UC Riverside
UC Riverside Electronic Theses and Dissertations

Title

Elucidation of G-Protein Signal Transduction in Neurospora crassa Using Chemical Genomics, Metabonomics, and Genetics

Permalink

Author

Kim, James Dong-Man

Publication Date

2011

UNIVERSITY OF CALIFORNIA
RIVERSIDE

Elucidation of G-Protein Signal Transduction in *Neurospora crassa* Using Chemical
Genomics, Metabonomics, and Genetics

A Dissertation submitted in partial satisfaction
of the requirements for the degree of

Doctor of Philosophy

in

Cell, Molecular, and Developmental Biology

by

James Dong-Man Kim

December 2011

Dissertation Committee:
        Dr. Katherine Borkovich, Chairperson
        Dr. Howard Judelson
        Dr. Cynthia Larive

The Dissertation of James Dong-Man Kim is approved:

_____

_____

_____
Committee Chairperson

University of California, Riverside

Acknowledgements

I humbly thank my mentor and advisor, Dr. Katherine A. Borkovich, for all of her efforts in training and supporting me for this journey. She has taught me so much about science and how to succeed in this field; she is a wonderful teacher. For that, I cannot thank her enough and will be grateful for all of my career.

Also, the members of the Borkovich lab, past and present, have really supported me over the years, not just as co-workers but more like family. They are Gyungsoon Park, Hyojeong Kim, Liande Li, Carol Jones, Sara Wright, Svetlana Krystofova, Jackie Servin, Carla Eaton, Asherie Campbell, Shouqiang Ouyang, Patrick Schacht, Alexander Michkov, Ilva Cabrera, Fitzgerald Diala, Amruta Garud, and Lorena Altamirano. Thank you very much for being such good friends.

I would also like to thank Dr. Larive and her lab. Starting from the collaboration and throughout, she has helped me greatly. Her patience and careful explanations really helped me out during the collaborative effort. Also, Kayla Kaiser, a good friend, was instrumental in helping me finish the project.

Dr. Judelson has given me good advice over the years, serving on my oral exam committee as well as the dissertation committee; thank you.

Ms. Kathy Redd has been a great assistance in the department.

Also, I would like to thank the IGERT program for giving me many opportunities as well as financial support for several years of my graduate program.

Last but not least is my family. My parents have always supported me, even during the really tough times; they've always been gracious. My wife, Inkyung, has been a true blessing through my Ph.D. She has given me so much energy and comfort; I cannot thank God enough.

Last, I thank God for giving me the strength to finish this journey in my life. Many times, I've cried out for help, and He has never failed me.

Only when you look back, do things make sense. That's the stage I am at now, and I see how blessed I've truly been.   Thank you all from the bottom of my heart.

Dedicated to

God, family, and friends

ABSTRACT OF THE DISSERTATION

Elucidation of G-Protein Signal Transduction in *Neurospora crassa* Using Chemical
Genomics, Metabonomics, and Genetics

by

James Dong-Man Kim

Doctor of Philosophy, Graduate Program in Cell, Molecular, and Developmental Biology
University of California, Riverside, December 2011
Dr. Katherine A. Borkovich, Chairperson

The filamentous fungus *Neurospora crassa* is a model organism for filamentous
fungi and has been studied for many years due to its many advantages as an organism for
study. Conidiation is a major mode of dispersal utilized by fungal pathogens, and it is
evident that conidiation is a common biological response to adverse conditions and a
means by which the fungus can reestablish itself in a more favorable environment. *N.
crassa* produces a type of asexual spore, the macroconidium (referred to as a conidium)
for dissemination in the environment.

In order to interact with its surroundings, fungi must be able to receive
extracellular signals. A major signaling pathway that detects and responds to external
signals in fungi and other eukaryotes is mediated by heterotrimeric GTP-binding proteins
(consisting of α, β, and γ subunits). Three Gα (GNA-1, GNA-2, and GNA-3), one Gβ
(GNB-1) and one Gγ subunit (GNG-1) have been identified in *N. crassa*. Loss of *gna-3*
has dramatic effects on conidiation, leading to production of short aerial hyphae and

premature conidiation in plate cultures and inappropriate conidiation in submerged cultures.

RIC8 is a novel guanine exchange factor (GEF) found in *Neurospora crassa* and has been shown to also interact with GNA-1 and GNA-3 in *N. crassa*. Yeast2Hybrid cDNA library screening has shown that RIC8 interacts with STE50, an adaptor protein working in the pathway of MAPK. A Δ*ric8* mutant shares several phenotypes with Δ*ste50* mutants. Also, without STE50, CAT formation is compromised. Localization of STE50 was investigated using a GFP-fused STE50; it localized to the cytoplasm as well as to the hyphal septa. Finally, coimmunoprecipitation (Co-IP) to verify that RIC8 and STE50 do physically interact was carried out.

As a participating student of the IGERT (Integrative Graduate Education and Research Traineeship), I was privileged to partake in a chemical genomics study; my goal was to find a chemical that perturbed asexual sporulation (conidiation) or spore germination in *Neurospora crassa*. From screens of the Chembridge library, I identified a compound that inhibited conidiation of Δ*gna-3* mutants. However, subsequent testing showed that newer batches of the chemical did not elicit the same phenotype; hence, this compound was dropped. However, during the screening of the Chembridge library, a unique phenotype was observed from one of the compounds that was tested. Compound #5979758 caused a "blebbing" effect on the conidia of all *Neurospora* strains tested so far.

Furthermore, I entered into a collaboration with Dr. Cythia Larive and Kayla Kaiser to use proton NMR to study metabonomics in Δ*gna-3* and wild-type strains under

different conditions. The metabolic profiles for wild type and Δ*gna-3* mutants were well-documented. From this study, it was revealed that the metabolome of Δgna-3 does not vary greatly from that of the wild-type, even though it conidiates in submerged conditions. Also, it was shown that GNA-3 is involved in a nutrient sensing pathway. A paper titled "Use of ¹H NMR to measure intracellular metabolite levels during growth and asexual sporulation in *Neurospora crassa*", with authors James Kim, Kayla Kaiser, Cynthia Larive and Katherine Borkovich, was published in the journal *Eukaryotic Cell*.

Table of Contents

List of Figures

List of Tables

Chapter 1: Introduction

I.   Introduction to *Neurospora crassa*

Neurospora crassa is a model organism for the filamentous fungi, serving as a model for fungal pathogens of plants and animals (20) . Its genome has been sequenced, facilitating research into genetic and signaling networks. *N. crassa* is an Ascomycete, a phylum of the Fungal kingdom (2). Also known as the "sac fungi", this is the largest phylum of the Fungal kingdom. The "sacs" are called asci and contain ascospores after meiosis (18).

Neurospora first came under scientific scrutiny in 1842 when an orange mold ruined baked goods at French bakeries (44). Even though it was originally seen as a pest, *Neurospora*'s ease of culturing soon brought it attention for use as a laboratory organism, and in the early 1920s, it blossomed in popularity for its utility as an experimental organism. Dr. Bernard Dodge performed much taxonomic work with *N. crassa,* and he was instrumental in convincing other researchers to use this organism as a model for laboratory experiments for biochemical and genetic research (44).

Perhaps, the most famous use of *Neurospora crassa* is Drs. Beadle and Tatum's "one gene-one enzyme" research that earned them a Nobel Prize in Physiology/Medicine in 1958 (21); their work showed that genes are responsible for the biochemistry of metabolism, bridging the disciplines of biochemistry and genetics (7). Briefly, they x-rayed *N. crassa* conidia to mutate genes responsible for control of specific chemical reactions. By testing the mutants (strains that did not grow on minimal medium) on

minimal medium with a particular supplementation (a nutrient that the mutant could no longer produce because the gene responsible was mutated and could no longer function correctly), Beadle and Tatum deduced that a gene was responsible for the biochemical reaction that sustained life.

The genome of *N. crassa* is approximately 40 megabases, with ~10,600 genes (20), and seven chromosomes (12). It is a heterothallic fungus with 29 different cell-types (10, 47) with two separate mating types, *mat A* and *mat a* (18). Even though most of its life cycle is spent as an asexual organism, *N. crassa* is able to grow indefinitely and establish new colonies with the aid of macro and microconidia that are clones of the original colony (18).

In warm, moist climates, *Neurospora* are often found in agricultural burn sites, probably due to the ascospores being activated to germinate after the fire (45). This explains why the Paris bakeries were such suitable environments for *N. crassa* to blossom: the warm bakeries with their ample nutrient supply provided the perfect environment for the fungus to thrive.

Fungi are found in many different environments (2). Hence, as a microorganism, they must be able to interact with these environments by responding to environmental stimuli. The mechanism by which fungi relate to stimuli and adapt is governed by signal transduction pathways (5). Fungi have adapted to their environment by evolving many ways to sense their immediate surroundings (5). Two main ways (shared with higher Eukaryotes) that occur are through the heterotrimeric G-protein signal transduction cascades and the Mitogen Activated Protein Kinase (MAPK) pathways (5).

II. Heterotrimeric G-Protein signal transduction pathways

Heterotrimeric G-Protein signaling comprises of a G-Protein Coupled Receptor (GPCR), a Gα subunit, a Gβ subunit, and a Gγ subunit (40). Figure 1 is a diagram illustrating the heterotrimeric G-protein signal transduction cascade. A binding of a ligand to the GPCR triggers a conformational change in the receptor such that the Gα exchanges its GDP for a GTP, separates from the GPCR and βγ heterodimer, and then interacts with downstream effectors.

GPCRs have a conserved 7 transmembrane helix domain (40). The amino terminus is exposed on the extracellular space, while the carboxy terminus is oriented towards the cytoplasm. GPCRs are necessary for a quick response to an external stimulus, such as chemical, environmental, and internal signals from within the organism (5). GPCRs make excellent drug targets, and a large percentage of phamaceuticals indeed target them (24).   Some examples are albuterol used to treat asthma that targets the adrenoceptor, and morphine, a powerful analgesic that targets the opioid receptor (50).

The *N. crassa* genome has predicted 29 GPCRs (12, 40). GPCRs of *N. crassa* can be divided into 8 groups: microbial opsins (an opsin called NOP-1 and opsin-related protein called ORP-1 (opsin related proteins are like opsins but lack the lysine residue necessary for retinal binding (13)), two pheromone receptors PRE-1 and PRE-2 (31), glucose sensors, nitrogen sensors, PTH11-related GPCRs, Homo sapiens mPR steroid receptor-related GPCRs, rat growth hormone releasing factor-like GPCR, and *Aspergillus* GprK-like GPCR (12, 40).

NOP-1 is a putative green-light receptor that binds all trans retinal (a chromophore that binds to opsins to form rhodopsin) (8). It is negatively regulated by the blue-light sensing pathway and influences conidiation-specific gene expression (9). PRE-1 and PRE-2 are pheromone receptors that are homologous to *Saccharomyces cerevisiae* Ste2p and Ste3p, respectively. PRE-1 is expressed solely in *mat A* strains (31) while PRE-2 is expressed only in *mat a* strains. Loss of *pre-1* does not block protoperithecial development. However, the protoperithecia do not become fertilized (cannot mature into perithecia) because trichogynes originating from protoperithecia of the Δ*pre-1* are not chemotropically attracted to the *mat a* cells (31). Hence, recruitment of the male gamete does not occur, preventing fertilization. This is also the case with loss of *pre-2*, the opposite pheromone receptor (30). Their respective pheromones ligands MFA-1 and CCG-4 (both polypeptides), are not recognized in these mutants due to loss of the cognate receptors.

Three GPCRs (GPR-1, GPR-2, and GPR-3) comprise one family, the cAMP Receptor-Like (CRL) GPCRs (40). Of these, GPR-1 is localized to protoperithecia (34). Loss of *gpr-1* leads to defective female structures in *N. crassa*, with weakly pigmented protoperithecia that are small and submerged in the agar and perithecia that have deformed beaks without ostioles (hole for ascospore ejection).

GPR-4 is a carbon-sensing receptor (39); Δ*gpr-4* has reduced mass accumulation on glycerol, mannitol, and arabinose compared to wild-type strain. Also, the increase in intracellular cAMP that accompanies the shift from a poor carbon source to a favorable one does not occur in Δ*gpr-4*, suggesting that GPR-4 is a carbon-sensor. It is similar to

Gpr1p of *Saccharomyces cerevisiae,* a GPCR whose agonists are glucose and sucrose. GNA-1 physically interacts with the carboxy terminus of GPR-4, and the former is epistatic to the latter (39).

GPR-5 and GPR-6 are homologous to *Schizosaccharomyces pombe* Stm1p (12). In *S. pombe,* Stm1p is upregulated in low nitrogen condition and also interacts with Gpa2 (one of two Gα subunits) via the carboxy-terminus (17). However, these observations could not be replicated in other laboratories, and the exact role of Stm1p in signaling is currently unknown.

There are 25 homologs related to *Magnaporthe grisea*'s PTH11 (40) which has been shown to be necessary for appressorium differentiation in this fungal plant pathogen (19). Out of these 25, only one has a CFEM domain (cysteine-rich EGF-like), which are characteristically present on extracellular regions of membrane proteins (35). Also, there are 2 *Homo sapiens* mPR steroid receptors in the *N. crassa* genome. One weak homolog to rat growth hormone releasing factor exists as well as one *Aspergillus* GprK-like GPCR that contains an RGS domain (36).

Regulators of G-Protein Signaling (RGS) proteins positively regulate the intrinsic GTPase activity of Gα subunits, speeding hydrolysis of GTP to GDP (25). This leads to a deactivation of the heterotrimeric G-protein signal transduction cascade (41). This is an excellent mechanism for fine-tuning the signal from the GPCR. There are five RGS proteins in the *N. crassa* genome, RGS-1 through -5. Similarly, *Aspergillus nidulans* also possesses 5 RGS proteins (53). One of the RGS proteins in *A. nidulans* called GprK

contains both a RGS domain and 7 transmembrane helices. Similarly, *N. crassa* also has a similar RGS called RGS-5 that shares similar domains (38).

There are 3 Gα subunits, 1 β, and 1 γ in the *Neurospora crassa* genome (12). The Gαs are GNA-1, GNA-2, and GNA-3. The Gβ is GNB-1, and the Gγ is GNG-1. This ratio of heterotrimeric G-protein subunits is also found in *Magnaporthe* and *Aspergillus* sp. (40). Judging from the fungal species that have been sequenced, it appears that filamentous fungi generally follow this rule of 3 Gα subunits, 1 β subunit, and 1 γ subunit. However, yeasts differ in that they generally only have 2 Gα subunits (14).

The predicted size of GNA-1 is 39 kiloDaltons, residing in the membrane fraction (49). It belongs in the mammalian $G\alpha_i$ superfamily. Using pertussis toxin (a toxin that ADP-ribosylates $G\alpha_i$ subfamily proteins) it was determined that the GNA-1 sequence contains a labeling site (ADP-ribosylation) for this toxin, showing that it is similar to $G\alpha_i$ family members in mammals. Also, it contains a myristoylation site for membrane targeting, characteristic of the $G\alpha_i$ superfamily. Loss of *gna-1* leads to reduced apical extension, decreased aerial hyphae, increased conidiation, and reduced colony size (51). Furthermore, deletion mutants of *gna-1* conidiate in submerged conditions (only at higher cell density of $3x10^6$ cells/ml) (22). Also, they are sensitive to KCl, NaCl and sorbitol. Furthermore, conidia of Δ*gna-1* are smaller than those of the wild type strain. Finally, *gna-1* protoperithecia are aberrant, appearing black and brown in color (whereas that of the wild-type are generally black). This phenotype brings to mind the Δ*gpr-1* that has weakly pigmented protoperithecia (34). Interestingly, without *gna-1*, trichogynes of *Neurospora crassa* are "blind" (31); they cannot sense the male cells.

On the other hand, constitutively activated *gna-1* strains (through disruption of the intrinsic GTPase activity; *gna-1**) have decreased carotenoid levels, but increased cAMP and sensitivity to heat and oxidative stress. These results suggest that GNA-1 controls aerial hyphae development and sensitivity to heat and oxidative stress (51). FadA (Gα subunit in *Aspergillus nidulans* in the same Gα class as *gna-1* (40)) controls asexual sporulation (1); without it, the fungus conidiates constitutively. Constitutively active *fadA* leads to no conidiation and a 'fluffy' phenotype, similar to a phenotype of *gna-1** (51).

gna-2 is the second Gα subunit in *N. crassa*. It is not part of any Gα superfamily of higher Eukaryotes (3). GNA-2 is 49.4% amino acid identical to GNA-1, indicating that it is due to a possible gene duplication event. No major abnormalities were discovered during vegetative or sexual development (3), except for a mass accumulation defect when cultured on poor carbon sources (39). However, g*na-1, gna-2* double deletion mutants have a slower rate of hyphal apical extension than *gna-1* deletion mutants on normal or hyperosmotic media. Also, the double deletion mutants show a more pronounced defect in female fertility than Δ*gna-l* strains; loss of *gna-2* causes even fewer perithecia after fertilization than loss of *gna-1* alone (3). Therefore, it has been proposed that *gna-1* and *gna-2* have overlapping functions and may constitute a gene family (3). Decreased adenylyl cyclase (enzyme that makes cAMP) levels in Δ*gna-1* and Δ*gna-1* Δ*gna-2* mutants means that GNA-1 regulates adenylyl cyclase protein levels (23). Lower cAMP levels in Δ*gna-2* on SCM suggests GNA-2 might be implicated in adenylyl cyclase or phosphodiesterase regulation during mating. Hence, GNA-1 and GNA-2 have

overlapping functions in the regulation of cAMP activity (either at the adenylyl cyclase (production) or phosphodiesterase (degradation) control). Also, further research has shown that a similar situation exists with Δ*gna-3*, such that Δ*gna-2* displays a strong phenotype only in conjunction with either Δ*gna-1* or Δ*gna-3* (29).

The last Gα subunit is GNA-3. Δ*gna-3* displays defects similar to Δ*cr-1*, the adenylyl cyclase deletion mutant (28). When *gna-3* is deleted, the mutant phenotype is shorter aerial hyphae, dense/premature conidiation, and inappropriate conidiation in submerged culture (28). When cAMP is supplied to the mutant in standing liquid culture, the short aerial hyphae and premature, dense conidiation phenotypes are corrected; however, inappropriate conidiation is not corrected with addition of cAMP. On the other hand, addition of peptone does correct the inappropriate conidiation phenotype in Δ*gna-3* mutants cultured in liquid medium. Some of the phenotypes of Δ*gna-3* can be attributed to lack of cAMP because, without GNA-3, CR-1 levels are reduced. Yet, this reduction was not due to reduced *cr-1* transcript levels, indicating that loss of *gna-3* affects translation or stability of adenylyl cyclase. Another interesting phenotype of Δ*gna-3* is that, in submerged conditions, the glucose-repressible gene *qa-2* is greatly derepressed, even more than that of carbon-starved wild-type strain, suggesting that GNA-3 is involved in a carbon-sensing pathway of *N. crassa*. Finally, Δ*gna-3* has reduced fertility, with smaller perithecia lacking beaks and reduced ascospore shooting.

Mutants lacking all three Gα genes have a severe growth phenotype (29). However, the triple deletion mutant (Δ*gna-1*, Δ*gna-2*, Δ*gna-3*) is viable, indicating that the Gαs are not essential for survival of *N. crassa*. The Δ*gna-1*, Δ*gna-2*, Δ*gna-3* mutants

display few and short aerial hyphae, are female infertile, produce aberrant protoperithecia, and exhibit inappropriate conidiation (which is not fully suppressed, even with the addition of 2% peptone). Interestingly, when all three Gαs are knocked out, GNB-1 levels also decrease.

GNB-1 is the sole Gβ-subunit of *N. crassa* (52). It is constitutively expressed throughout the lifecycle. Interestingly, it is 65% identical to the human Gβ. When deleted, Δ*gnb-1* conidiates profusely on solid medium. The mutant also inappropriately conidiates under submerged conditions (which can be corrected with addition of 2% peptone). Moreover, cAMP levels decrease to approximately 60% of that of wild type on VM plate. Δ*gnb-1* is female sterile; it forms small perithecia without any ascospores (a phenotype identical to Δ*gna-1*). Also, without GNB-1, all Gα levels are decreased significantly. This decrease in Gα proteins is due to a post-transcriptional mechanism, because *gna-1* and *gna-2* mRNA levels are normal in Δ*gnb-1* mutants.

Many of the phenotypes of Δ*gnb-1* (such as female sterility, lower cAMP levels and inappropriate conidiation) can be explained by low levels of Gα proteins. Two phenotypes that are independent of the influence of Gα proteins are apical extension rate (slightly less than wild type) and mass accumulation.

N. crassa only has one Gγ-subunit (33). It possesses a characteristic CaaX box motif at the carboxy-terminus. This motif is posttranslationally modified by isoprenylation (for plasma membrane targeting). Deletion of the Gγ-subunit leads to phenotypes similar to the Δ*gnb-1* in that the Δ*gng-1* inappropriately conidiates, has a

9

negative influence on the stability of all three Gαs, has decreased intracellular cAMP levels, and is female sterile, with formation of aberrant perithecia, and blind trichogynes that are not attracted to opposite mating type cells (a trait that is shared by *Δgnb-1* and *Δgna-1*). The requirement of these genes for trichogyne chemotropism is also shared by the pheromone GPCRs PRE-1 and PRE-2 (30), indicating that these genes are an integral component of the female fertility signaling pathway. Using co-immunoprecipitation, GNB-1 was shown to associate with GNG-1, indicating that these two proteins form a functional heterodimer and are interdependent for stability (33).

III. MAPK signaling pathways

Mitogen-Activated Protein Kinase (MAPK) signaling pathways are ubiquitous in all known Eukaryotes (15). These pathways transduce external signals to the nucleus by involving 3 sequentially activated serine/threonine protein kinases (6). A complex co-regulatory circuit that incorporates MAPK pathways exists to coordinate differentiation mechanisms in cells (16).

In *N. crassa*, there are three MAPK pathways (12): osmosensing, cell integrity, and pheromone response/filamentation pathways (43, 44, 54). Figure 2 shows a diagram of the MAPK pathways in *N. crassa*. MAPK signaling can be regulated by heterotrimeric G-proteins; In *Saccharomyces cerevisiae*, it was shown that pheromones binding to a pheromone receptor (a GPCR) can lead to signal transduction from the heterotrimeric G-proteins to the MAPK cascade (comprised of Ste11p (MAPKKK), Ste7 (MAPKK), and Fus3p (MAPK) (42). Additionally, Gpa1p (Gα) physically interacts with Fus3p (MAPK)

to downregulate the pheromone-induced mating signal by binding to activated Fus3p and keeping it out of the nucleus (to prevent transcriptional activation of mating-related genes) (11).

In *N. crassa*, the *mak-2* MAPK is a homolog of Fus3p and Kss1p (involved in pheromone and filamentation signaling) of *Sacchromyces cerevisiae* (37). It is 43 kDa and has a TEY (Thr-Glu-Tyr) dual phosphorylation motif (residing in the catalytic core of the protein) that is specific to this group of MAPKs. MAK-2 is highly similar to ERK1 and ERK2 (Extracellular signal-Related Kinase) of mammalian cells that are involved in regulation of meiosis, mitosis, and postmitotic functions. The target of MAK-2 is a transcription factor called PP-1 (*protoperithecium-1*), a homolog of *S. cerevisiae* Ste12p that contains zinc-finger motifs for DNA binding. Deletion mutants of *mak-2* and *pp-1* share several phenotypes: reduced growth rate on solid medium (only 25% of wild type), short aerial hyphae, no protoperithecial formation (hence female sterility), and ascospore lethality. Both of the genes are necessary for protoperithecial development, normal filamentous growth, and aerial hyphae formation. NRC-1 is the MAPKKK of the MAK-2 MAPK pathway (32). NRC-1 (Non-Repressible Conidiation gene 1) is homologous to Ste11p of *Saccharomyces cerevisiae* (12). Δ*nrc-1* conidiates inappropriately, is female infertile, and ascospore lethal (32). Furthermore, Δ*nrc-1*, Δ*mak-2*, and Δ*pp-1* all are defective in hyphal fusion, further confirmation that these components function in the same pathway (43). Phosphorylation study of MAK-2 (using phospho-p44/42 antibody that recognizes phosphorylated threonine and tyrosine residues of the TEY motif of ERK1/2 which are highly conserved) shows that phosphorylated

MAK-2 is associated with germ tube elongation, branching, and hyphal fusion among germlings. Logically, loss of NRC-1 (MAPKKK) causes defect in the phosphorylation of MAK-2, corraborating that they are indeed part of the same MAPK pathway. Finally, parallel to the pheromone pathway in *S. cerevisiae*, *N. crassa* pheromone pathway signal transduction could be traveling from the pheromone (CCG-4/MFA-1) to the pheromone receptor GPCRs PRE-1/PRE-2, to Gα GNA-1, to MAPK pathway from NRC-1 to MAK-2 (29).

The second MAPK pathway in *N. crassa* is homologous to the Slt2p cell wall integrity MAPK pathway of *Saccharomyces cerevisiae* (44). Its components are MIK-1 (MAPKKK), MEK-1 (MAPKK), and MAK-1 (MAPK). When any one of these components is deleted, the mutants share the following phenotypes: reduced basal hyphae growth on solid medium (30% ~ 40% of wild type by comparison), short aerial hyphae, no protoperithecial formation (hence, female sterility), and arthroconidial formation. Also, loss of *mik-1* leads to reduced conidiation, whereas loss of either *mek-1* or *mak-1* completely prevents conidiation. MAK-1 is approximately 50 kDa, and its phosphorylation can be checked by using the same antibody for detection of MAK-2 phosphorylation. MAK-1 phosphorylation was greatest at 16 – 24 hours on solid medium. When the phosphorylation level of MAK-1 was checked, neither Δ*mik-1* or Δ*mek-1* showed any phosphorylation, evidence that these three components function in the same MAPK pathway. Interestingly, in Δ*mek-1* and Δ*mik-1* grown in SCM medium (nitrogen-starved condition), tyrosinase mRNA and protein levels are elevated (this is an enzyme for production of secondary metabolite L-DOPA melanin).

The last MAPK pathway (osmosensing) to be discussed is intertwined with the two-component signaling system (4). Basically, the two-component system requires 3 proteins, the hybrid histidine kinase, the histidine phosphotransfer protein (HPT) and the response regulator. The hybrid histidine kinase protein contains both domains, histidine kinase and response regulator. This protein transfers phosphate from histidine to aspartate of same protein and then transfers the phosphate to another protein with a histidine phosphotransfer (HPT) domain. Finally, the phosphate is transferred to a conserved aspartate residue on a response regulator that regulates the MAPK cascade. The most well-known two-component system is probably the one that regulates the Hog1 MAPK cascade in *Saccharomyces cerevisiae*: The osmosensor Sln1p (hybrid histidine kinase) transfers the phosphate group to Ypd1p (HPT protein) then to Ssk1p (response regulator), which inhibits phosphorylation of the MAPKKK Ssk2p/Ssk22p, MAPKK Phb2p, and finally Hog1p (46). Finally, since histidine kinases are not found in humans, they make a great drug targets (12).

N. crassa possesses 11 putative hybrid histidine kinases (12). One of the well-characterized hybrid histidine kinases is OS-1 (also known as NIK-1). With HPT-1 (the HPT protein), and RRG-1 (a response regulator) (12) OS-1 regulates the osmosensing pathway of *N. crassa* by affecting the MAPK pathway with components OS-4 (MAPKKK), OS-5 (MAPKK), and OS-2 (MAPK) (27). The OS-2 MAPK is homologous to Hog1p of *Saccharomyces cerevisiae* (12). It also regulates osmosensitivity. It is a p38 class MAPK, a MAPK group that is activated by environmental stresses rather than mitogenic stimuli in mammals (48). *os* mutants have

fragile conidia, having a tendency to lyse. They are also female-sterile and sensitive to osmotic stress (due to the inability to properly stimulate glycerol production) (26). This last phenotype is related to resistance to fungicides (such as Fludioxonil, a phenylpyrrole) that target the hyperosmotic stress pathway and activates the *os-2* MAPK pathway, causing production of glycerol that leads to intracellular accumulation and eventual bursting of cells (54).

A general conclusion that can be drawn from studying the three MAPK pathways of *N. crassa* is that, since all three MAPK mutants show defects in sexual development and conidiation, MAK-1, MAK-2, and OS-2 MAPK pathways play a crucial role in these processes (27, 37, 44).

IV.   Objectives

Small compound library was screened for "hits" that had an effect on conidiation of *N. crassa*. Specifically, wild-type and Δ*gna-3* were tested to see if wild-type could be induced to conidiate in submerged condition while Δ*gna-3*'s 'inappropriate conidiation' could be corrected. Initially, a compound was found to correct the Δ*gna-3* phenotype. However, subsequent lots of the chemical failed to reproduce the phenotype. On the other hand, a unique chemical (compound #5979758) showed an unusual phenotype, causing strange blebbing to occur on the surface of all strains tested.

To determine if the metabolome of *N. crassa* was influenced by GNA-3, wild-type and Δ*gna-3* strains were subjected to a metabolic study utilizing ^{1}H NMR. Results showed that loss of GNA-3 does not greatly influence the overall metabolic profile of this

filamentous fungus. However, by examining the metabolic profile, we learned that without GNA-3 *N. crassa* does not detect presence of an environmental carbon source.

In order to explore RIC8-involved signaling pathways, a Yeast2Hybrid screening of *N. crassa* cDNA library was undertaken. 8 interactors were found, one of which was a protein called STE50; it is an adaptor protein involved in MAPK signaling in *Saccharomyces cerevisiae*. Furthermore, a co-immunoprecipitation experiment showed that STE50 physically interacts with RIC8. The deletion mutant of ste50 was made and phenotyped. Phenotypes of Δ*ste50* shared many similarities with Δ*ric8*, providing genetic evidence that these two proteins associate in cellular processes.

Figure 1. Diagram illustrating the heterotrimeric G-protein signal transduction cascade. (a) GPCR sits on the plasma membrane with the heterotrimeric G-proteins attached on cytoplasm side. (b) As the ligand binds to the GPCR (on the extracellular side), a conformational change occurs on the receptor, leading to an exchange of GTP for GDP on the Gα-subunit. (c) Then, the Gα dissociates from the βγ-heterodimer. (d) Both Gα and the βγ-heterodimer are free to interact with downstream effectors. (e) The intrinsic hydrolysis activity of Gα causes GTP to be converted to GDP (RGS proteins can greatly facilitate this activity), and the Gα can reassociate with the βγ-heterodimer at the GPCR.
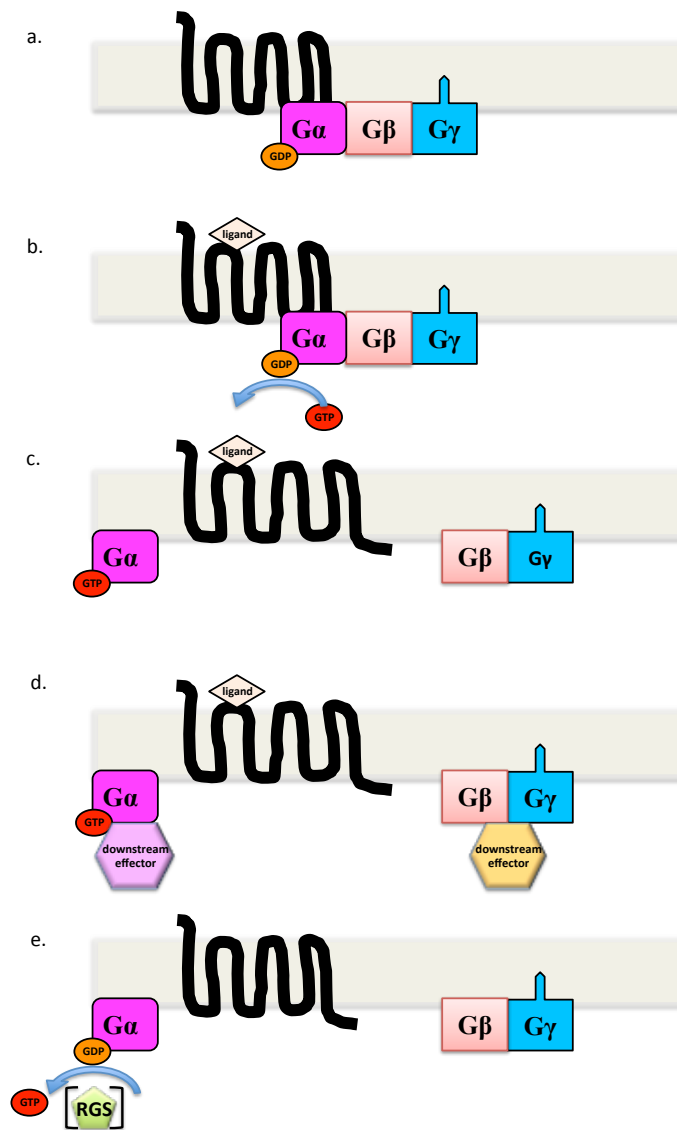
Figure 2. MAPK pathways of *Neurospora crassa*. The three MAPK pathways in *Neurospora crassa* are the cell wall integrity pathway (MIK-1, MEK-1, MAK-1), the cell fusion/female fertility pathway (NRC-1, MEK-2, MAK-2), and the osmosensing pathway (OS-4, OS-5, OS-2).
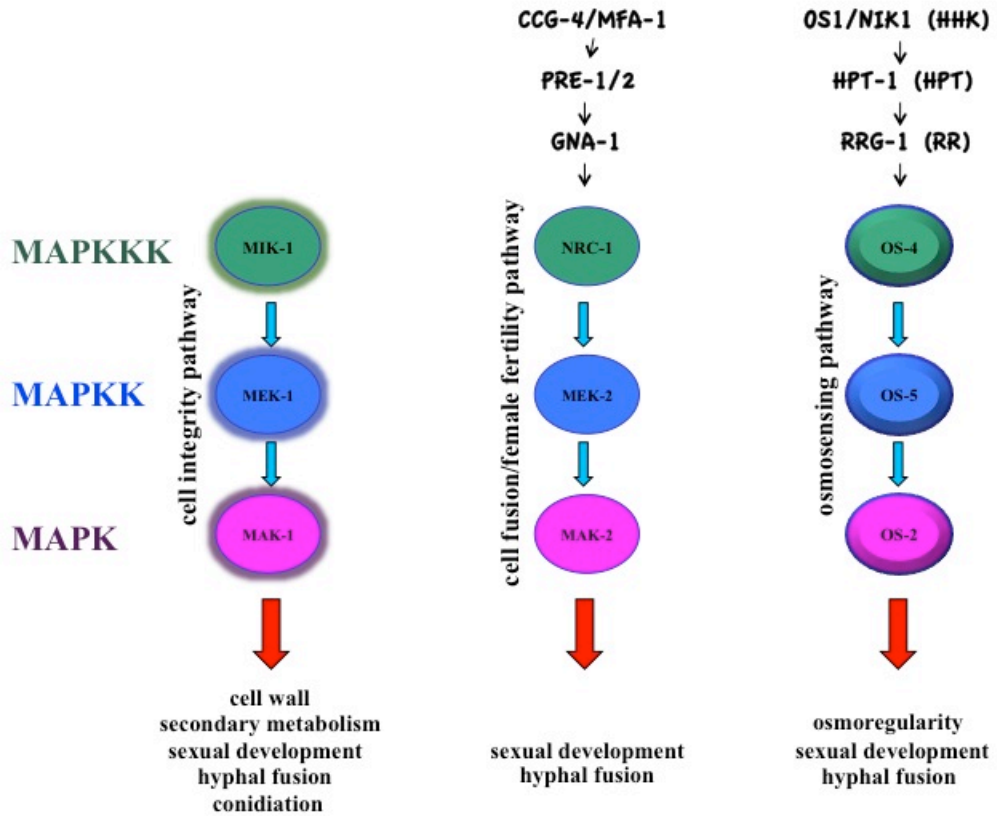
REFERENCES

1. **Adams T. H., and J. H. Yu**. 1998. Coordinate control of secondary metabolite production and asexual sporulation in *Aspergillus nidulans*. Current Opinion in Microbiology **1**:674-677.

2. **Alexopoulos C. J., C. W. Mims, and M. Blackwell**. 1996. Introductory Mycology, 4th ed. Wiley, New York.

3. **Baasari R. A., X. Lu, P. S. Rowley, K. A. Borkovich, and E. Turner**. 1997. Overlapping Functions for Two G Protein α subunits in *Neurospora crassa*. Genetics **147**:137-145.

4. **Bahn Y.S.** 2008. Master and commander in fungal pathogens: the two-component system and the HOG signaling pathway. Eukaryotic Cell **7**:2017-36.

5. **Bahn Y.S., C. Xue, A. Idnurm, J. C. Rutherford, J. Heitman, and M. E. Cardenas**. 2007. Sensing the environment: lessons from fungi. Nature Reviews. Microbiology **5**:57-69.

6. **Bardwell L.** 2006. Mechanisms of MAPK signalling specificity. Information Processing and Molecular Signalling **34**:837-41.

7. **Beadle G. W., and E. L. Tatum**. 1941. Genetic control of biochemical reactions in *Neurospora*. Proceedings of the National Academy of Sciences of the United States of America **27**:499-506.

8. **Bieszke J. A., E. L. Braun, L. E. Bean, S. Kang, D. O. Natvig, and K. A. Borkovich**. 1999. The *nop-1* gene of *Neurospora crassa* encodes a seven transmembrane helix retinal-binding protein homologous to archaeal rhodopsins. Proceedings of the National Academy of Sciences of the United States of America **96**:8034-9.

9. **Bieszke J. A., L. Li, and K. A. Borkovich**. 2007. The fungal opsin gene *nop-1* is negatively-regulated by a component of the blue light sensing pathway and influences conidiation-specific gene expression in *Neurospora crassa*. Current Genetics **52**:149-57.

10. **Bistis G. N., D. D. Perkins, and N. D. Read**. 2003. Different cell types in *Neurospora crassa*. Fungal Genetics Newsletter 17-19.

11. **Blackwell E., I. M. Halatek, H. J. Kim, A. T. Ellicott, A. A. Obukhov, and D. E. Stone**. 2003. Effect of the Pheromone-Responsive Gα and Phosphatase Proteins of *Saccharomyces cerevisiae* on the Subcellular Localization of the Fus3 Mitogen-Activated Protein Kinase. Molecular and Cellular Biology **23**:1135-1150.

12. **Borkovich K. A., L. A. Alex, O. Yarden, M. Freitag, G. E. Turner, N. D. Read, S. Seiler, D. Bell-pedersen, J. Paietta, N. Plesofsky, M. Plamann, M. Goodrich-tanrikulu, U. Schulte, G. Mannhaupt, F. E. Nargang, A. Radford, C. Selitrennikoff, J. E. Galagan, J. C. Dunlap, J. J. Loros, D. Catcheside, H. Inoue, R. Aramayo, M. Polymenis, E. U. Selker, M. S. Sachs, G. A. Marzluf, I. Paulsen, R. Davis, D. J. Ebbole, A. Zelter, E. R. Kalkman, R. O. Rourke, and F. Bowring**. 2004. Lessons from the Genome Sequence of *Neurospora crassa*: Tracing the Path from Genomic Blueprint to Multicellular Organism. Microbiology and Molecular Biology Reviews **68**:1-108.

13. **Brown L. S.** 2004. Fungal rhodopsins and opsin-related proteins: eukaryotic homologues of bacteriorhodopsin with unknown functions. Photochemical & Photobiological Sciences **3**:555-65.

14. **Bölker M.** 1998. Sex and crime: heterotrimeric G proteins in fungal mating and pathogenesis. Fungal Genetics and Biology **25**:143-56.

15. **Chang L., and M. Karin**. 2001. Mammalian MAP kinase signalling cascades. Nature **410**:37-40.

16. **Chavel C. A., H. M. Dionne, B. Birkaya, J. Joshi, and P. J. Cullen**. 2010. Multiple signals converge on a differentiation MAPK pathway. PLoS Genetics **6**:e1000883.

17. **Chung K. S., M. Won, S. B. Lee, Y. J. Jang, K. L. Hoe, D. U. Kim, J. W. Lee, K. W. Kim, and H. S. Yoo**. 2001. Isolation of a novel gene from *Schizosaccharomyces pombe*: stm1+ encoding a seven-transmembrane loop protein that may couple with the heterotrimeric Gα2 protein, Gpa2. The Journal of Biological Chemistry **276**:40190-201.

18. **Davis R.** 2000. *Neurospora*: Contributions of a Model Organism. Oxford University Press, USA.

19. **DeZwaan T. M., A. M. Carroll, B. Valent, and J. A. Sweigard**. 1999. *Magnaporthe grisea* pth11p is a novel plasma membrane protein that mediates appressorium differentiation in response to inductive substrate cues. The Plant Cell **11**:2013-30.

20. **Galagan J. E., S. E. Calvo, K. A. Borkovich, E. U. Selker, N. D. Read, D. Jaffe, W. FitzHugh, L. J. Ma, S. Smirnov, S. Purcell, B. Rehman, T. Elkins, R. Engels, S. Wang, C. B. Nielsen, J. Butler, M. Endrizzi, D. Qui, P. Ianakiev, D. Bell-Pedersen, M. A. Nelson, M. Werner-Washburne, C. P. Selitrennikoff, J. A. Kinsey, E. L. Braun, A. Zelter, U. Schulte, G. O. Kothe, G. Jedd, W. Mewes, C. Staben, E. Marcotte, D. Greenberg, A. Roy, K. Foley, J. Naylor, N. Stange-Thomann, R. Barrett, S. Gnerre, M. Kamal, M. Kamvysselis, E. Mauceli, C. Bielke, S. Rudd, D. Frishman, S. Krystofova, C. Rasmussen, R. L. Metzenberg, D. D. Perkins, S.**

Kroken, C. Cogoni, G. Macino, D. Catcheside, W. Li, R. J. Pratt, S. A. Osmani, C. P. C. DeSouza, L. Glass, M. J. Orbach, J. A. Berglund, R. Voelker, O. Yarden, M. Plamann, S. Seiler, J. Dunlap, A. Radford, R. Aramayo, D. O. Natvig, L. A. Alex, G. Mannhaupt, D. J. Ebbole, M. Freitag, I. Paulsen, M. S. Sachs, E. S. Lander, C. Nusbaum, and B. Birren. 2003. The genome sequence of the filamentous fungus *Neurospora crassa*. Nature **422**:859-68.

21. **Horowitz N. H.** 1991. Fifty Years Ago: The *Neurospora* Revolution. Genetics **127**:631-635.

22. **Ivey F. D., P. N. Hodge, G. E. Turner, and K. A. Borkovich**. 1996. The Gα_i homologue *gna-1* controls multiple differentiation pathways in *Neurospora crassa*. Molecular Biology of the Cell **7**:1283-97.

23. **Ivey F. D., Q. Yang, and K. A. Borkovich**. 1999. Positive regulation of adenylyl cyclase activity by a gα_i homolog in *Neurospora crassa*. Fungal Genetics and Biology **26**:48-61.

24. **Jacoby E., R. Bouhelal, M. Gerspacher, and K. Seuwen**. 2006. The 7 TM G-protein-coupled receptor target family. ChemMedChem **1**:761-82.

25. **Jean-Baptiste G., Z. Yang, and M. T. Greenwood**. 2006. Regulatory mechanisms involved in modulating RGS function. Cellular and Molecular Life Sciences **63**:1969-85.

26. **Jones C. A., and K. A. Borkovich**. 2010. Analysis of Mitogen-Activated Protein Kinase Phosphorylation in Response to Stimulation of Histidine Kinase Signaling Pathways in *Neurospora*. Methods Enzymol. **471**:319-334.

27. **Jones C. A., S. E. Greer-phillips, and K. A. Borkovich**. 2007. The Response Regulator RRG-1 Functions Upstream of a Mitogen-activated Protein Kinase Pathway Impacting Asexual Development, Female Fertility, Osmotic Stress, and Fungicide Resistance in *Neurospora crassa*. Molecular Biology of the Cell **18**:2123-2136.

28. **Kays A. M., P. S. Rowley, R. A. Baasiri, and K. A. Borkovich**. 2000. Regulation of conidiation and adenylyl cyclase levels by the Gα protein GNA-3 in *Neurospora crassa*. Molecular and Cellular Biology **20**:7693-705.

29. **Kays A. M., and K. A. Borkovich**. 2004. Severe impairment of growth and differentiation in a *Neurospora crassa* mutant lacking all heterotrimeric Gα proteins. Genetics **166**:1229-40.

30. **Kim H. J., and K. A. Borkovich**. 2006. Pheromones are essential for male fertility and sufficient to direct chemotropic polarized growth of trichogynes during mating in *Neurospora crassa*. Eukaryotic Cell. Am Soc Microbiol **5**:544-554.

31. **Kim H. J., and K. A. Borkovich**. 2004. A pheromone receptor gene, *pre-1*, is essential for mating type-specific directional growth and fusion of trichogynes and female fertility in *Neurospora crassa*. Molecular Microbiology **52**:1781-98.

32. **Kothe G. O., and S. J. Free**. 1998. The Isolation and Characterization of *nrc-1* and *nrc-2*, Two Genes Encoding Protein Kinases That Control Growth and Development in *Neurospora crassa*. Genetics **149**:117-130.

33. **Krystofova S., and K. A. Borkovich**. 2005. The Heterotrimeric G-Protein Subunits GNG-1 and GNB-1 Form a Gβγ Dimer Required for Normal Female Fertility, Asexual Development, and Gα Protein Levels in *Neurospora crassa*. Eukaryotic Cell **4**:365-378.

34. **Krystofova S., and K. A. Borkovich**. 2006. The predicted G-protein-coupled receptor GPR-1 is required for female sexual development in the multicellular fungus *Neurospora crassa*. Eukaryotic Cell **5**:1503-16.

35. **Kulkarni R. D., M. R. Thon, H. Pan, and R. A. Dean**. 2005. Novel G-protein-coupled receptor-like proteins in the plant pathogenic fungus *Magnaporthe grisea*. Genome Biology **6**:R24.

36. **Lafon A., K.-H. Han, J.-A. Seo, J.-H. Yu, and C. D'Enfert**. 2006. G-protein and cAMP-mediated signaling in aspergilli: a genomic perspective. Fungal Genetics and Biology **43**:490-502.

37. **Li D., P. Bobrowicz, H. H. Wilkinson, and D. J. Ebbole**. 2005. A mitogen-activated protein kinase pathway essential for mating and contributing to vegetative growth in *Neurospora crassa*. Genetics **170**:1091-104.

38. **Li L.** 2008. Ph.D. Thesis. G protein coupled receptors in *Neurospora crassa*. University of California, Riverside, CA.

39. **Li L., and K. A. Borkovich**. 2006. GPR-4 is a predicted G-protein-coupled receptor required for carbon source-dependent asexual growth and development in *Neurospora crassa*. Eukaryotic Cell **5**:1287-300.

40. **Li L., S. J. Wright, S. Krystofova, G. Park, and K. A. Borkovich**. 2007. Heterotrimeric G protein signaling in filamentous fungi. Annual Review of Microbiology **61**:423-52.

41. **McCudden C. R., M. D. Hains, R. J. Kimple, D. P. Siderovski, and F. S. Willard**. 2005. G-protein signaling: back to the future. Cellular and Molecular Life Sciences **62**:551-77.

42. **Metodiev M. V., D. Matheos, M. D. Rose, and D. E. Stone**. 2002. Regulation of MAPK Function by Direct Interaction with the Mating-Specific G α in Yeast. Science **296**:1483-6.

43. **Pandey A., M. G. Roca, N. D. Read, and N. L. Glass**. 2004. Role of a Mitogen-Activated Protein Kinase Pathway during Conidial Germination and Hyphal Fusion in *Neurospora crassa*. Eukaryotic Cell **3**:348-358.

44. **Park G., S. Pan, and K. A. Borkovich**. 2008. Mitogen-activated protein kinase cascade required for regulation of development and secondary metabolism in *Neurospora crassa*. Eukaryotic Cell **7**:2113-22.

45. **Perkins D. D.** 2004. *Neurospora*: The Organism Behind the Molecular Revolution. Genetics **168**:1105-9.

46. **Posas F., S. M. Wurgler-Murphy, T. Maeda, E. A. Witten, T. C. Thai, and H. Saito**. 1996. Yeast HOG1 MAP kinase cascade is regulated by a multistep phosphorelay mechanism in the SLN1-YPD1-SSK1 "two-component" osmosensor. Cell **86**:865-75.

47. **Roca M. G., J. Arlt, C. E. Jeffree, and N. D. Read**. 2005. Cell Biology of Conidial Anastomosis Tubes in *Neurospora crassa*. Eukaryotic Cell **4**:911-919.

48. **Roux P. P., and J. Blenis**. 2004. ERK and p38 MAPK-Activated Protein Kinases : a Family of Protein Kinases with Diverse Biological Functions. Microbiology and Molecular Biology Reviews **68**:320-344.

49. **Turner G. E., and K. A. Borkovich**. 1993. Identification of a G protein α subunit from *Neurospora crassa* that is a member of the G_i family. The Journal of Biological Chemistry **268**:14805-11.

50. **Wilson S., D. J. Bergsma, J. K. Chambers, A. I. Muir, K. G. Fantom, C. Ellis, P. R. Murdock, N. C. Herrity, and J. M. Stadel**. 1998. Orphan G-protein-coupled receptors: the next generation of drug targets? British Journal of Pharmacology **125**:1387-92.

51. **Yang Q., and K. A. Borkovich**. 1999. Mutational activation of a $G\alpha_i$ causes uncontrolled proliferation of aerial hyphae and increased sensitivity to heat and oxidative stress in *Neurospora crassa*. Genetics **151**:107-17.

52. **Yang Q., S. I. Poole, and K. A. Borkovich**. 2002. A G-Protein β Subunit Required for Sexual and Vegetative Development and Maintenance of Normal Gα Protein Levels in *Neurospora crassa*. Eukaryotic Cell. **1**:378-390.

53. **Yu J.-H.** 2006. Heterotrimeric G protein signaling and RGSs in *Aspergillus nidulans*. Journal of Microbiology **44**:145-54.

54. **Zhang Y., R. Lamm, C. Pillonel, S. Lam, and J. R. Xu**. 2002. Osmoregulation and fungicide resistance: the *Neurospora crassa os-2* gene encodes a HOG1 mitogen-activated protein kinase homologue. Applied and Environmental Microbiology. **68**:532-538.

Chapter 2: Chemical genomics approach to study signal transduction in
Neurospora crassa.

I. Introduction

Chemical genomics is a powerful tool that is analogous to genetic mutation leading to information regarding gene function (31). Using small molecules, this discipline endeavors to study biological processes by delving into protein function. The small molecule can act as an agonist or an antagonist against its protein target to affect cellular processes. For example, chemical genomics has been used to target specific protein kinases for inhibition, leading to understanding of cellular processes (4). Also, polyamides have been designed to easily penetrate cell membranes to bind specific DNA sequences, inhibiting gene expression (12). Finally, chemical genetics has demonstrated that small molecules can be used to understand function of proteins by taking advantage of natural pharmacogenetic (individual genetic makeup that influences affect of a drug) variation in organisms (46).

Just as there is the concept of forward genetics (random mutagenesis followed by gene identification) and reverse genetics (mutation of a specific gene and phenotypic characterization), a similar concept exists in chemical genomics. David Spring illustrates this point by comparing chemical genomics with traditional genetics where forward chemical genomics, using a small molecule screen on an organism to investigate a particular phenotype is analogous to random mutation (38). On the other hand, reverse chemical genomics involves using small molecules on a protein target of interest. This

can be analogous to mutation of a specific gene (38). The interesting protein is purified

and assayed against the small molecule by using an expression system that can be

measured. A caveat to this approach is that a small compound might interact with its

protein target, but when put into the cell, it could also interact with other cellular

components, diminishing or obscuring its original effect on the target protein.

A "chemical intervention" coupled with genetic interference is doubly powerful. In

this scenario, the desired phenotype is displayed by the mutant. The screen would then

be to identify the chemical that changes either of the two phenotypes: mutant or wild-

type. Cutler and McCourt (2005) explain this scenario using the traditional genetic

analysis of "Phenotype = Genotype + Environment" (9); they point out that the chemical

"hit" can be a factor of the environment. Therefore, not only can the chemical "hit"

complement the mutation, but it can also reveal functions for a gene in an aphenotypic

mutant.

A. Advantages of chemical genomics

There are several advantages to using chemical genomics: it can be used to induce

biological effects rapidly and even reversibly (due to metabolism of the small compound)

(21). For this to occur in traditional genetics, a conditional allele of the gene must be

identified (such as a temperature-sensitive mutant), a difficult task (38). Also, it can be

used to study the development of an organism at different stages of growth. For example,

a small molecule screen on zebrafish was used to find small molecules that can modulate

the developmental processes of this model organism (35).

If a gene is deleted, then all of the functions of the resultant protein are lost. However, with chemical genomics, instead of turning up or down the expression of a particular protein, a finer control of the protein can be achieved by modulating just one of its functions (22). Small molecules have the potential to target only one function of that protein by binding to a particular domain (40); hence, only one aspect of that protein is blocked while the others are left operative.

Sometimes, a gene deletion does not lead to a phenotype due to the redundancy of the system; there may be duplicated functions among genes of the same class within the genome. However, a small molecule that targets one of the gene products could theoretically affect others with same function due to the similarity of a shared domain. This is the case with kinase inhibitors that bind to ATP-binding pocket (45). Structures of the ATP-binding pockets are conserved, so that ATP-competitive inhibitors have a broad-range of interactions.

Chemical genomics also gives great temporal control (40); for cell-based assays, the media containing the small molecule can simply be washed out and replaced. In cases where the compound does not bind irreversibly to the protein target, the cell can reverse to the original phenotype once the chemical is removed from the environment.

Finally, doing research with small molecules can lead to new drug discovery. In fact, chemical genomics is a sibling of the discipline of pharmacology that first searched for biologically active small molecules (7, 11). Also, chemical genomics supplements pharmacology by determining the mode of action of drugs (18). The advent of

combinatorial chemistry and the explosion of the molecular genetics revolution led the burgeoning field of chemical genomics to follow pharmacology (17).

B. Difficulties associated with chemical genomics

Chemical genomics is not without its share of disadvantages. The main issue is that a chemical that has a direct effect on the organism of study must be found. This may require screening many small-compound libraries. And even then, success is not guaranteed. Advances in combinatorial chemistry have provided a staggering number of small molecules (43). However, the size of the library is not a guarantee that a "hit" can be found. The of diversity in the chemical library is of paramount importance (5). If assembled without careful scrutiny and forethought, a chemical library may include only a small subset of unique compounds that are capable of being bioactive. Libraries for the academic scientist can be purchased from companies that provide them as bio-active compounds derived from nature or by diversity-oriented synthesis (DOS) (38). Natural product libraries have a proven track record in that they are solely composed of bioactive compounds. These can range from chemicals such as lovastatin (derived from *Aspergillus terreus*) that lowers LDL cholesterol (2) to taxol (derived from the Pacific Yew (*Taxus brevifolia*), an important anticancer drug that works by interrupting microtubule systems (34). A disadvantage of libraries composed solely of natural products is that purification of these products is extremely difficult. Hence, oftentimes a mixture is being marketed. As for commercial libraries, their disadvantage is that the compounds included are of limited structural diversity (6). The solution is to combine different libraries in order to achieve a diverse chemical space (29); chemical space is

defined as "total descriptor space encompassing all possible small organic molecules that are possible for creation (including those present in biological systems)" (14).

Also, there's the problem of "lack of generality" in chemical genomics; drugs found so far only cover a small subset of all proteins residing in the cell (37). On the other hand is the problem of "selectivity". A small molecule with a biological activity must not show significant promiscuity against other targets. This is especially true in the case of proteins that share homology. In order to circumvent this problem, structural complexity of the compound must increase in order to increase the specificity of interaction with the desired protein (29).

Cell permeability of a small molecule is an issue that needs to be empirically determined. A commonly held rule is Lipinski's 'Rule of 5': a small molecule should have no more than 5 H-bond donors, less than 10 H-bond acceptors, have a molecular weight of less than 500, have Log P (partition coefficient) value of less than 5, and compound classes that act as substrates for biological transporters are exceptions (28). However, designing compounds with such restrictions are difficult, and much more so in libraries constructed using combinatorial chemistry.

A disadvantage of the organism screening method (although it is simpler to set up) is that even though a chemical hit has been identified that is showing the phenotype of interest, the target of this protein is still unknown. To complicate the matter even more, the interacting partner may not be a protein (42).

A way to alleviate the problem of finding a chemical that has a biological activity against the protein of interest or a particular phenotype is using high-throughput

screening (HTS). This is a process where many different compounds are tested using the same biological test for their effect on the cellular process of interest (40). Usually, it involves automating the screening process so that a massive number of compounds can be checked at a fast rate in order to find the "hit".

C. Research strategy

Neurospora crassa grows asexually by producing conidia that separate from the conidiophores attached to the main colony (41). There are many factors that influence conidiation: limiting carbon or nitrogen environment, blue-light, oxygen level or desiccation and the circadian rhythm (15, 39). However, it is clear that the wild-type strain does not conidiate in submerged conditions when there are ample nutrients in the liquid medium (26). Interestingly, loss of the Gα-subunit GNA-3 leads to inappropriate conidiation, whereby the fungus forms conidiophores and chains of conidia under submerged conditions, even with ample nutrients (26).

The purpose of this experiment was three-fold: 1) identify a chemical that would either correct the inappropriate conidiation phenotype of Δ*gna-3* or cause the wild-type strain to exhibit inappropriate conidiation when exposed to the chemical (thus targeting the conidiation pathway), 2) identify a novel chemical that would have a fungicidal effect on *Neurospora crassa* (possibly leading to new class of fungicides), and 3) identify a chemical that would have a significant phenotype (that can be readily observed under the screening conditions).

Using the results from this chemical screening, the goal is to shed light into the signaling pathway of *Neurospora crassa*, mainly the conidiation pathway. By

discovering a compound that affects conidiation, the mechanism by which the fungus initiates this process can be better understood. Without GNA-3, *N. crassa* conidiates profusely (26). If a chemical "hit" can be found, is it preventing inappropriate conidiation by interacting with a downstream effector that is negatively regulated by GNA-3 in a wild-type strain? Another aspect of this research is from an applied perspective: fungal pathogens cause an enormous amount of crop damage, and the asexual spore is their main mode of dispersal (1). Hence, a conidiation inhibitor could result in a better understanding of this mechanism, possibly leading to a chemical solution.

And, if possible, the ultimate goal is to find the target of the "hit" and figure out its mode of action.

II. Materials and Methods

A. Chemicals tested

ChemBridge Microformat library (Cambridge Corporation, San Diego, CA) is a diverse small-compound library, housed at UC Riverside Core Facility, that has been aliquoted into 96-well PCR plates for ease of use using the Beckman Biomek 200 fluid-handling robot. A common approach is to store the compounds in 100% DMSO, with low humidity at -20°C so that the chemicals stay in solution (16). Chemical library was aliquoted 2μl of the original library to a new plate with the addition of 18μl of 100% DMSO by a former student in the lab (Susan Won) and stored in the Borkovich lab freezer at -20°C. Since solubility data were not available for each compound, the

chemical library was aliquoted into DMSO (13), a solvent commonly used in pharmaceutical research to keep small molecules in solution (28). The advantages of DMSO—readily crossing the biological membrane, co-transport of non-ionized molecules of low molecular weight (25), and freezing point of 18˚C (16)—make it a convenient solvent for chemical screening.

The Spectrum Collection library (Microsource Discovery Systems, CT, USA), another library at UC Riverside, was also screened. This library is a collection of known drugs, bioactive compounds, and natural products that have been identified previously. This library was screened with the help of Mr. Mike Qin, an REU (Research Experience for Undergraduates) student from UC Berkeley who interned in the Borkovich lab during the summer of 2008. This library was aliquoted to a set of 96-well PCR plates utilizing pintools designed for minute liquid handling and also the Beckman Biomek 200 fluid-handling robot. Using pintools (96 pins oriented to fit a PCR plate), 0.4 μl of chemical was aliquoted from the original library stock into a PCR plate with each well containing 9.6 μl of 100% DMSO (sterile), diluting the chemical stock from 10mM to 400μM concentration.

Finally, five compounds previously reported to have a phenotypic effect on fungi were also gathered and screened to see if they had an effect on *N. crassa* for the phenotypes in question (See table 1). First, 2-(4-hydroxyphenyl) ethanol (also known as tyrosol) is a quorum-sensing molecule identified in *Candida albicans*, an opportunistic, dimorphic, pathogenic yeast (8); tyrosol stimulates formation of germ-tubes in this fungal pathogen when added to a freshly exchanged medium. Quorum-sensing, a mechanism by

which the microorganism can gauge the size of the collective population, is due to

extracellular chemical signals produced in response to increasing density of the cell

population (36). Tyrosol is continuously released by the fungus to gauge its cell density

(8). When a threshold level of tyrosol is detected in the environment, then *C. albicans*

can sense this change and convert to a yeast form. Second, 3,4-dimethoxycinnamic acid

is a self-inhibitor of conidia germination of rusts (uredospores) (33). Third, farnesol is a

chemical with much biological activity across many fungal groups. In *C. albicans*,

farnesol (a regulator of quorum-sensing) blocks the transition from yeast to filamentous

growth (24); hence, it has the opposite biological effect as that of tyrosol. In *Aspergillus*

niger (a non-yeast-like fungus), farnesol was shown to inhibit conidiation in plate

cultures (30). Also, it was shown that cAMP levels were greatly diminished after

treatment, a most interesting phenomenon since Δ*gna-3* deletion mutant of *N. crassa* also

leads to low levels of cAMP (due to low levels of adenylyl cyclase protein) (26).

Farnesol was shown to inhibit growth of *Saccharomyces cerevisiae* by interfering with

the phosphatidylinositol-type signaling during cell cycle progression (32). Finally,

salicylic acid is a mild fungal-growth retardant exuded by the plant (23).

B. Phenotypic assay

A forward, chemical genetic screen was designed using *N. crassa* as the test

organism. For each chemical, both wild-type and Δ*gna-3* strains would be tested against

it (See Table 2 for all strains tested in this research). Finally, since 'inappropriate

conidiation' requires liquid culturing, and that the other 2 phenotypes examined in this

chemical screening experiment could be conducted in liquid culture also, it was decided that screening *N. crassa* in VM-liquid medium would be most ideal.

Both wild type and Δ*gna-3* strains were inoculated onto VM-agar media in a sterile 125 ml Erlenmeyer flask with a foam plug. These flasks were incubated at 30˚C in the dark for 2 days and then moved to room temperature with a 12 hour photoperiod. After 3 more days of incubation, the conidia from these flasks were collected with sterile water by agitation (via a vortexer) and filtered through sterile layer of shop towel (Chix masslin; Benson, NC) to remove all tissue types except conidia. After counting the conidial concentration using a hemacytometer, a concentrated, conidial stock was prepared so that the final concentration of 1×10^6 conidia/ml in the test medium could be prepared.

1. Preliminary experiments

To determine which culturing format would be best for optimal growth of the fungus with the effective amount of the chemical, preliminary tests were conducted. This involved using cell-culture plates of different dimensions: 96-well, 48-well, and 24-well plates. Initially, 350 µl of standard VM liquid-medium was used for growing *N. crassa*. Onto each plate was placed a pair of negative controls (wild-type and Δ*gna-3*) where instead of supplying the chemical, 100% DMSO (same amount) was added. The plate was fastened to the plate holder inside a shaker set at 30˚C, 200 rpm, dark conditions. Initially, after 16 hours of incubation, 20 µl of hyphal suspension was pipetted (using a pipet with tip cut off with scissors) onto a microscope glass, covered with coverglass, and examined under a compound microscope at 40X. From this experiment, it was

determined that the 24-well plate showed the most consistent results, with the wild type strain not conidiating and Δ*gna-3* conidiating inappropriately. Hence, it was decided that all future screens would be conducted using a 24-well plate with 150µl of VM liquid-medium per well (Greiner Bio-One, Monroe, NC). See Figure 1 for a diagram of the screening process. A plastic lid was used to cover the plates in order to prevent dessication during incubation. The plate was incubated in the platform shaker for 16 hours at 30˚C, 200rpm in the dark. The next day (after the 16 hour incubation), the plate was removed from the platform shaker and observed under the dissecting microscope at maximum zoom (5.6X) for various phenotypes: activation/prevention of inappropriate conidiation, suppression of growth, or miscellaneous morphological abnormalities. If a well exhibited one of the forementioned phenotypes, then it was noted for a secondary screening.

2. Chemical concentrations

Small molecules from the Cambridge ExpressPick library were tested at range of 5 µM to 10 µM concentration. The Microsource Spectrum Bioactive compounds library were tested at 10 µM concentration. For the small molecules found from reviewing the literature, tyrosol, 3,4-dimethylcinnamic acid, farnesol, and salicylic acid were tested at various concentrations, including 10 µM, 7.5 µM, 5 µM, and 2.5 µM.

C. Follow-up experiments

For the compounds from the chemical library, those small molecules that had an effect on either the wild-type strain, Δ*gna-3*, or both, were tested again under identical conditions to ensure that the experiment was reproducible. Only then were the individual

compounds purchased in small amounts (usually 1 mg) from the Chembridge hit2lead
website (www.hit2lead.com), an affiliate of Chembridge corporation, or from
SigmaAldrich (www.sigmaaldrich.com). With the newly acquired compound, the
experiment was performed again, but with the following modifications: the experiment
was scaled up to a 1ml volume using a borosilicate glass test-tube (13 x 100mm) under
the same environmental conditions. This was repeated 3 times to ensure reproducibility
of the effect of the small molecule on *N. crassa*.

Also for the compounds from the chemical library, after identification of the "hit",
analogs of the small molecule were checked to see if they also had activity. The analogs
were identified by ChemMine, an online database resource for bioactive chemical
discovery projects that was created at UC Riverside
(http://bioweb.ucr.edu/ChemMineV2/) (19). Under the same screening conditions, these
analogs were tested to see if they had similar biological activity and also if their effect
was stronger. Identifying an analog with similar biological activity could potentially lead
to association of a chemical motif that both the analog and the original "hit" shares, that
is ultimately responsible for the biological activity.

III. Results

Approximately 4880 compounds from the Chembridge Small-Compound
ExpressPick library previously aliquoted and stored in the Borkovich lab freezer (-20°C)
were screened using the screening method described above. Table 1 summarizes the list
of compounds from the Chembridge ExpressPick library that were identified as "hits"

during the 1st and 2nd screening. A conidiation inhibitor of Δ*gna-3* was identified during this screening. It is annotated as compound # 6238725 in the Chembridge library (Figure 2). This small molecule had no effect on wild-type strain but inhibited the submerged conidiation phenotype of Δ*gna-3*. Using ChemMine, 49 compounds were identified when a similarity search was conducted with compound #6238725. These compounds were subsequently screened to determine whether their structural similarity conferred similar biological activity as #6238725. Unfortunately, none of the compounds had any effect on wild-type or Δ*gna-3* strains.

Chemical #6238725 was tested for prevention of conidiation in submerged conditions on the heterotrimeric G protein mutants Δ*gna-1,* Δ*gna-2,* Δ*gnb-1*, and Δ*gng-1*. With the exception of Δ*gna-2*, all were previously shown to inappropriately conidiate in submerged cultures. None of the mutants exhibited inhibition of conidiation with the addition of compound #6238725. These results suggested that compound #65238725 is fairly specific for a target in the conidiation signaling pathway uniquely mediated by GNA-3 and not by other heterotrimeric G-proteins.

To determine whether a certain motif of the compound was the actual ligand, compounds were tested that contained each portion of the molecule connected by the ester bridge in the middle of the compound #6238725: these are veratrole (1,2-dimethoxybenzene) and 4-methoxybenzaldehyde (Figure 2b & c). These were tested under the same experimental conditions to check for their ability to prevent conidiation. However, neither chemical had an effect on *N. crassa*.

Finally, another aliquot of the chemical purchased from Chembridge hit2lead website (www.hit2lead.com) was tested. However, it did not behave like the original compound from the stock library; it had no effect in preventing submerged conidiation. The newly purchased chemical was tested by mass spectrometry (UCR Core Facility) to determine if it had the same molecular weight as the compound designated in the original chemical library (Figure 3). Even though the mass spec results showed that the molecular weight of the compound was 272 (same as that described in the library database), it didn't have the desired effect. Unfortunately, this prevented any further work from being conducted because the purchased compound was not a conidiation inhibitor, while the original stock from the library had run dry.

Another compound from the Chembridge ExpressPick library numbered as #5979758 was identified through the screening process. Initially, this compound completely inhibited germination, but was later shown to cause swelling of the conidia at much lower concentrations (Figure 4). Compound #5979758 caused a most unusual phenotype: strange blebbing on the surface of the conidia. From a time-course experiment, it was determined that the first appearance of the blebbing occurred at about the sixth hour after incubation, and the phenotype got steadily more severe with time (Figure 4c). Unfortunately, the exact concentration that caused this phenotype could not be ascertained because the reordered compound was not completely soluble. Dissolving in 100% DMSO, methanol, or water (even with heating) failed to get all of the compound into solution. However, approximately 10 µl of the chemical (not completely dissolved) in 1ml of VM-liquid medium was able to induce the blebbing phenotype in wild-type

strain. Since 1mg of compound #5979758 was dissolved in 1 ml of 100% DMSO (even though it does not dissolve completely), and that compound has a molecular weight of 397, the concentration would be 2.52 mM. When 10 μl of this solution was inoculated into 1 ml of VM/conidial suspension, the maximum concentration of the compound would be 25.2 μM. However, since the solubility of the compound is quite poor, it would be safer to estimate the concentration on a much lower range.

One possibility was that the blebbing was a morphological structure that the chemical induced inappropriately. I tested the hypothesis that compound #5979758 was inducing Conidial Anastamosis Tubes (CATs), which are small hyphal tubes formed by conidia and young germlings that allow fusion between neighboring cells and formation of a network. I tested the Δ*ste50* mutant, defective in CAT formation, with compound #5979758. Δ*ste50* also showed strange blebbing on the surface of its conidia and hyphae after 16 hours of germination. Other deletion mutants were also checked for the effect of compound #5979758: Δ*gna-1*, Δ*gna-2*, Δ*gnb-1*, Δ*gng-1*, Δ*ric8*: all were affected by this compound.

In order to find any additional information regarding this small molecule, scientific literatures were searched for possible reference. The only lead according to the SciFinder Chemical database (scifinder.cas.org), a molecule with 81% similarity to compound #5979758, quinazoline, 6-bromo-4-phenyl-2-(1-piperazinyl)-6-Bromo-4-phenyl-2-piperazin-1-ylquinazoline, is a quinazolinyl norepinephrine reuptake inhibitor for treatment of central nervous system disorders (Fig. 4d). It has been patented for this

purpose, but there are no other information regarding its properties. However, it was impossible to obtain this compound for testing.

An additional 1200 compounds from the Spectrum Bioactive Compounds library (Microsource, CT) were screened in 2008. The screening process was identical to the Chembridge library screening. The primary screen was conducted by an REU student who was supervised while the secondary screen was conducted collaboratively. This library contains known fungicides, and their effects were well-correlated with the screening results; hence, they served as an internal control during the screening process. Two compounds that induce conidiation in wild-type were identified from this screen: eserine and rutilantinone (Figure 5).

Eserine (physostigmine salicylate) has been previously shown to induce conidiation in the fungus *Trichoderma viride* when added to the growth medium in conjunction with acetylcholine (20). Also known as physostigmine, eserine is a cholinesterase inhibitor that is obtained from calabar beans. This chemical showed results in both the primary and the secondary screening process, but the phenotype was not reproducible when the compound was re-purchased. Also, although this library contained physostigmine sulfate (considered as an analog), this compound did not have any effect on *N. crassa.*

Rutilantin (a pyrromycin) is an antibiotic that also has antiphage activity (3), but it has not been demonstrated to have activity against fungi. The Spectrum library contained rutilantinone, a derivative of rutilantin. Li *et al*. described rutilantinone as an inhibitor of fatty acid uptake (27). Unfortunately, the purchased compound (Sigma Aldrich) had no effect on *N. crassa.*

In conclusion, excluding the known fungicides, none of the "hits" from the Spectrum library were reproducible after the primary and secondary screening. Furthermore, of the compounds found in literature that have a biological activity in other fungi (listed in Table 1), none showed any effect in *N. crassa* in the submerged culture morphology assay.

III. Discussion

One of the main goals of chemical genomics is to identify the target of the small molecule in the signaling pathway. To this end, testing on *N. crassa* has a distinct advantage: many deletion mutants are already available. By testing the effect of the "hit" on gene deletion mutants, a resistant mutant could indirectly point to the target: the mutant could be resistant because the target (deleted gene's product) is absent. Alternatively, the small molecule could be binding downstream of the pathway that the deletion is in.

Chemical genomic screening is very difficult. Speaking with first-hand experience, testing is fraught with difficulties. In order to conduct a perfect screen, many factors must come together to ensure that false positives are minimized and that true "hits" are not passed over during the screening process. When dealing with forward screens, it is crucial that the organism used is amenable to the particular phenotypic assay that it is used for.

An issue that came up several times during the chemical screening was that of consistency. The reliability of the screening could be jeopardized if care is not taken into

consideration. This is especially true when dealing with organism screening; experimenting on organisms means another variable is added to the mix. It still is not known why the chemical "hits" behaved so erratically during the primary and the secondary screening or why the purchased compounds did not display the identical phenotype as the compound from the stock. One possibility is that the library could have been contaminated. Another is that during the synthesis process, a completely pure compound was not created, leading to contaminants that piggybacked with the desired molecule. Such occurrences can lead to false positives that end in ambiguous results and lack of reproducibility (44).

Another factor to take into consideration is that since the original chemical library has been used by several other groups, there's no guarantee that the compound designated to be in that well on a particular plate is what you are getting. Contamination problems can puzzle the true identity of the biologically active molecule.

It was a huge disappointment to learn that the purchased compound #6238725 did not behave as that from the Chembridge library. One lesson to take away from this experience is that the original small-molecule from the library should immediately be analyzed once it is confirmed to be a "hit". This action prevents waste of time and effort, averting future headaches. Unfortunately, depending on when you use the library, a compound could be present in a low amount so that it is not possible to analyze it chemically.

The one bright light in this research was finding a consistent "hit", compound #5979758. So far, the target of compound #5979758 is yet unknown. Consequently, no

mutant has been discovered that is resistant to the compound. Continuing to screen more

deletion mutants could yield one that is resistant to the compound. However, it is a long

process and might not lead to success. Another strategy is to use an on-bead matrix

approach (10). This chemical method would involve modifying the "hit" so that it can be

tethered to a resin and incubated with whole cell extract of *N. crassa*. Then, the

immobilized chemical-protein complex can be separated from the rest of cell extract,

protein removed from the bead, and identified by tandem mass-spectrometry.

Figure 1. Diagram of the screening process. a) The chemical screening is carried out in a 24-well cell culture plate. 150µl of VM liquid-medium is pipetted into each well and inoculated with wild-type strain conidia at $1x10^6$ conidia/ml (alternate rows are inoculated with Δ*gna-3* conidia at the same concentration). Each chemical is tested pairwise on both wild-type and Δ*gna-3* strain. A pair of wells (wild-type and Δ*gna-3*) are reserved for the controls: 100% DMSO is pipetted into the wells instead of the chemical from the library. After all wells are inoculated, the plates are covered with the plastic lid and incubated at the following conditions: 16 hours, 200 rpm, 30°C, dark. b) Plates are examined under the dissecting microscope at 5.8X magnification. Each well is visually checked for presence of conidia/conidiophores. The results are noted; any chemicals that cause a phenotype in either the wild-type strain or Δ*gna-3* are arranged for the secondary screening. c) When a sufficient number of potential "hits" are discovered through the primary screening, then a secondary screening is conducted in the exact same manner as a).

a.

negative control
(DMSO only)

1st chemical
screened

wild-type

Δgna-3

wild-type

Δgna-3

Incubation conditions:
30˚C, 200rpm, dark

b.

negative control
(DMSO only)

1st "hit"
re-screened

2nd "hit"
re-screened

wild-type

Δgna-3

wild-type

Δgna-3
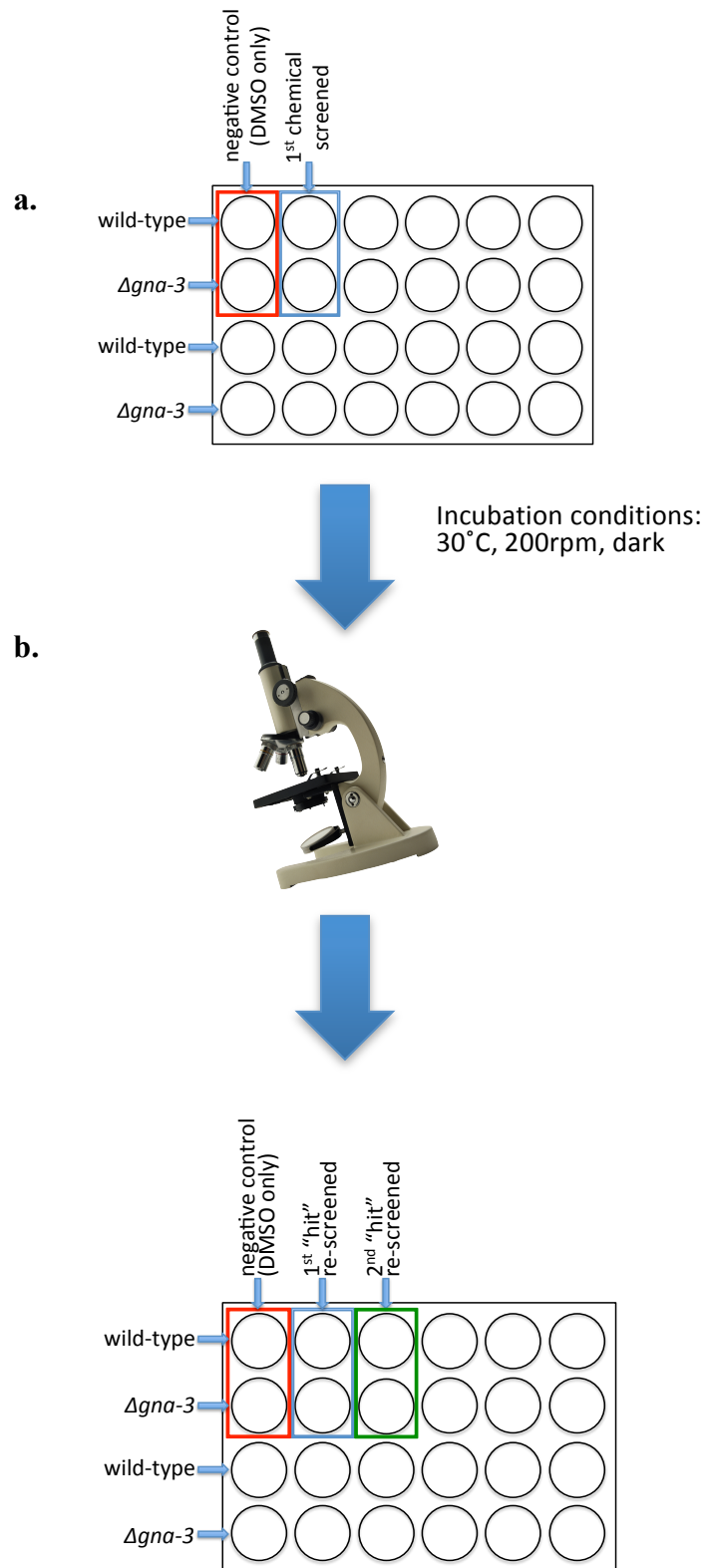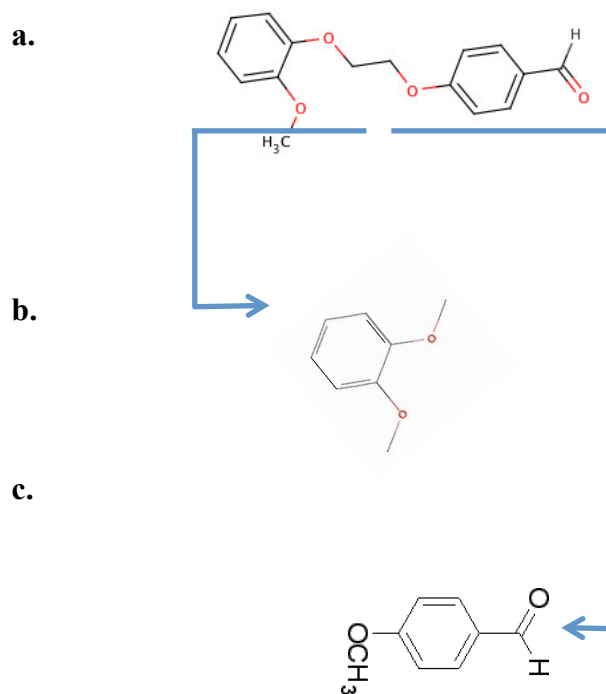
Figure 2. Analysis of compound #6238725 from the Chembridge ExpressPick library. a) Chemical structure of the compound #6238725 from Chembridge ExpressPick library. In the initial screens, this compound showed promise as a conidiation inhibitor of Δ*gna-3*. Two possible derivatives of compound #6238725 were ordered and tested under same conditions (Their structures are shown in b. and c.). b) Structure of veratrole (1,2-dimethoxybenzene), an analog of compound #6238725. Veratrole did not have any effect on Δ*gna-3*. c) Structure of 4-methoxybenzaldehyde, another analog of compound #6238725. This compound also failed to correct inappropriate conidiation in Δ*gna-3*.

Figure 3. Mass Spectrometry data of compound #6238725 re-purchased from Chembridge. a) Top chromatogram indicates the presence of compound #6238725 (indicated with an asterisk). The bottom chromatogram indicates the blank. b) This is a magnified portion of the chromatogram indicating the representative peak of the compound #6238725. It is the region boxed in blue of the top chromatogram of (a). c) This is a magnified portion of the top chromatogram in (a) that is not representative of compound #6238725 and yet is not present in the negative control chromatogram. It seems to indicate contamination with other compounds beside #6238725.

a.

272-Kim

1: TOF MS ES+
BPI
7.00e3

(b) (c)

*

29.50
151.05

29.83
151.05

33.87
313.23

34.26
313.24

19.34
182.17

25.54
433.17

18.00
102.08

8.15
149.01

11.80
149.01

21.35
149.01

47.81
149.01

50.34
149.01

54.34
149.01

272-control

1: TOF MS ES+
BPI
3.74e3

19.34
182.17

35.92
149.01

35.79
149.01

30.76
415.17

27.01
256.27

25.17
226.16

36.34
149.01

18.20
102.08

35.64
149.01

24.71
149.01

8.65
149.01

12.67
149.01

31.55
149.01

40.10
285.23

42.26
637.25

47.11
149.02

49.91
149.01

51.57
149.01

54.81
149.01

Time

b.

273.0840

387.1595

152.0719

274.0924

295.0720

388.1718

429.0779

m/z

c.

272-Kim 1513 (32.893)

313.2401

271.0729

331.2555

348.2858

353.2448

151.0637

358.3431

445.0854

702.1577

m/z

Figure 4. Compound #5979758 from Chembridge ExpressPick library. a) Chemical structure of compound #5979758. b) Swelling phenotype of compound # 5979758 on wild-type conidia using dark-field light microscopy @ 40X. c) Effect of compound #5979758 on wild-type strain after 6 hours of incubation. d) Quinazoline, 6-bromo-4-phenyl-2-(1-piperazinyl)-6-Bromo-4-phenyl-2-piperazin-1-ylquinazoline. This molecule shares 81% similarity to compound #5979758 and is also biologically active.

a.
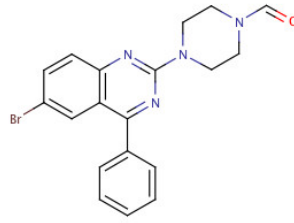
b.
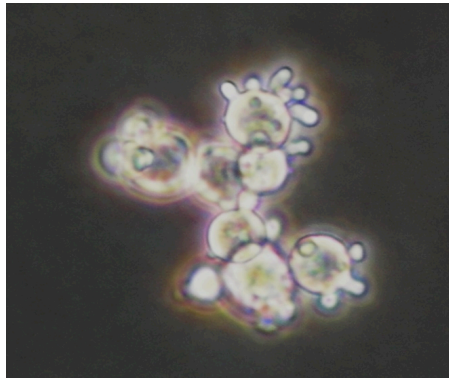
c.
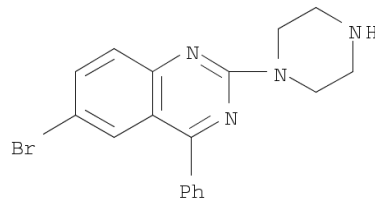
d.
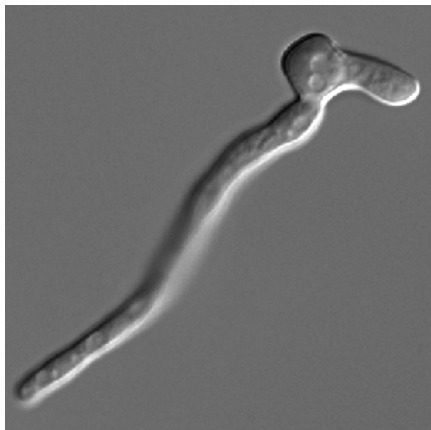
Wild Type, untreated   Wild Type, treated
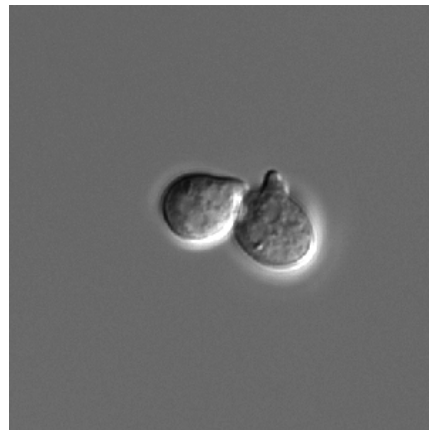
a.
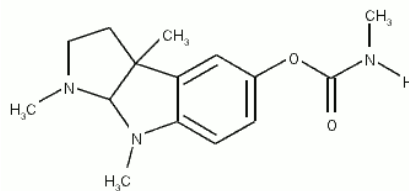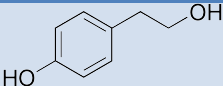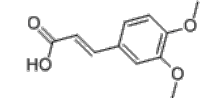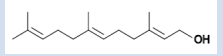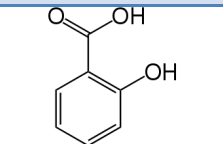
b.
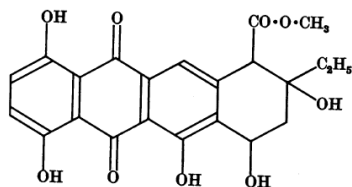
Figure 5. Chemical structures of (a) eserine and (b) rutilantinone identified as conidiation inhibitors of the Spectrum Bioactive Compounds library. In the primary and secondary screening, these two compounds inhibited inappropriate conidiation of Δ*gna-3*. However, when the compounds were purchased separately, they no longer showed any biological activity.
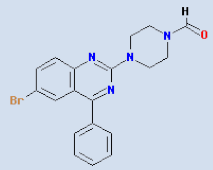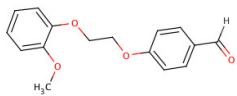
Table 1. Compounds with biological activity in other fungi included in the screening. Although they were shown to have an effect in other fungi, none had any biological activity on *N. crassa*, under the conditions tested.

Name	Molecular Weight	Formula	Structure	citation	Effect on fungus
2-(4-hydroxyphenyl) ethanol (tyrosol)	138.166	$C_8H_{10}O_2$		Chen et al., 2004	Quorum sensing molecule in *Candida albicans*
3,4-dimethoxycinnamic acid	208.2106	$C_{11}H_{12}O_4$		Macko et al., 1972	Self-inhibitor of conidia germination of rusts (uredospores)
farnesol	222.37	$C_{15}H_{26}O$		Hornby et al., 2001 Lorek et al., 2008	In *Candida albicans*, farnesol (a regulator of quorum-sensing) blocks change from yeast to filamentous growth transition In *Aspergillus niger*, farnesol was shown to inhibit conidiation on plate culture
salicylic acid	138.12	$C_7H_6O_3$		Medina, 2003	Mild fungal-growth retardant exuded by the plant

Table 2. *Neurospora crassa* **strains used in these experiments.**

Borkovich lab strain #	Strain	Relevant genotype	Comments	Source/reference
541	wild type	wild type	74A-OR23-1A (74A), FGSC #987	FGSC
276	Δ*gna-1*	Δ*gna-1::hph$^+$*	Δ*gna-1* homokaryon	
2216	Δ*gna-2*	Δ*gna-2::hph$^+$*	Δ*gna-2* homokaryon	
479	Δ*gna-3*	Δ*gna-3::hph$^+$*	Δ*gna-3* homokaryon	
360	Δ*gnb-1*	Δ*gnb-1::hph$^+$*	Δ*gnb-1* homokaryon	
650	Δ*gng-1*	Δ*gng-1::hph$^+$*	Δ*gng-1* homokaryon	
1811	Δ*ric8*	Δ*ric8::hph$^+$*	Δ*ric8* homokaryon	Sara Wright
2333	Δ*ste50*	Δ*ste50::hph$^+$*	Δ*ste50* homokaryon	James Kim

Table 3. Hits identified from screening the Cambridge ExpressPick library. Only compound #5979758 showed same activity in subsequent purchases from the manufacturer.

Phenotype	Compound ID#	Results	Chemical Structure
No germination of both wild-type and Δ*gna-3*	5979758	1	
Inhibition of conidiation in Δ*gna-3*	6238725	1	
Conidiation in wild-type	None	None	None

REFERENCES

1. **Agrios G. N.** 2005. Plant Pathology, 5th ed. Academic Press, San Diego, CA.

2. **Alberts A. W.** 1988. Discovery, biochemistry and biology of lovastatin. The American Journal of Cardiology **62**:10J-15J.

3. **Asheshov I. N., and J. J. Gordon**. 1961. Rutilantin: an antibiotic substance with antiphage activity. The Biochemical Journal **81**:101-4.

4. **Bishop A. C., J. A. Ubersax, D. T. Petsch, D. P. Matheos, N. S. Gray, J. Blethrow, E. Shimizu, J. Z. Tsien, P. G. Schultz, M. D. Rose, J. L. Wood, D. O. Morgan, and K. M. Shokat**. 2000. A chemical switch for inhibitor-sensitive alleles of any protein kinase. Nature **407**:395-401.

5. **Brenk R., A. Schipani, D. James, A. Krasowski, I. H. Gilbert, J. Frearson, and P. G. Wyatt**. 2008. Lessons learnt from assembling screening libraries for drug discovery for neglected diseases. ChemMedChem **3**:435-44.

6. **Burke M. D., and S. L. Schreiber**. 2004. A planning strategy for diversity-oriented synthesis. Angew. Chem. Int. Ed. **43**:46-58.

7. **Cases M., and J. Mestres**. 2009. A chemogenomic approach to drug discovery: focus on cardiovascular diseases. Drug Discovery Today **14**:479-85.

8. **Chen H., M. Fujita, Q. Feng, J. Clardy, and G. R. Fink**. 2004. Tyrosol is a quorum-sensing molecule in Candida albicans. Proceedings of the National Academy of Sciences of the United States of America **101**:5048-52.

9. **Cutler S., and P. Mccourt**. 2005. Dude, Where's My Phenotype? Dealing with Redundancy in Signaling Networks. Plant Physiology **138**:558-559.

10. **Das R. K., A. Samanta, W. Xu, D. Su, C. Leong, K. Ghosh, D. Zhai, and Y. T. Chang**. 2011. Target Identification : A Challenging Step in Forward Chemical Genetics. Interdisciplinary Bio Central **3**:1-16.

11. **Dean P. M.** 2007. Chemical genomics: a challenge for de novo drug design. Molecular Biotechnology **37**:237-45.

12. **Dervan P. B., and R. W. Bürli**. 1999. Sequence-specific DNA recognition by polyamides. Current Opinion in Chemical Biology **3**:688-93.

13. **Di L., and E. H. Kerns**. 2006. Biological assay challenges from compound solubility: strategies for bioassay optimization. Drug Discovery Today **11**:446-51.

14. **Dobson C. M.** 2004. Chemical space and biology. Nature **432**:824-8.

15. **Dunlap J. C., and J. J. Loros**. 2004. The *Neurospora* circadian system. Journal of Biological Rhythms **19**:414-24.

16. **Engeloch C., U. Schopfer, I. Muckenschnabel, F. Le Goff, H. Mees, K. Boesch, and M. Popov**. 2008. Stability of screening compounds in wet DMSO. Journal of Biomolecular Screening **13**:999-1006.

17. **Frearson J. A., and I. T. Collie**. 2009. HTS and hit finding in academia-from chemical genomics to drug discovery. Drug Discovery Today **14**:1150-8.

18. **Giaever G.** 2003. A chemical genomics approach to understanding drug action. Trends in Pharmacological Sciences **24**:444-6.

19. **Girke T., L. C. Cheng, and N. Raikhel**. 2005. ChemMine . A Compound Mining Database for Chemical Genomics. Plant Physiology **138**:573-577.

20. **Gressel J., L. Strausbauch, and E. Galun**. 1971. Photomimetic Effect of Acetylcholine on Morphogenesis in *Trichoderma*. Nature **232**:648-649.

21. **Guengerich F. P.** 2000. Metabolism of chemical carcinogens. Carcinogenesis **21**:345-51.

22. **Haggarty S. J., K. M. Koeller, J. C. Wong, C. M. Grozinger, and S. L. Schreiber**. 2003. Domain-selective small-molecule inhibitor of histone deacetylase 6 (HDAC6)-mediated tubulin deacetylation. Proceedings of the National Academy of Sciences of the United States of America **100**:4389-4394.

23. **Herrera Medina M.** 2003. Root colonization by arbuscular mycorrhizal fungi is affected by the salicylic acid content of the plant. Plant Science **164**:993-998.

24. **Hornby J. M., E. C. Jensen, A. D. Lisec, J. J. Tasto, B. Jahnke, R. Shoemaker, P. Dussault, and K. W. Nickerson**. 2001. Quorum Sensing in the Dimorphic Fungus *Candida albicans* Is Mediated by Farnesol. Applied and Environmental Microbiology **67**:2982-2992.

25. **Jacob S. W., and R. Herschler**. 1986. Pharmacology of DMS0. Cryobiology **27**:14-27.

26. **Kays A. M., P. S. Rowley, R. A. Baasiri, and K. A. Borkovich**. 2000. Regulation of conidiation and adenylyl cyclase levels by the Gα protein GNA-3 in *Neurospora crassa*. Molecular and Cellular Biology **20**:7693-705.

27. **Li H., P. N. Black, A. Chokshi, A. Sandoval-Alvarez, R. Vatsyayan, W. Sealls, and C. C. DiRusso**. 2008. High-throughput screening for fatty acid uptake inhibitors in humanized yeast identifies atypical antipsychotic drugs that cause dyslipidemias. Journal of Lipid Research **49**:230-44.

28. **Lipinski C. A., F. Lombardo, B. W. Dominy, and P. J. Feeney**. 2001. Experimental and computational approaches to estimate solubility and permeability in drug discovery and development settings. Advanced Drug Delivery Reviews **46**:3-26.

29. **Lipinski C., and A. Hopkins**. 2004. Navigating chemical space for biology and medicine. Nature **432**:855-861.

30. **Lorek J., S. Pöggeler, M. R. Weide, R. Breves, and D. P. Bockmühl**. 2008. Influence of farnesol on the morphogenesis of *Aspergillus niger*. Journal of Basic Microbiology **48**:99-103.

31. **MacBeath G.** 2001. Chemical genomics: what will it take and who gets to play? Genome Biology **2**:1-6.

32. **Machida K., T. Tanaka, Y. Yano, S. Otani, and M. Taniguchi**. 1999. Farnesol-induced growth inhibition in *Saccharomyces cerevisiae* by a cell cycle mechanism. Microbiology **145**:293-299.

33. **Macko V., R. C. Staples, J. A. A. Renwick, and J. Pirone**. 1972. Germination self-inhibitors of rust uredospores. Physiological Plant Pathology **2**:347-355.

34. **Markman M.** 1991. Taxol: an important new drug in the management of epithelial ovarian cancer. The Yale Journal of Biology and Medicine **64**:583-90.

35. **Peterson R. T., B. A. Link, J. E. Dowling, and S. L. Schreiber**. 2000. Small molecule developmental screens reveal the logic and timing of vertebrate development. Proceedings of the National Academy of Sciences of the United States of America **97**:12965-9.

36. **Reading N. C., and V. Sperandio**. 2006. Quorum sensing: the many languages of bacteria. FEMS Microbiology Letters **254**:1-11.

37. **Spandl R. J., A. Bender, and D. R. Spring**. 2008. Diversity-oriented synthesis; a spectrum of approaches and results. Organic & Biomolecular Chemistry **6**:1149-58.

38. **Spring D. R.** 2005. Chemical genetics to chemical genomics: small molecules offer big insights. Chemical Society Reviews **34**:472.

39. **Springer M. L.** 1993. Genetic Control of Fungal Differentiation: The Three Sporulation Pathways of *Neurospora crassa*. BioEssays **15**:365-374.

40. **Stockwell B. R.** 2004. Exploring biology with small organic molecules. Nature **432**:846-54.

41. **Turian G., and N. Matikian**. 1966. Conidiation of *Neurospora crassa*. Nature **212**:1067-1068.

42. **Ward G. E., K. L. Carey, and N. J. Westwood**. 2002. Using small molecules to study big questions in cellular microbiology. Cellular Microbiology **4**:471-82.

43. **Weber L.** 2000. High-diversity combinatorial libraries. Current Opinion in Chemical Biology **4**:295-302.

44. **Yan B., L. Fang, M. Irving, S. Zhang, A. M. Boldi, F. Woolard, C. R. Johnson, T. Kshirsagar, G. M. Figliozzi, C. A. Krueger, and N. Collins**. 2003. Quality control in combinatorial chemistry: determination of the quantity, purity, and quantitative purity of compounds in combinatorial libraries. Journal of Combinatorial Chemistry **5**:547-59.

45. **Zhang J., P. L. Yang, and N. S. Gray**. 2009. Targeting cancer with small molecule kinase inhibitors. Nature Reviews. Cancer **9**:28-39.

46. **Zhao Y., T. F. Chow, R. S. Puckrin, S. E. Alfred, A. K. Korir, C. K. Larive, and S. R. Cutler**. 2007. Chemical genetic interrogation of natural variation uncovers a molecule that is glycoactivated. Nature Chemical Biology **3**:716-21.

Chapter 3: Use of ^{1}H NMR to measure intracellular metabolite levels during growth and asexual sporulation in *Neurospora crassa*

I. Introduction

The filamentous fungus *Neurospora crassa* is a model organism that has been extensively studied for over a hundred years. *N. crassa* possesses a predominantly haploid life-cycle, with 28 different cell types and three sporulation pathways (4). The genome has been sequenced (4), and knock-out mutants are available for most of its ~10,000 genes (11). Since *N. crassa* has simple nutritional requirements, being able to synthesize all cellular constituents (except for the vitamin biotin) from a medium containing simple salts, trace elements, and a carbon and nitrogen source, it is an ideal system for analysis of biochemical pathways and metabolic flux (20).

N. crassa produces a type of asexual spore, the macroconidium (referred to as a conidium) for dissemination in the environment (67). Conidiation initiates with production of aerial hyphae that rise perpendicular to the substratum (66). The tips of aerial hyphae form constrictions that eventually develop into complete crosswalls (septa) and finally sever, leading to release of the mature macroconidia. Since conidiation is a major mode of dispersal utilized by fungal pathogens (8), it also plays an important role in pathogenesis in these organisms.

Several factors have been shown to cause conidiation in *N. crassa*, including carbon or nitrogen deprivation, desiccation, heat-shock or blue light exposure. Lowering the sucrose concentration from 1.5% to 0.15% (w/v) or imposing nitrogen limitation will

cause wild type to form conidiophores in shaking submerged cultures (56, 69).

Desiccation-induced conidiation is observed when *N. crassa* is cultured on solid medium

or in standing liquid cultures (66). Heat-shocking *N. crassa* submerged liquid cultures at

46°C, followed by incubation at 25°C, causes inappropriate conidiogenesis (68). Finally,

exposing *N. crassa* to blue light induces conidiation (45). From these findings, it is

evident that conidiation is a common biological response to adverse conditions and a

means by which the fungus can reestablish itself in a more favorable environment.

A major signaling pathway that detects and responds to external signals in fungi

and other eukaryotes is mediated by heterotrimeric GTP-binding proteins (consisting of

α, β, and γ subunits) (39, 43). Briefly, binding of a ligand to a G-protein coupled

receptor (GPCR) leads to a conformational change that causes the associated Gα subunit

to exchange GDP for GTP. Consequently, the βγ-heterodimer dissociates from the Gα

protein, allowing both to interact with downstream effectors that influence cell growth

and development.

Three Gα (GNA-1, GNA-2, and GNA-3), one Gβ (GNB-1) and one Gγ subunit

(GNG-1) have been identified in *N. crassa* (37, 43). Loss of *gna-3* has dramatic effects

on conidiation, leading to production of short aerial hyphae and premature conidiation in

plate cultures and inappropriate conidiation in submerged cultures (Fig. 1) (38). The

phenotypes of Δ*gna-3* mutants are consistent with GNA-3 as a negative regulator of

conidiation in *N. crassa*. Δ*gna-3* mutants have low levels of adenylyl cyclase protein

(CR-1) and cyclic-AMP (cAMP), and Δ*cr-1* mutants produce conidiophores in

submerged cultures, revealing a link between low cAMP levels and conidiation.

59

Interestingly, supplementation of submerged cultures of Δ*gna-3* and Δ*cr-1* mutants with 2% peptone reverses the submerged conidiation phenotype (38), hinting at a nutrient-sensing function for GNA-3 and CR-1. These observations are also supported by work showing that loss of *gna-3* or *cr-1* leads to reduced mass accumulation on poor carbon sources (42).

Previous work has identified metabolites present in *N. crassa* tissues under various conditions. Most of the amino acids have been detected in cell extracts from conidia and hyphal cultures using high pressure liquid chromatography (HPLC) followed by ninhydrin staining (62-63). Alanine, glutamine and glutamate have also been quantified in intact hyphal cells using ^{15}N NMR (35). Several sugars/carbon sources have been detected in hyphal cultures, including trehalose (enzymatic detection); (21), glucose (enzymatic detection); (12), glycerol (enzymatic detection); (55), and tricarboxylic acid intermediates and organic acids (HPLC); (53).

The goals of this research were two-fold. First, we sought to determine the metabolite profile of wild-type *N. crassa* hyphae grown under high and low carbon (sucrose) conditions and conidia cultured in high sucrose. Secondly, we wanted to explore whether lack of a single gene (*gna-3*) causes a significant metabolite shift in conidia or hyphae under the same conditions used for wild type. The latter objective addresses whether the Δ*gna-3* mutant conidiates in submerged conditions due to interruption of a signal transduction relay from outside stimuli or because of a metabolic block that leads to nutrient deprivation. A metabonomics approach using ^{1}H NMR (34, 46-47, 60, 72, 74) was used to create a metabolite fingerprint of tissue extracts to

60

compare levels of amino acids and other metabolites present in wild type and the Δ*gna-3*

mutant. ^{1}H NMR was chosen as the method for recording metabolite profiles, because it

is rapid, direct, and the quantitative information from multiple metabolites in a single

experiment has been shown to correlate well with quantitative enzymatic assays in other

systems (6, 47). This was a collaboration between members of the Borkovich lab (James

Kim and Dr. Borkovich) and the Larive lab (Kayla Kaiser and Dr. Larive).

II. Materials and Methods

A. Cell Growth and Extraction of Metabolites.

N. crassa strains used in this study were wild-type ORS-SL6a (74a; *mat a*; Fungal

Genetics Stock Center #4200; Kansas City, MO) and Δ*gna-3* strain 43c2 (38) (See table

1). Tissue was collected from a total of six biological replicates for each treatment per

strain. Each strain was grown in three different types of media: Vogel's minimal medium

(VM) with 1.5% sucrose (w/v), VM with 0.15% sucrose (w/v), and VM with 1.5%

sucrose (w/v) plus 2% peptone (w/v). Solid medium contained 1% agar.

Conidia were propagated as follows. A small amount of conidia from a slant

culture was used to inoculate 50 ml of VM agar medium in a 250-ml foam-stoppered

flask. Flasks were then incubated at 30˚C in the dark for two days before being moved to

25˚C in constant light for an additional five days. Conidia that were used to inoculate

liquid cultures were collected by filtration using sterile water (20) and used immediately,

while those to be used directly for metabonomics studies were collected using Soltrol

(see below).

Glass Erlenmeyer flasks (25 ml total volume) to be used for liquid cultures were treated with dichlorodimethylsilane (5% v/v in chloroform; TCI America) in order to prevent hyphae from adhering to the inside walls of the flask, possibly leading to dessication-induced conidiation. Cultures containing 6 ml of liquid VM were inoculated with water-harvested conidia to a final concentration of 1×10^6 conidia/ml and then incubated at 30˚C with shaking at 200 RPM in the dark for 16 hours. Cultures were collected by vacuum-filtration using filter paper (Whatman #3), transferred to 2-ml screw-cap tubes and stored at -80°C until extraction.

To determine the metabolite profile of pure conidia, conidia were collected from the agar flasks described above using Soltrol® 170 isoparaffin, a nonaqueous solvent that has previously been shown to prevent germination of conidia (5). Approximately 50 ml of Soltrol was poured into the flask, the contents vortexed, and then filtered using Handi-wipe towels (autoclaved sterile) into a sterile flask. The conidial suspension was then collected on a Whatman #3 filter paper using vacuum filtration. The conidia were scraped off the filter paper using a spatula and transferred to a 2-ml screw-cap tube before freezing at -80˚C.

Similar to recent work in the filamentous fungus *Fusarium graminearum* (47), the metabolite extraction protocol used in this study was developed using Arabidopsis (33). To extract the metabolites, the frozen tissues in 2-ml tubes were pulverized using a glass rod after addition of liquid nitrogen. After the tissue reached the consistency of a fine powder, 750 μl of extraction buffer was added to each tube. The extraction buffer consisted of 1:1 (v/v) acetonitrile-d_3 (CD$_3$CN):deuterium oxide (D$_2$O) containing 50 mM

62

sodium acetate-d_3 (CD$_3$COOD), and 100 μM 3-trimethylsilylpropionic acid-d_4 sodium salt (TMSP), as a chemical shift reference (0.000 ppm). Acetonitrile (50%) has been shown to precipitate proteins without small molecule loss (3). Tissue homogenization in the presence of the extraction buffer was carried out at room temperature for 4 minutes.

Extracts were clarified by centrifugation at 2,300 x g for 5 min. and supernatants transferred to a new tube, while cellular debris was discarded. Kayla found a simple evaporation and reconstitution step provided selectivity for hydrophilic metabolites, removing broad resonances contributed by long hydrocarbon chains (which obscure the region around 0.9 ppm) alleviating spectral crowding and allowing accurate integration of resonances from aliphatic amino acids, without appreciable loss of amino acids, sugars, and nitrogen-containing metabolic intermediates (73). Extracts were evaporated using a speed vacuum overnight (16 hours) at room temperature and reconstituted in 700 μl of D$_2$O containing 100 mM CD$_3$COOD, 100 μM TMSP and 500 μM NaN$_3$ as a biocide.

Hydrophobic interferents were removed by the addition and removal of 100 μL deuterated chloroform (CDCl$_3$) at room temperature. The D$_2$O/CDCl$_3$ phases were vortexed for 60 s and the emulsion was broken by centrifugation at 2,300 x g for 5 min. This step further improved our ability to quantify organic acids (occupying the region around 1.3 ppm) by removing endogenous polar lipids (44). This protocol is summarized in Kaiser, K. A., et al. 2009 (33). The aqueous portion, in the amount of 600 μl, was transferred to a microcentrifuge tube wherein the pD of the each extract was adjusted to 7.40 ± 0.08 using deuterium chloride and sodium deuteroxide. All deuterated reagents

were from Cambridge Isotope Laboratories (Andover, MA). The solution was stored at -80˚C until measurement of metabolites by ^{1}H NMR.

^{1}H NMR. Each sample was thawed and transferred to a 5 mm NMR tube (Wilmad, Buena, NJ) for analysis. Spectra were acquired for bioreplicate samples with selective saturation of the solvent resonance using a Bruker Avance NMR spectrometer operating at 600.06 MHz. Free induction decays (FIDs) were acquired into 25860 time points and zero filled to 131072 points. A spectral width of 7716 Hz was excited using a 90º pulse. A relaxation delay of 1.5 sec. was used, and 640 scans were co-added following 16 dummy scans for a total experiment time of 34 min. The temperature of the sample was maintained at 298 K. FIDs were apodized by multiplication by an exponential function equivalent to 1.0 Hz line-broadening prior to Fourier transformation. Manual shimming was performed for each sample, and the TMSP line width at half-height after application of 1.0 Hz exponential line broadening was 2.43 + 0.16 Hz. (NMR data acquisition and analysis were aided by Kayla Kaiser and Dr. Larive.)

Metabonomics and metabolite profiling. Spectra were processed using Topspin 2.0 (Bruker, Billerica, MA), phasing was applied automatically, while baseline correction applied by manual fitting with a sine function. Conidia spectra were baseline-corrected using a cublic spline function with approximately 100 user-defined baseline points utilized in the operation. This was necessary due to residual contributions from Soltrol in the aliphatic region of the spectra, which could not be completely removed by chloroform treatment. Prior to integration, each spectrum was aligned such that the chemical shift reference (TMSP) was at 0.00 ppm. Spectra were integrated for the purpose of

metabonomics using equidistant integral regions of 0.02 ppm width over the range of 0.50 to 9.00 ppm, excluding the regions containing the resonances of solvent constituents: acetate and acetonitrile (1.96 - 2.04 ppm), and residual water (4.28 - 4.72 ppm). For metabolic profiling, a second set of integration regions were manually defined for the quantitation of well-resolved peaks. The relative amounts of metabolites present were determined by normalizing each integral to the constant sum of the NMR spectrum (48, 75). Kayla found the method of normalization to a constant sum to be superior to mass normalization (data not shown), even though approximately equal tissue weights were used in these experiments. Normalization to a constant sum better compensates for variability in the recovery of metabolites by extraction, allowing us to better apply PCA to identify metabolite abundances which are altered by the applied biological treatment(s).

Confirmation of analyte resonance assignments was made by comparison to standard solutions. NMR spectra of standards were measured using the same NMR parameters as for the extracts, except that fewer scans were required.

Statistical Analysis. The goal in this work was to record metabolic fingerprints and compare treatments for their effect on the global metabolome, therefore principal components analysis (PCA)(59)) was selected as the appropriate technique for dimensionality reduction and data visualization. PCA, an unsupervised pattern recognition method, was performed with the statistical analysis program Minitab version 15 (Minitab Inc., State College, PA) using the equidistant integrals obtained from the NMR spectra. These calculations were performed in accordance with the

recommendations of Broadhurst and Kell (7) to avoid false discoveries through aggressive cross-validation. Mean centering was applied in this study (2, 71). No scaling was applied prior to PCA.

One of our objectives was to determine whether loss of GNA-3 and/or sucrose limitation directly influences metabolite profiles. Some of our growth conditions were conidiogenic, while others supported a predominantly hyphal mycelium (Fig. 1). In order to study metabolites specifically accumulated in conidia, Soltrol® 170 isoparaffin was added to a set of conidial suspensions to prevent germination. However, residual Soltrol remaining after our extraction procedure interfered with the routine baseline correction of the NMR spectra. Because of the resonances due to residual soltrol and the different modes of baseline correction, the conidia spectra are not directly compared with the submerged culture profiles represented in Fig. 3A and 3B. Importantly, Soltrol did not affect integration and univariant analysis of many conidia metabolites in regions of the spectrum unaffected by the presence of Soltrol (Fig. 4-6).

Univariate statistical analyses (metabolite profiling) were carried out in Excel 2008 (Microsoft, Redmond, WA). Each integral region was treated as an independent variable with six replicates/treatment/strain. The Q-test was conducted to exclude up to one replicate/treatment/strain that was considered an outlier.

Identification of metabolites. Resonances were assigned to individual metabolites by comparison with spectra recorded for approximately 100 authentic metabolite standards (Sigma-Aldrich, St. Louis, MO), chemical shifts and multiplicities reported in the published literature, and also in the Madison Metabolomics Consortium

66

Database (http://mmcd.nmrfam.wisc.edu/), (15). In cases of ambiguity, a pure standard

was spiked into the fungal extract and the resulting NMR spectra were recorded (See

Table 2). For the metabolites listed in Table 2, good agreement was obtained for all the

resolved resonances of a given metabolite. Metabolite identification was performed by

Kayla and I, with confirmation by Dr. Larive.

III. RESULTS

The global metabolome of Δ*gna-3* mutants is similar to that of wild-type strains

In this study, we analyzed the endometabolome, or intracellular metabolites (32)

of *N. crassa*. Levels of extractable, water-soluble metabolites (lipids were removed)

were measured under several conditions using ^{1}H NMR. We assessed liquid cultures

from wild-type and Δ*gna-3* strains in the presence of high (1.5%) sucrose, low (0.15%)

sucrose, and 1.5% sucrose + 2% peptone (Fig. 1A,B). As previously reported, wild-type

strains produce only hyphae in high sucrose submerged cultures, but form hyphae with

associated conidia in low sucrose submerged cultures (Fig. 1A,B) (38). In contrast,

Δ*gna-3* mutants form hyphae and conidia under both high and low sucrose conditions in

submerged cultures (Fig. 1A,B) and peptone reverses the submerged conidiation

phenotype of Δ*gna-3* mutants in high sucrose (Fig. 1A,B), (38). Thus, analysis of

submerged cultures under these varied conditions could reveal a possible contribution of

altered metabolite levels in inducing conidiation as well as a role for the G-protein GNA-

3 in regulating metabolite levels in *N. crassa*. We also recorded metabolite profiles of

purified conidia harvested from wild-type and Δ*gna-3* cultures grown in solid medium

containing 1.5% sucrose. Together with the results for high-sucrose submerged cultures, these studies produce a baseline metabolome for purified conidia and vegetative hyphae from submerged cultures under high carbon growth conditions.

Six biological replicates were used to generate the initial data, with up to one outlier discarded per treatment (see Methods). Representative spectra of extracts obtained from submerged cultures of wild-type and Δ*gna-3* strains grown in high sucrose (Fig. 2) reveal both similarities and differences between the two strains; this pattern was repeated with the other treatments (see below). We examined the spectra for the presence of peaks corresponding to 102 metabolites, with a total of 21 being unambiguously identified (Table 2).

The data were subjected to PCA, an unsupervised statistical method that can be used to compare large data sets, reducing multidimensional data to two principal component axes which represent the differences between samples in a two-dimensional graphical format (59). We initially conducted PCA (Fig. 3A) omitting the peptone medium data, since peptone is a rich source of metabolites that could influence the observed clustering. The analysis revealed that principal component 1 (PC1) is responsible for 55.3% of the variance, while PC2 accounts for 24.9%. The PCA scores plot (Fig. 3A) revealed two major groupings, with separation of all samples. The grouping on the left side of the plot consisted of submerged cultures from wild type cultured on high sucrose and Δ*gna-3* mutants grown on high and low sucrose. The second grouping on the right side of the plot was wild type cultured on low sucrose. These results suggest several conclusions. First, there is a large shift in the metabolite

profile produced in wild-type *N. crassa* when cultured on high vs. low sucrose conditions. Second, the observation that Δ*gna-3* strains cultured in high and low sucrose are more similar to wild-type high sucrose than low sucrose cultures suggests that loss of *gna-3* does not have a global effect on the metabolome of *N. crassa* in adequate carbon, and that Δ*gna-3* mutants are relatively "blind" to reduced carbon levels in submerged cultures. Third, the closer grouping between conidiating Δ*gna-3* strains and non-conidiating (high sucrose) rather than conidiating (low sucrose) wild-type cultures suggests that any effect of the Δ*gna-3* mutation on conidiation does not involve large changes in the metabolome.

The results from the PCA scores plot that included peptone-supplemented cultures (Fig. 3B) reinforced the conclusions of the initial analysis. This plot revealed two major groupings; the first, on the left side of the plot, contained separable clusters for wild-type and Δ*gna-3* high sucrose submerged cultures. The second grouping on the right side of the plot consisted of both strains cultured in high sucrose plus peptone. The results from peptone-supplemented cultures suggest that, analogous to the observations in high sucrose medium, Δ*gna-3* strains have a metabolome similar to wild type and/or that small molecules in the nutrient-rich peptone have a dominant effect on the metabolic profile that obscures any effect due to the Δ*gna-3* mutation.

The Soltrol solvent used to isolate conidia was present as an interference in the aliphatic region (0.8 ~ 1.1ppm) of the NMR spectra of conidia extracts. Therefore, the conidial samples were not directly compared with other treatments by multivariate analysis (PCA), and only univariate statistical analyses of metabolites from conidia were

performed.

It has been postulated that "metabolic network robustness" in a gene knockout results from gene redundancy and alternate metabolic pathways (40). The PCA scores plots (Fig. 3) are consistent with this premise, as the overall global metabolome does not significantly change with loss of *gna-3*. This could be due to the presence of the other two Gα subunits (GNA-1 and GNA-2) in the *N. crassa* genome. Loss of *gna-1* also leads to inappropriate conidiation, although a higher cell density is required ($3x10^6$ conidia/ml). Furthermore, mutation of *gna-2* in the Δ*gna-3* background leads to more severe effects on submerged conidiation and overall growth (37). Thus, the observed overlapping roles of Gα subunits may explain the overall similarity in the metabolomes of Δ*gna-3* and wild-type strains.

Initial research design included a treatment with the conidiation inhibitor MPEB that was identified in a chemical screen (detailed in chapter 2) at 10 μM concentration in VM + 1.5% sucrose. However, the data generated did not make sense in that metabolite levels did not correlate with either conidiating or non-conidiating conditions. For example, levels of trehalose were much lower in both strains than in that of any other hyphal tissue. Also, mannitol levels were even higher than conidiating tissues for both strains. Hence, data relating to treatment with conidial inhibitor were not included in the overall metabonomics research. Instead, it is included as Appendix 1.

Levels of individual metabolites differ in Δ*gna-3* and wild type

Although PCA analysis showed that the metabolomes were comparable in wild-type and Δ*gna-3* strains, visual inspection of the NMR spectra revealed significant

70

changes in several metabolites between treatments and also between strains (Fig. 2; Fig. 4). Stacking of the spectra was used to identify changes in metabolite levels and to assess reproducibility of replicates (Fig 2; Supplementary Fig. 1). Taking into account all sample preparation steps, relative standard deviations (RSD) of ~10% were observed between bioreplicates, which is comparable to the most widely used GC/MS metabolomics method of Fiehn, O., et al. (24) who reported 8% RSD. The work of Dieterle, F., et al. (22) demonstrates that with a sample size of 4000+ bioreplicates, relative standard deviations on the order of 7% could be achieved for creatinine, a proposed "housekeeping metabolite" using NMR-based metabolomics in small mammals. A majority of the amino acids and a number of sugars were cataloged, as well as other metabolites (see below). In many cases, supplementation of cultures with peptone led to elevation of amino acid levels, presumably because peptone is a rich source of amino acids (Fig. 5).

Amino acids and related metabolites

Alanine, glutamate and glutamine. Alanine serves as a convenient reservoir of amino groups and pyruvate during nitrogen and carbon sufficiency. Alanine is made from glutamate by reverse transamination (35) and can be converted back to glutamate by alanine transaminase. Glutamine is synthesized from glutamate by glutamine synthetase (18).

The results from our analysis validate earlier reports that alanine is the most abundant amino acid in *N. crassa* hyphal cultures, followed by glutamate and glutamine (35, 63). In wild type, the NMR spectra show that alanine and glutamate levels are

elevated in high vs. low sucrose (Fig. 5). In Δ*gna-3* strains, the same trend is observed

for alanine, while glutamate levels are relatively similar under high and low carbon

conditions. For glutamine, levels in both strains are not appreciably influenced by carbon

availability. However, the relative glutamine amount is higher in Δ*gna-3* mutants than in

wild type cultured on low sucrose medium. This effect cannot be explained by the

greater conidiation of Δ*gna-3* strains, as conidia from Δ*gna-3* mutants have the lowest

relative levels of glutamine detected in the six biological treatments.

On a relative basis, conidia have much lower levels of alanine and glutamine than

hyphae. Glutamate amounts in Δ*gna-3* conidia are similar to those in hyphal cultures,

whereas levels in wild-type conidia are significantly less. The relative levels of these

three amino acids roughly correlate with those measured in conidia in a previous study

(62). Furthermore, our results demonstrating that alanine, glutamate, and glutamine are

some of the most abundant amino acids in conidia support earlier work showing that

levels of these three compounds constituted nearly 70% of free amino acids in conidia

(Fig. 5) (62).

Aspartate and asparagine. Aspartate can be synthesized from the citric acid

cycle intermediate oxaloacetate using aspartate aminotransferase (50). Evidence for

synthesis of aspartate in a pathway involving catabolism of glutamate using glutamatic

acid decarboxylase during conidial germination has been obtained (10). Asparagine is

produced by transamination of aspartate (50). Since levels of aspartate and asparagine

varied greatly among the biological replicates for high and low sucrose cultures,

conclusions can only be drawn for conidia and high-sucrose peptone-supplemented

cultures. With the exception of Δ*gna-3* high sucrose peptone cultures, where asparagine could not be detected, relative levels of aspartate and asparagine are similar in wild-type and Δ*gna-3* strains and are much greater in peptone-supplemented cultures than in conidia (Fig. 5).

Serine and glycine. Serine is formed from 3-phospho-hydroxypyruvate, which in turn is derived from glycerate-3-phosphate, a metabolic intermediate of glycolysis (1). Glycine is then produced from serine by serine hydroxymethyltransferase (14). We detected serine in wild-type strains grown in high sucrose, low sucrose or the presence of peptone, and in Δ*gna-3* mutants cultured in high and low sucrose (data not shown). However, it was not possible to reliably quantify serine levels because overlap of the serine resonance with the shoulder of the much more intense trehalose peak at 3.88 ppm made integration unreliable. Serine could not be detected in conidia isolated from wild-type and Δ*gna-3* strains or in peptone-treated cultures of Δ*gna-3* (data not shown).

Glycine could only be detected and quantified in the Δ*gna-3* strain grown in peptone-supplemented medium (Fig. 5).

Threonine, valine, leucine and isoleucine. Threonine is derived from glycine and serine and, along with pyruvate, is a direct precursor to isoleucine (19, 58). Pyruvate is a precursor of valine, and leucine is formed from the last intermediate in the valine biosynthetic pathway (19, 58). Although they are formed from different initial substrates, the pathways for synthesis of isoleucine and valine share four enzymes (19, 58).

Under high-sucrose conditions, relative levels of threonine are comparable in wild-type and Δ*gna-3* submerged cultures (Fig. 5). However, the relative threonine

amount is greater in wild type, but not in Δ*gna-3* strains, under low sucrose conditions. This suggests that *gna-3* is required for increased threonine in response to poor carbon availability. Peptone supplementation did not significantly affect relative threonine levels. Finally, threonine levels are much greater in conidia from the Δ*gna-3* mutant than from wild type (Fig. 5).

Relative valine levels are not affected by sucrose in submerged cultures from the two strains (Fig. 5). Similar to the results for threonine, valine amounts are slightly higher in conidia from the Δ*gna-3* mutant than in wild type. Relative valine levels are highest in peptone-supplemented cultures (Fig. 5).

Leucine was only detected in low-sucrose wild-type cultures and peptone-supplemented cultures from both strains (Fig. 5). Interestingly, although isoleucine could not be detected in high or low sucrose submerged cultures from the Δ*gna-3* strain, Δ*gna-3* conidia possessed the highest relative levels of isoleucine detected in our study (Fig. 5). In wild type, the isoleucine amount was low in high sucrose cultures, and greater and similar in low sucrose, high-sucrose peptone-supplemented cultures and conidia (Fig. 5). Finally, peptone-supplemented cultures from Δ*gna-3* strains had isoleucine amounts comparable to wild type. The results for Δ*gna-3* strains suggest that GNA-3 is required for isoleucine production in submerged cultures, but not under peptone supplementation or in conidia.

Arginine and ornithine. Ornithine is produced in the mitochondrion and then transported into the cytoplasm to serve as a precursor for arginine and polyamine synthesis (19). In *N. crassa* cultured on minimal medium, >98% of cellular arginine and

74

ornithine are stored in the vacuole. Arginine or nitrogen starvation results in release of stored arginine and ornithine into the cytoplasm, where these compounds can be used for protein synthesis and/or as nitrogen sources (70).

Comparison of high vs. low sucrose demonstrates that the arginine level decreases slightly in wild type, while Δ*gna-3* mutants show the opposite trend (Fig. 5). Levels of arginine are highest in peptone-supplemented cultures. Relative levels of ornithine are similar in wild-type and Δ*gna-3* submerged cultures (Fig 5), with lesser amounts in low vs. high sucrose. Ornithine could not be detected in peptone-supplemented cultures (Fig. 5). The results for ornithine are consistent with positive regulation of this amino acid by sucrose levels in the growth medium in both strain backgrounds.

Arginine and ornithine could not be detected in conidia from either strain. The observation of lower arginine levels in conidia vs. hyphae is consistent with results from previous work (62) and also supported by the hypothesis (70) that arginine is metabolized to glutamate during conidiation, and then eventually converted back into arginine after conidial germination.

Lysine. Lysine is synthesized using the α-aminoadipate pathway in *N. crassa* (54), with the majority of lysine utilized for protein synthesis (31). Our results demonstrate that sucrose deprivation leads to an almost two-fold increase in lysine levels in wild-type submerged cultures (Fig. 4). Lysine amounts are similar in peptone-supplemented cultures of both strains. Lysine could not be detected in low-sucrose Δ*gna-3* cultures or in conidia from either wild-type or Δ*gna-3* strains (Fig. 5).

Tyrosine. In *N. crassa*, tyrosine, phenylalanine and tryptophan are produced from the shikimate pathway (18). Tyrosine is synthesized starting with conversion of chorismate to prephenate by chorismate mutase, and then prephenate to tyrosine by prephenate dehydrogenase (18-19). Tyrosine is a precursor to the secondary metabolite DOPA-melanin, through a pathway involving the enzyme tyrosinase (41). In our study, tyrosine levels were very low in submerged cultures and this amino acid could only be quantified in conidia of both wild-type and Δ*gna-3* strains (Fig. 5). The relatively high levels of tyrosine in conidia suggest a function for this amino during conidial biogenesis and/or germination.

Amino acids that could not be quantitated and/or detected. Amino acids that could not be detected and/or quantitated in our studies were serine (as mentioned above), cysteine, histidine, methionine, phenylalanine, proline and tryptophan.

Sugars and related metabolites

Trehalose and glucose. Previously published studies have shown that metabolites that can be readily used as carbon sources, such as glutamate and trehalose, are found in dormant spores of *N. crassa* (62). A role for trehalose as a thermal protectant has been established for *N. crassa* (57). This previous work also demonstrated that although trehalose is a large component of the metabolite pool in conidia, relative levels in of trehalose are similar in conidia and hyphae of wild-type strains.

In our study, we observed that relative levels of trehalose are greater in high sucrose submerged cultures compared to all other submerged cultures from wild type (Fig. 6). In contrast, relative trehalose amounts are similar in high and low-sucrose

76

submerged cultures of Δ*gna-3* strains, with lower levels under peptone-supplementation (Fig. 6). The results for high and low sucrose submerged cultures are consistent with a defect in nutrient sensing for the Δ*gna-3* strains.

Relative glucose levels are higher in low-sucrose relative to high-sucrose submerged cultures for both wild-type and Δ*gna-3* strains (Fig. 6). Still lower relative amounts are found in peptone-supplemented cultures (Fig. 6).

Our attempts to measure relative amounts of trehalose and glucose in conidial extracts were unsuccessful due to residual enzymatic activity of trehalase, which we did not observe in hyphal extracts (data not shown). Trehalase is known to be extremely stable in solution, at a range of temperatures and within a wide pH range (23). Levels of trehalose are high in fungal conidia and activation of trehalase has been shown to accompany conidial germination in numerous fungi (16-17, 30). Previous studies have demonstrated that ungerminated conidia contain the highest levels of trehalase detected during *N. crassa* development (28), effectively priming conidia for germination and colonization.

Fumarate. Fumarate is an intermediate of the citric acid cycle. In our study, it could not be detected in high or low sucrose submerged cultures from either strain or in peptone-supplemented cultures from Δ*gna-3* mutants (Fig. 6). There was wide variation in fumarate amount in the biological replicates for peptone-supplemented cultures from wild type. Fumarate levels were similar in conidia from both Δ*gna-3* and wild-type strains (Fig. 6).

Mannitol. Mannitol is an abundant sugar alcohol in fungal tissue that is derived from fructose (65). In wild type, relative mannitol levels are greater in low sucrose than in high sucrose submerged cultures (Fig. 6). In contrast, the relative mannitol amount in Δ*gna-3* mutants is similar in high and low sucrose cultures and greater than levels detected in wild type submerged cultures (Fig. 6). Conidia of both wild-type and Δ*gna-3* strains contain the highest relative levels of mannitol detected in our studies (Fig. 6). Taken together, these results reveal a positive correlation between the proportion of conidia in a culture and the relative level of mannitol.

Miscellaneous metabolites

Adenosine. Adenosine is a precursor of AMP, ADP and ATP and the second messenger cAMP (52). We observed that adenosine levels were similar in all three submerged cultures of wild type (Fig. 7). Relative adenosine levels exhibited high variability in high-sucrose cultures of the Δ*gna-3* mutant. Levels in low sucrose cultures were lower than those observed in wild type, while adenosine amount in peptone-supplemented cultures was similar to wild type (Fig. 7). Relative adenosine levels were similar in conidia from wild-type and Δ*gna-3* strains and were greatly reduced relative to levels in submerged cultures.

Allantoin. As a small molecule (158.12 MW) with four nitrogen atoms, allantoin is an ideal nitrogen storage compound (13). Allantoin is an intermediate in purine catabolism and can be utilized as a nitrogen source after sequential degradation to urea and then ammonium (49). We could not detect allantoin in high sucrose cultures +/- peptone of either strain or in low-sucrose Δ*gna-3* cultures (Fig. 7). Relative allantoin

78

amounts are the highest in low sucrose submerged cultures and conidia from wild-type strains, with lower levels observed in Δ*gna-3* conidia (Fig. 7).

In *S. cerevisiae*, allantoin is stored as a nitrogen reserve during starvation (49). Our results are also consistent with a storage function in *N. crassa* conidia, with allantoin being sequestered in conidia and possibly serving as a nitrogen reserve for germination. In contrast to wild type, the presence of lower relative allantoin levels in Δ*gna-3* samples, suggests that loss of GNA-3 disrupts the normal storage mechanism, particularly in submerged cultures that produce conidia.

Choline. Choline is an important component of cellular membranes (29). We noted that choline is present at similar levels in wild-type and Δ*gna-3* strains cultured on high sucrose (Fig. 7). However, in low sucrose conditions, relative levels of choline are much higher in wild-type strains. Relative choline levels in conidia from both strains are similar and are higher than those in high-sucrose submerged cultures. Peptone supplementation results in marked elevation of choline in Δ*gna-3* cultures (Fig. 7).

Data from previous mRNA profiling experiments support metabolite profiling results for several amino acids

An earlier study by Kasuga et al., 2005 (36) used long-oligomer microarray profiling to detect transcript levels for 3366 predicted genes in wild-type *N. crassa* during a time course of conidial germination. Among the analyzed genes are numerous loci encoding amino acid biosynthetic and degradative enzymes. We took advantage of this dataset by comparing levels of amino acids that could be detected and quantified in wild-type conidia and high-sucrose submerged cultures to the corresponding available mRNA

levels for amino acid metabolic genes in conidia and at various times during germination. Within these constraints, we were able to analyze pathways for nine amino acids: threonine, glutamate, glutamine, ornithine, arginine, lysine, valine, isoleucine and tyrosine (Table 3). In general, the mRNA and metabolic profiling data correlate. In most instances, transcript levels for amino acid biosynthetic genes increase during conidial germination (usually within 0.5-1 h), and this is reflected in higher levels of the relevant amino acid in hyphae relative to ungerminated conidia (Table 3). The only exceptions are isoleucine and tyrosine, where levels of these amino acids are lower in hyphae than in conidia. However, metabolism of isoleucine is complicated by the sharing of four enzymes with valine biosynthesis, as well as inhibition of the first common enzyme (acetolactate synthase) by valine, but not isoleucine (19). In the case of tyrosine, this amino acid shares several intermediates with phenyalanine, tryptophan and the vitamin p-aminobenzoic acid (25-27) and is a precursor for DOPA melanin (41). Finally, transcripts for genes that metabolize glutamate, glutamine and arginine to other compounds are also upregulated during conidial germination (Table 3).

Results from a study that used Northern analysis to measure mRNA expression further validate our metabolite profiling results for arginine and ornithine levels in wild-type conidia and hyphae (61). This work showed that mRNA levels for *arg-2* (encoding the small subunit of arginine-specific carbamoyl phosphate synthetase, required for arginine and ornithine biosynthesis; (19)) are low in conidia and then become elevated during germination (51).

IV. DISCUSSION

To our knowledge, this is the first report of profiling *N. crassa* metabolites using ^{1}H NMR. The advantage of ^{1}H-NMR is that an entire cellular "snapshot" of metabolites can be produced from a single experiment, thus allowing comparative global analysis of multiple strains and growth conditions. We first determined whether there were large differences in the metabolomes in a non-targeted approach using PCA analysis, and then turned to identification of specific metabolites using relative integrals of resolved resonances. To our knowledge, we are the first to report relative quantitation of several metabolites, including allantoin and mannitol, in *N. crassa*.

Schmit and Brody previously conducted a metabolic study with *N. crassa* in which they measured levels of amino acids and other compounds in conidia and hyphae of wild type using column chromatography and detection with ninhydrin (62). Overall, our results are consistent with this earlier work, validating the accuracy of the two methods for metabolite profiling of *N. crassa*. However, there were some differences in the results obtained using the two methodologies. Proline, methionine, and cysteine could not be detected in conidia and levels were very low in hyphae in the Schmit and Brody study. We could not detect these three amino acids in either conidia or hyphae. Schmit and Brody reported that the predominant amino acids in conidia were glutamate, alanine, and glutamine, with glutamate in greatest abundance. Similar results were obtained in our experiments, except that glutamate and alanine were present at similar levels in conidia. Schmit and Brody also found that ornithine and arginine amounts were lower in conidia than in hyphal cultures; this trend was also noted in our study, except

that ornithine and arginine could not be detected in conidia.

Our extraction method produced hyphal extracts that were stable for more than 105 min of incubation at room temperature prior to acquiring spectra. The same was true for conidial extracts, with the exception of trehalose, glucose and citrate (data not shown). Citrate levels were too low to quantitate in any sample in our analysis. We were unable to quantitate the other two sugars in conidia, due to apparent metabolism of trehalose to glucose, which resulted in large errors for these two compounds in our univariate analysis (data not shown). Future experiments to measure trehalose and glucose levels in conidia will require an alternative extraction method, possibly that recently reported by Lowe *et al.*, 2010 (47).

PCA analysis revealed somewhat surprising results, in that although Δ*gna-3* mutants produce conidia under all growth conditions (with the exception of peptone), they did not group with low-sucrose, conidiating wild-type cultures on the scores plot, but instead clustered near wild type high-sucrose cultures. This suggests that the Δ*gna-3* mutation does not have a global effect on the metabolome in high sucrose conditions. However, major differences were observed in the PCA analysis for wild type and Δ*gna-3* mutants cultured in limiting sucrose. Taken together, these data and those from previous work in our group (42) suggest that GNA-3 regulates carbon sensing and conidiation using different pathways. One interpretation is that without GNA-3, *N. crassa* will initiate conidiation, but at the same time will not be able to sense available carbon and so will metabolically resemble a strain cultured in abundant carbon.

As mentioned above, conidiation and conidial germination in *N. crassa* are

influenced by nutrient availability (63), and changes in the levels of several intracellular metabolites have been reported during these processes. We inspected our data for metabolite(s) that correlated with (1) sucrose level in the growth medium, (2) the Δ*gna-3* mutation or (3) the presence of conidia. There were three metabolites that associated with low or high sucrose in submerged cultures of both wild-type and Δ*gna-3* strains: alanine, ornithine and glucose. Alanine and ornithine are positively correlated, while glucose amount varies inversely with sucrose levels in the growth medium.

There were several metabolites that could be associated with the Δ*gna-3* mutation, but not under all growth conditions. Relative threonine levels are higher in wild type than in Δ*gna-3* strains under low sucrose conditions. Isoleucine cannot be detected in high or low-sucrose submerged cultures from Δ*gna-3* mutants. Leucine cannot be detected and levels of adenosine and choline are low in low-sucrose Δ*gna-3* submerged cultures. The observation of lower metabolite levels in Δ*gna-3* mutants cultured on limiting carbon hints at a requirement for *gna-3* in response to poor carbon availability.

Regarding metabolites that were associated with conidiation, we noted that the sugar alcohol mannitol was elevated in tissues that contain conidia, with highest levels in ungerminated conidia (Fig. 5). Mannitol has been proposed to play roles as a carbohydrate reserve in environmental stress tolerance and during conidiation in the wheat pathogen fungus *Stagonospora nodorum* (64-65). In the insect pathogenic fungus *Metarhizium anisopliae*, mannitol is the most abundant metabolite in conidial extracts (9).

Reduced carbon level signals to the fungus that the immediate environment is no longer suitable for sustained vegetative hyphal growth and that a new location must be sought to ensure survival in more favorable surroundings. In the absence of a mating partner, this is accomplished by conidiation and the subsequent spread of mature spores by animals or wind currents in many species of filamentous fungi. The Δ*gna-3* mutant appears to possess two defects. First, Δ*gna-3* strains are deficient in a negative control mechanism for conidiation that is independent of major changes in metabolite levels. Second, Δ*gna-3* mutants are lacking in the ability to detect abundant sucrose in growth media. These malfunctions suggest that GNA-3 plays separate roles in the signal transduction cascades responsible for conidiation and nutrient sensing in *N. crassa*.
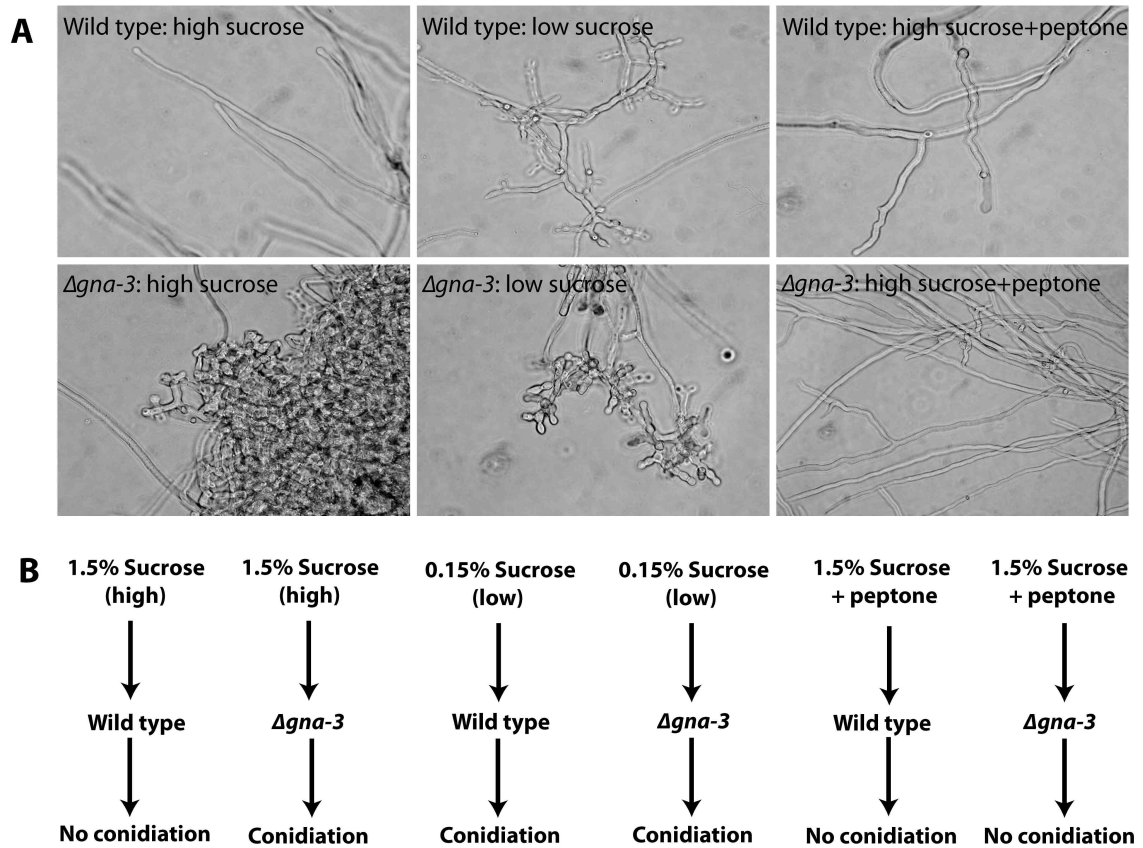
Figure 1. Submerged culture phenotypes
    A. Morphology of submerged cultures. Cultures were grown in high or low sucrose +/- peptone, as indicated in the figure. Photos were taken after 16 hr of growth. Conidia are indicated with arrows.
    B. Summary of treatments used for submerged cultures. The strains and media used to grow cultures, as well as the final conidiation phenotype, are indicated.

Table 1. The strains used for the metabonomics research project.

Borkovich lab strain #	Strain	Relevant genotype	Comments	Source/ reference
1749	wild type	wild type	74A-ORS-SL61 (74a), FGSC #4200	FGSC
479	Δgna-3	Δgna-$3::hph^+$	Δgna-3 homokaryon; 43c2	

Table 2. Metabolites Examined in this Study. These metabolites were run as a standard or checked in the MMCD database for their NMR signature and compared with the spectra of *N. crassa*.

[1]+ , metabolite could be detected at least one sample; -, metabolite could not be detected in any sample.
[2]+ , metabolite could be quantified in at least one sample where it was detected; -, metabolite could not be quantified in any sample where it was detected.
[3]NA, Not Applicable.
[4]MMCD, Madison Metabolomics Consortium Database, University of Wisconsin, Madison

Metabolite	Source of Standard	Detected[1]	Quantified[2]
Abscisic acid	This Study	-	NA[3]
Acetaldehyde	"	-	NA
Acetate	"	-	NA
Adenosine	"	+	+
Adenosine diphosphate	"	-	NA
Adenosine monophosphate	"	-	NA
Adenosine triphosphate	"	-	NA
Alanine	"	+	+
α-ketoglutarate	"	-	NA
Arginine	"	+	+
Arginosuccinate	"	-	NA
Ascorbate	"	-	NA
Asparagine	"	+	+
Aspartate	"	+	+
β-alanine	"	-	NA
Biotin	"	-	NA
Choline	"	+	+
Citrate	"	+	-
Citrulline	"	-	NA
Cyclic adenosine monophosphate	"	-	NA
Cysteine	"	-	NA
Cytidine	"	-	NA
Erythrose-4-phosphate	MMCD[4]	-	NA
Ethanol	This Study	-	NA
Flavin adenine dinucleotide	"	-	NA
Folic acid	"	-	NA
Fructose	"	-	NA
Fructose-1,6-diphosphate	MMCD	-	NA
Fructose-6-phosphate	This Study	-	NA
Fumarate	"	+	+
Fucose	"	-	NA
Galactose	"	-	NA
γ-aminobutyric acid	"	-	NA
γ-hydroxybutyrate	"	-	NA
Gibberellic acid	"	-	NA
Gluconate	This Study	-	NA

Metabolite	Source of Standard	Detected[1]	Quantified[2]
Glucose	"	+	+
Glucose-1-phosphate	MMCD	-	NA
Glucose-6-phosphate	This Study	-	NA
Glucuronate	"	-	NA
Glutamate	"	+	+
Glutamine	"	+	+
Glycerol	MMCD	-	NA
Glycerol-3-phosphate	"	-	NA
Gycine	This Study	+	+
Glyoxylate	"	-	NA
Guanosine triphosphate	"	-	NA
Guanosine	"	-	NA
Guanosine triphosphate	"	-	NA
Gulonate	This Study	-	NA
Histidine	"	+	+
Homocysteine	"	-	NA
Indole acetic acid	"	-	NA
Isocitrate	"	-	NA
Isoleucine	"	+	+
Lactate	"	-	NA
Lactose	"	-	NA
Leucine	"	+	+
Lysine	"	+	+
Malate	"	-	NA
Maltose	"	-	NA
Mannitol	"	+	+
Mannose	"	-	NA
Methionine	"	-	NA
Myoinositol	"	-	NA
Nicotinamide adenine dinucleotide	"	-	NA
Nicotinic acid	"	-	NA
Ornithine	"	+	+
Oxaloacetate	"	-	NA
Phenylalanine	"	+	-
Phosphoenolpyruvate	"	-	NA
3-Phosphoglycerate	"	-	NA
6-Phosphogluconate	MMCD	-	NA
Proline	This study	-	NA
Putrescine	"	-	NA

Metabolite	Source of Standard	Detected[1]	Quantified[2]
Pyruvate	"	+	-
Raffinose	"	-	NA
Ribose	"	-	NA
Ribose-5-phosphate	This Study	-	NA
Salicylic acid	"	-	NA
Sarcosine	"	-	NA
Serine	"	-	NA
Shikimate	"	-	NA
Spermidine	"	+	-
Stearate	"	-	NA
Succinate	"	-	NA
Succinic semialdehyde	"	-	NA
Sucrose	"	-	NA
Threonine	"	+	+
Thymidine	"	-	NA
Trehalose	"	+	+
Tryptophan	"	-	NA
Tyrosine	"	-	NA
Uridine	"	-	NA
Uridine-5-monophosphate	"	-	NA
Urea	"	-	NA
Valine	"	+	+
Xylose	"	-	NA
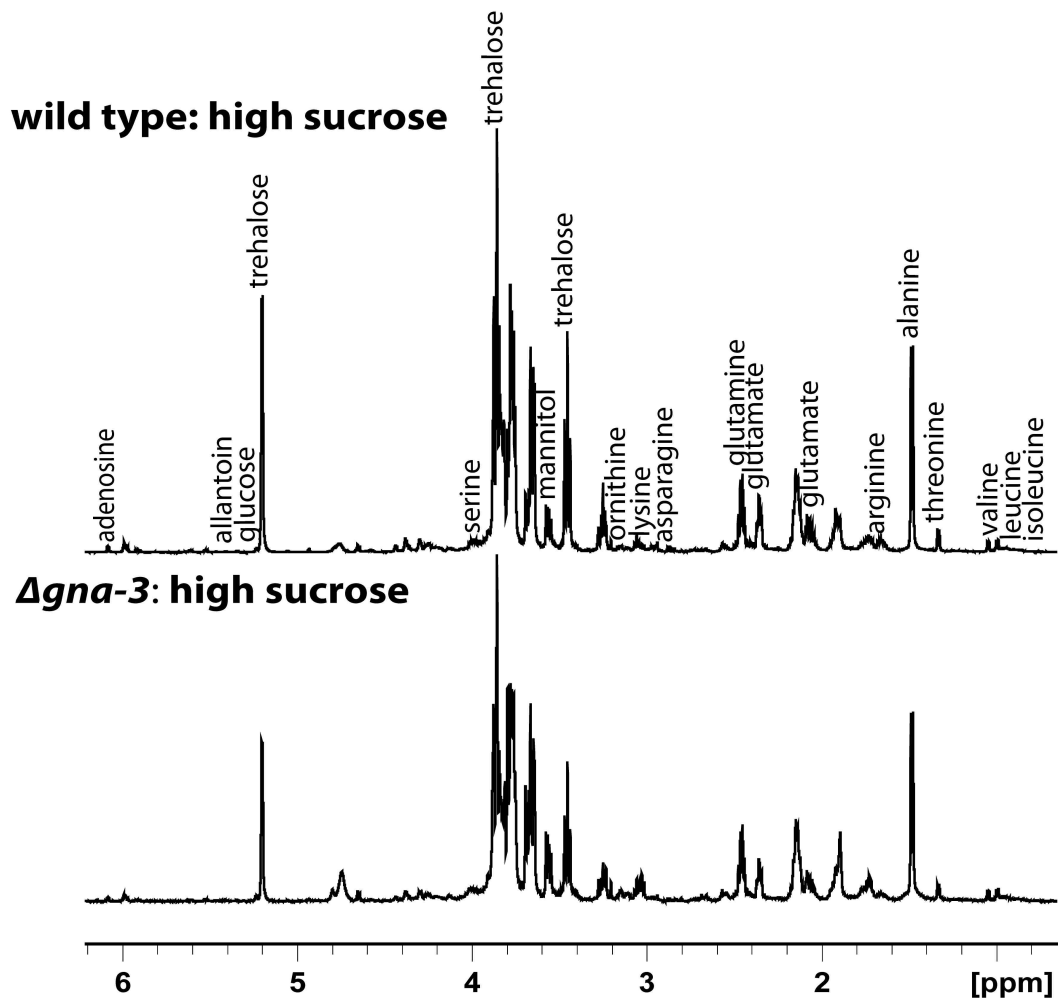
Figure 2. Representative ¹H-NMR spectra for extracts of wild type and Δ*gna-3* submerged cultures
Strains were cultured in high sucrose medium for 16 hr and metabolites extracted as described in the methods. Major identified peaks are labeled.
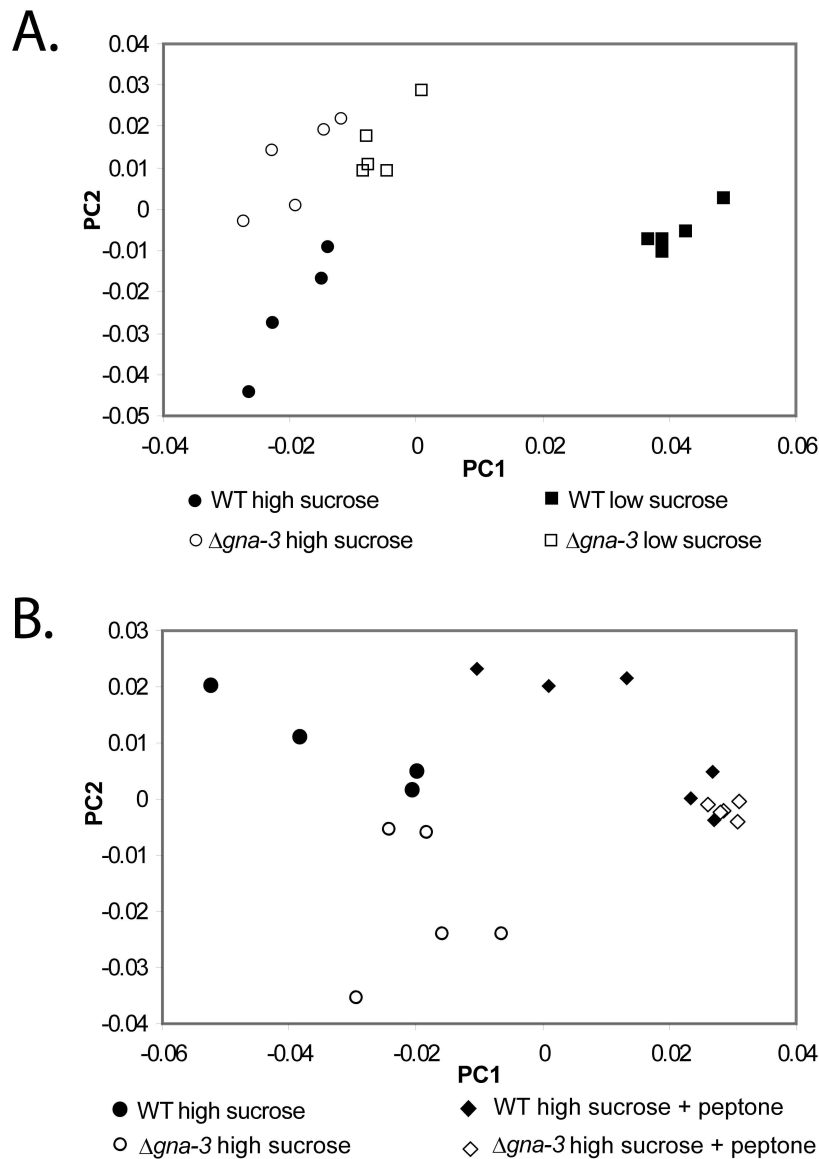
Figure 3: Principal components analysis (PCA) scores plot
A. Low and high sucrose cultures. PCA analysis of relative integrals from ^{1}H-NMR spectra measured for replicate samples of both strains grown under high sucrose and low sucrose conditions. In this plot of PC1 vs PC2, the x-axis is the value of the first principal component explaining 55.3 % of the variance, while the y-axis indicates the second principal component, explaining 24.9 % of the variance. **B. High sucrose cultures +/- peptone.** PCA analysis of ^{1}H NMR data was performed for the strains described in (A), except that high sucrose cultures +/- peptone were compared. X and Y-axes are as in (A); the first principal component explains 55.4 % of the variance, while the second principal component accounts for 18.3 % of the variance.

92
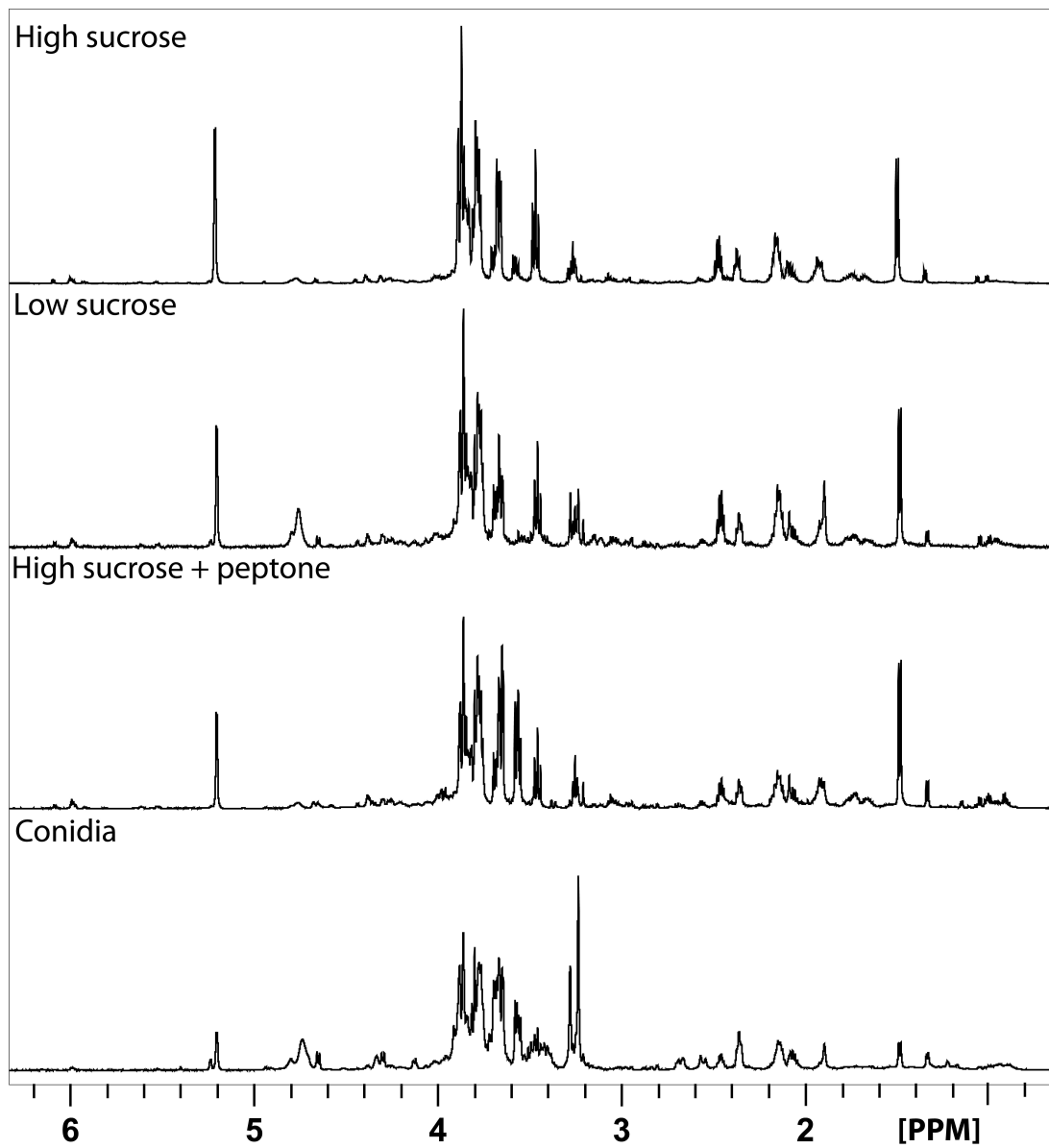
Figure 4. Spectra of wild-type strain under all conditions. All four treatments (high sucrose, low sucrose, high sucrose + peptone, and conidia) are shown together for visual comparison.
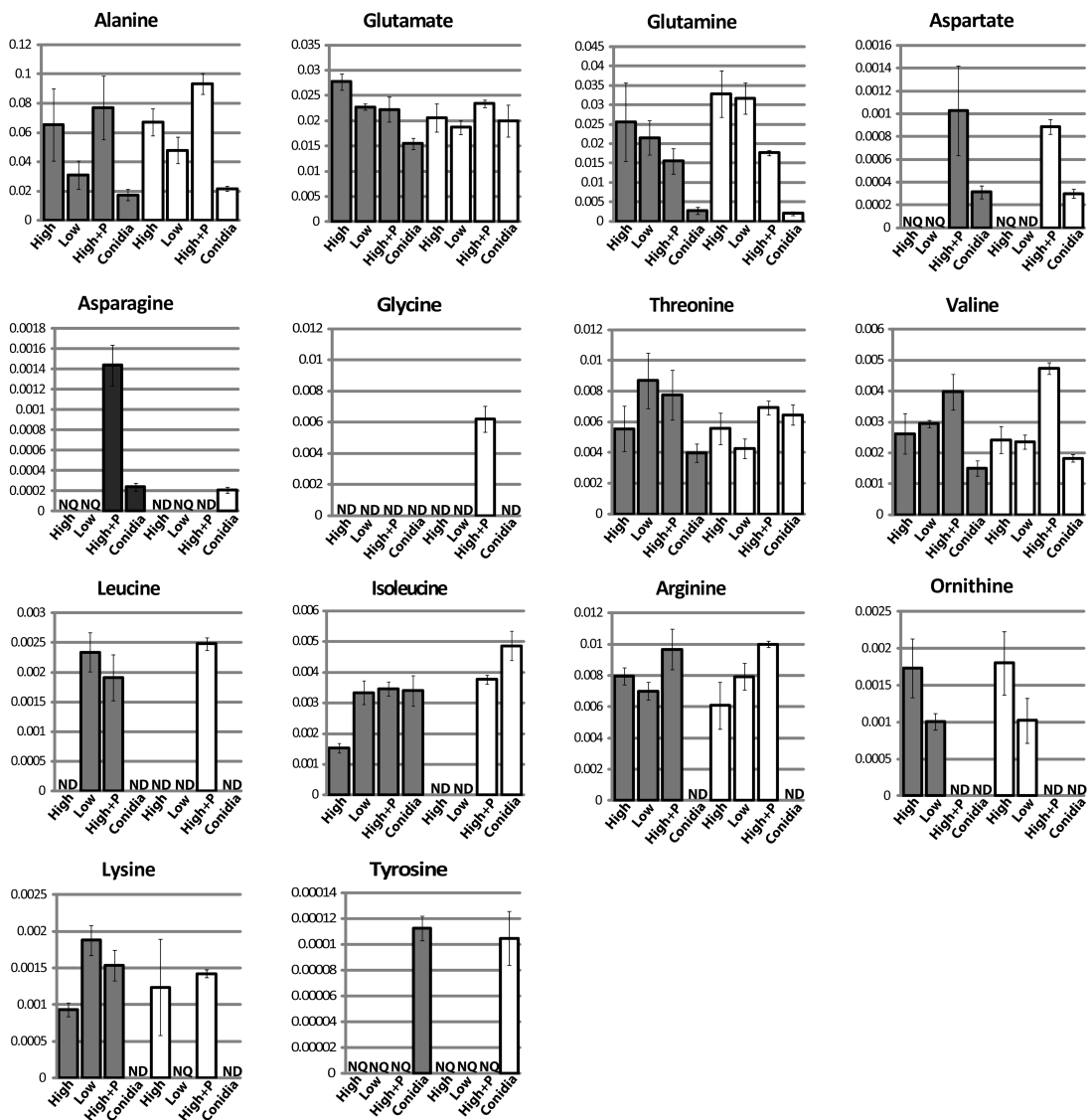
Figure 5. Relative amino acid levels.
Metabolites extracted from both wild-type (dark bars) and Δ*gna-3* (white bars) strains grown under various conditions were subjected to ^{1}H-NMR analysis and relative resonance intensities determined. On the x-axis, "HIGH" indicates metabolites extracted from tissue grown in high sucrose medium, "LOW" refers to low-sucrose medium, "HIGH+P" denotes high-sucrose with addition of 2% peptone, and "CONIDIA" represents conidia collected from strain grown on high sucrose solid medium. "ND" indicates that metabolite was not detected in that treatment. "NQ" denotes that metabolite was detected, but not quantifiable due to low concentration. The y-axis represents the quantity of a metabolite that has been normalized to the total pool of metabolites present in that particular sample.
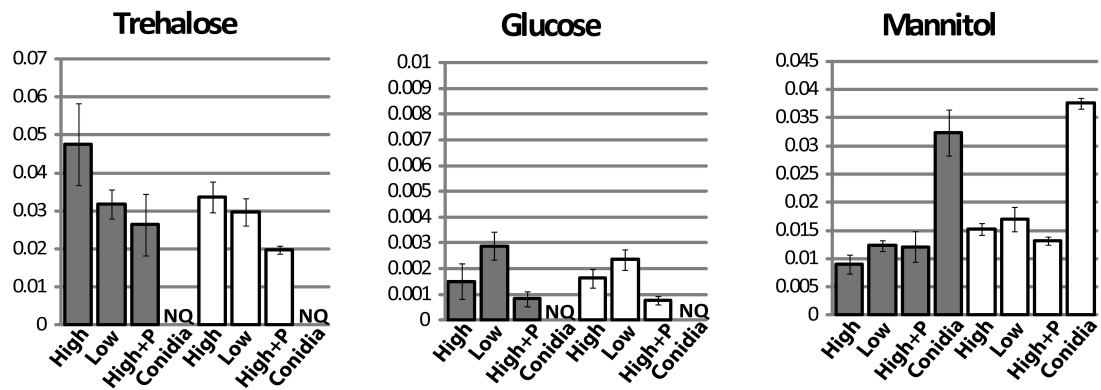
Figure 6. Relative levels of sugar metabolites.
Metabolites were extracted and analyzed and x and y axes labeled as indicated in the legend to Figure 5.
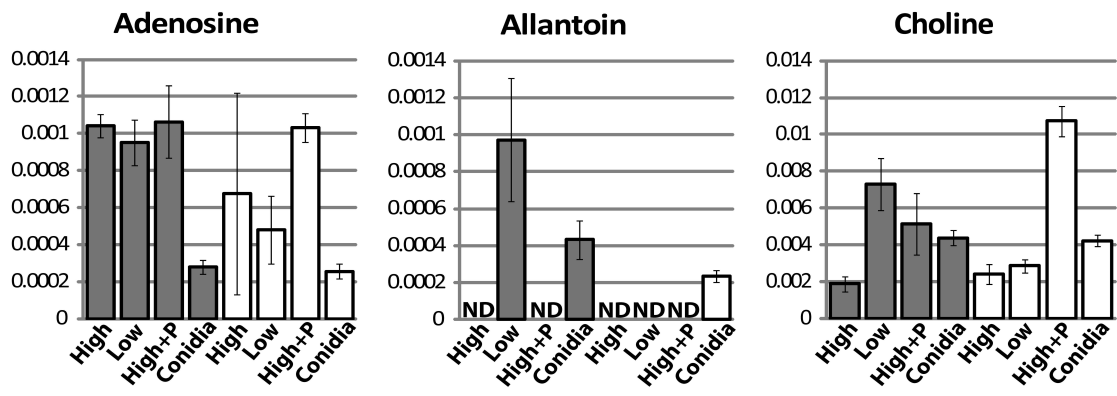
Figure 7. Relative levels of adenosine, allantoin and choline.
Metabolites were extracted and analyzed and x and y axes labeled as indicated in the legend to Figure 5.

Table 3. Comparison of mRNA profiling by Kasuga et al. (2005). This is a comparison of mRNA levels and metabolite levels during conidial germination and early hyphal stage in *Neurospora crassa*. Generally, there is correlation between the comparisons.

[1] All Broad gene numbers are from Version 1.
[2] Gene names are taken from references Perkins et al., The Neurospora Compendium, 2001; Radford, Adv. Genetics 52, 2004, and Davis, Cellular and Molecular Biology of Filamentous Fungi, 2010.
[3] mRNA data from Kasuga et al., 2005. Range of relative values are shown; complete data is available in supplementary table "gki953_S2_Expression_Data" in Kasuga et al., 2005.
[4] First time point with increased value. Number in parentheses corresponds to time after onset of germination.
[5] Amino acid produced or consumed by indicated enzymes.
[6] Data obtained from Figure 4 for wild-type conidia and high-sucrose submerged hyphal cultures.
[7] NQ = Not quantifiable; amino acid was detected, but levels were too low to quantitate.
[8] Reannotated as *ilv-3* based on linkage to *met-2* in genetic and physical maps.

Amino Acid	Broad #[1]	EC#	Enzyme	Gene name[2]	mRNA expression[3]		Relevant Metabolite[5]	Relative Metabolite Level (x10^3)[6]	
					Conidia	Hyphae[4]		Conidia	Hyphae
Threonine synthesis	NCU04118	2.7.2.4	Aspartate kinase		0.68 - 1.66	(0.5h) 2.32 - 5.87	Threonine	4.0±0.6	5.6±1.5
"	NCU03935	1.1.1.3	Homoserine dehydrogenase		0.92 - 1.23	(0.5h) 6.79 - 8.88	"	"	"
"	NCU04277	2.7.1.39	Homoserine kinase	thr-4	0.44 - 0.79	(0.5h) 3.44 - 6.18	"	"	"
"	NCU03425	4.2.3.1	Threonine synthase	thr-2	0.64 - 1.34	(0.5h) 1.53 - 3.12	"	"	"
Glutamate synthesis	NCU01195	1.4.1.4	Glutamate dehydrogenase (NADP+)	am	0.51 - 1.08	(1h) 3.15 - 4.30	Glutamate	16.0±1.1	27.0±1.6
"	NCU01744	1.4.1.14, 1.4.1.13	Glutamate synthase (NADPH) GOGAT	en (am)-2	0.99 - 3.44	(0.5h) 10.40 - 22.38	"	"	"
Glutamate degradation	NCU00461	1.4.1.2	Glutamate dehydrogenase (NAD+)	gdh	0.61 - 1.46	(0.5h) 2.26 - 2.16	"	"	"
Glutamine synthesis	NCU06724	6.3.1.2	Glutamine synthetase (β subunit)	gln-1	0.34 - 0.52	(1h) 1.32 - 1.52	Glutamine	2.7±0.9	25.6±10.0
"	NCU04856	6.3.1.2	Glutamine synthetase (α subunit)	gln-2	0.95 - 2.58	(0.5h) 1.51 - 2.60	"	"	"
Glutamine degradation	NCU04216	2.4.2.14	Amidophosphoribosyl transferase	ad-7	1.04 - 2.48	(0.5h) 3.89 - 7.42	"	"	"
Asparagine synthesis	NCU04303	6.3.5.4	Asparagine synthase	asn-1	0.49 - 1.10	(0.5h) 1.43 - 2.71	Asparagine	0.24±0.04	NQ[7]
Threonine synthesis	NCU04118	2.7.2.4	Aspartate kinase		0.68 - 1.66	(0.5h) 2.32 - 5.87	Threonine	4.0±0.6	5.6±1.5
"	NCU03935	1.1.1.3	Homoserine dehydrogenase		0.92 - 1.23	(0.5h) 6.79 - 8.88	"	"	"
"	NCU04277	2.7.1.39	Homoserine kinase	thr-4	0.44 - 0.79	(0.5h) 3.44 - 6.18	"	"	"
"	NCU03425	4.2.3.1	Threonine synthase	thr-2	0.64 - 1.34	(0.5h) 1.53 - 3.12	"	"	"
Valine and isoleucine synthesis	NCU07982	2.2.1.6	Acetolactate synthase, large subunit	ilv-3[8]	1.62 - 2.95	(1h) 2.73 - 3.74	Valine/ Isoleucine	1.5±0.3 / 3.4±0.5	2.6±0.7 / 1.5±0.2
"	NCU01666	2.2.1.6	Acetolactate synthase small subunit	ilv-4	0.36 - 0.70	(1h) 6.44 - 6.85	"	"	"
"	NCU03608	1.1.1.86	Ketol-acid reductoisomerase	ilv-2	0.47 - 1.19	(1h) 23.37 - 27.84	"	"	"
"	NCU04579	4.2.1.9	Dihydroxy-acid dehydratase	ilv-1	1.22 - 2.62	(0.5h) 6.02 - 12.57	"	"	"
"	NCU04754	2.6.1.42	Branched-chain-amino-acid aminotransferase		0.85 - 1.86	(0.5h) 3.67 - 7.13	"	"	"
Ornithine synthesis	NCU01295 / NCU10468	2.3.1.1	Glutamate N-acetyltransferase	arg-14	0.49 – 0.99	(0.5h) 3.23 – 6.56	Ornithine	NQ	1.7±0.4
"	NCU00567	2.7.2.8, 1.2.1.38	Acetylglutamate kinase and N-acetylglutamyl phosphate reductase	arg-6	0.41 - 0.80	(0.5h) 1.22 - 2.57	"	"	"
"	NCU05410	2.6.1.11	Acetylornithine aminotransferase	arg-5	0.63 - 1.27	(0.5h) 1.68 - 2.62	"	"	"
Arginine synthesis	NCU07732	6.3.5.5	Carbamoyl-phosphate synthase (small	arg-2	0.69 - 1.46	(1h) 8.18 - 8.71	Arginine	NQ	8.0±0.6

			chain, arginine-specific)						
"	NCU01667	2.1.3.3	Ornithine carbamoyl transferase	*arg-12*	0.71 - 1.83	(0.5h) 3.66 - 7.59	"	"	"
Arginine degradation	NCU02333	3.5.3.1	Arginase	*aga*	1.31 - 2.09	(0.5h) 5.11 - 3.82	"	"	"
Lysine synthesis	NCU05526	2.3.3.14	Homocitrate synthase (mitochondrial precursor)	*lys-5*	0.50 - 1.33	(0.5h) 2.28 - 4.81	Lysine	NQ	0.9±0.1
"	NCU08898	4.2.1.36	Homoaconitase	*lys-6*	0.57 - 1.61	(1h) 3.33 - 3.44	"	"	"
"	NCU02954	1.1.1.87	Homoisocitrate dehydrogenase	*lys-7*	0.40 - 0.70	(0.5h) 4.01 - 7.43	"	"	"
"	NCU03010	1.2.1.31	L-aminoadipate-semialdehyde dehydrogenase (large subunit)	*lys-3*	0.55 - 1.04	(0.5h) 2.27 - 3.63	"	"	"
"	NCU03748	1.5.1.10	Saccharopine dehydrogenase	*lys-2*	1.23 - 1.85	(0.5h) 7.26 - 8.22	"	"	"
Tyrosine synthesis	NCU01632		Pentafunctional arom polypeptide	*aro-1*	0.63 - 1.62	(0.5h) 2.78 – 5.44	Tyrosine	0.11±0.01	NQ
"	NCU05420		Chorismate synthase/flavin reductase (NADPH)	*aro-3*	0.49 - 1.39	(0.5h) 2.07 – 5.20	"	"	"

REFERENCES

1.   **Abelson, P. H., and H. J. Vogel**. 1954. Amino Acid Biosynthesis in *Torulopsis utilis* and *Neurospora crassa*. J. Biol. Chem. **213**:355-364.

2.   **Berg, R. A. v. d., H. C. J. Hoefsloot, J. A. Westerhuis, A. K. Smilde, and M. J. v. d. Werf**. 2006. Centering, scaling, and transformations: improving the biological information content of metabolomics data. BMC Genomics **7**:142.

3.   **Boernsen, K. O., S. Gatzek, and G. Imbert**. 2005. Controlled protein precipitation in combination with chip-based nanospray infusion mass spectrometry. An approach for metabolomics profiling of plasma. Anal Chem **77**:7255-7264.

4.   **Borkovich, K. A., L. A. Alex, O. Yarden, M. Freitag, G. E. Turner, N. D. Read, S. Seiler, D. Bell-Pedersen, J. Paietta, N. Plesofsky, M. Plamann, M. Goodrich-Tanrikulu, U. Schulte, G. Mannhaupt, F. E. Nargang, A. Radford, C. Selitrennikoff, J. E. Galagan, J. C. Dunlap, J. J. Loros, D. Catcheside, H. Inoue, R. Aramayo, M. Polymenis, E. U. Selker, M. S. Sachs, G. A. Marzluf, I. Paulsen, R. Davis, D. J. Ebbole, A. Zelter, E. R. Kalkman, R. O'Rourke, F. Bowring, J. Yeadon, C. Ishii, K. Suzuki, W. Sakai, and R. Pratt**. 2004. Lessons from the genome sequence of *Neurospora crassa*: tracing the path from genomic blueprint to multicellular organism. Microbiol. Mol. Biol. Rev. **68**:1-108.

5.   **Brambl, R.** 1975. Presence of polyribosomes in condiospores of *Botryodiplodia theobromae* harvested with nonaqueous solvents. J. Bacteriol. **122**:1394-1395.

6.   **Branco-Price, C., K. A. Kaiser, C. J. H. Jang, C. K. Larive, and J. Bailey-Serres**. 2008. Selective mRNA translation coordinates energetic and metabolic adjustments to cellular oxygen deprivation and reoxygenation in *Arabidopsis thaliana*. Plant J. **56**:743-755.

7.   **Broadhurst, D. I., and D. B. Kell**. 2006. Statistical strategies for avoiding false discoveries in metabolomics and related experiments. Metabolomics **2**:171-196.

8.   **Brown, J. K. M., and M. S. Hovmoller**. 2002. Aerial Dispersal of Pathogens on the Global and Continental Scales and Its Impact on Plant Disease. Science **297**:537-541.

9.   **Carollo, C. A., A. L. Calil, L. A. Schiave, T. Guaratini, D. W. Roberts, N. P. Lopes, and G. U. Braga**. 2010. Fungal tyrosine betaine, a novel secondary metabolite from conidia of entomopathogenic *Metarhizium* spp. fungi. Fungal Biol **114**:473-480.

10. **Christensen, R. L., and J. C. Schmit**. 1980. Regulation and glutamic acid decarboxylase during *Neurospora crassa* conidial germination. J. Bacteriol. **144**:983-990.

11. **Colot, H. V., G. Park, G. E. Turner, C. Ringelberg, C. M. Crew, L. Litvinkova, R. L. Weiss, K. A. Borkovich, and J. C. Dunlap**. 2006. A high-throughput gene knockout procedure for *Neurospora* reveals functions for multiple transcription factors. Proc. Natl. Acad. Sci. USA **103**:10352-10357.

12. **Colvin, H. J., B. L. Sauer, and K. D. Munkres**. 1973. Glucose utilization and ethanolic fermentation by wild type and extrachromosomal mutants of *Neurospora crassa*. J. Bacteriol. **116**:1322-1328.

13. **Cooper, T. G., V. T. Chisholm, H. J. Cho, and H. S. Yoo**. 1987. Allantoin transport in *Saccharomyces cerevisiae* is regulated by two induction systems. J. Bacteriol. **169**:4660-4667.

14. **Cossins, E. A., S. H. Y. Pang, and P. Y. Chan**. 1980. Glycine synthesis in a *Neurospora* mutant deficient in serine hydroxymethyltransferase. Plant Cell Physiol. **21**:719-729.

15. **Cui, Q., I. A. Lewis, A. D. Hegeman, M. E. Anderson, J. Li, C. F. Schulte, W. M. Westler, H. R. Eghbalnia, M. R. Sussman, and J. L. Markley**. 2008. Metabolite identification via the Madison Metabolomics Consortium Database. Nat. Biotech. **26**:162-164.

16. **d'Enfert, C., B. M. Bonini, P. D. A. Zapella, T. Fontaine, A. M. d. Silva, and H. F. Terenzi**. 1999. Neutral trehalases catalyse intracellular trehalose breakdown in the filamentous fungi *Aspergillus nidulans* and *Neurospora crassa*. Molecular Microbiology **32**:471-483.

17. **d'Enfert, C., and T. Fontaine**. 1997. Molecular characterization of the *Aspergillus nidulans treA* gene encoding an acid trehalase required for growth on trehalose. Mol Microbiol **24**:203-216.

18. **Davis, R. H.** 2000. *Neurospora*: contributions of a model organism. Oxford University Press, New York, N.Y.

19. **Davis, R. H.** 2010. Amino Acids and Polyamines: Polyfunctional Proteins, Metabolic Cycles, and Compartmentation, p.339-358. *In* K. A. Borkovich, and D. J. Ebbole (eds.). Cellular and Molecular Biology of Filamentous Fungi, ASM press, Washington, DC.

20. **Davis, R. H., F. J. de Serres, H. Tabor, and C. W. Tabor**. 1970. [4] Genetic and microbiological research techniques for *Neurospora crassa*, p. 79-143. Metabolism of Amino Acids and Amines Part A, vol. Volume 17, Part 1. Academic Press.

21. **de Pinho, C. A., M. de Lourdes, T. M. Polizeli, J. A. Jorge, and H. F. Terenzi**. 2001. Mobilisation of trehalose in mutants of the cyclic AMP signalling pathway, *cr-1* (CRISP-1) and *mcb* (microcycle conidiation), of *Neurospora crassa*. FEMS Microbiol. Lett. **199**:85-89.

22. **Dieterle, F., A. Ross, G. Schlotterbeck, and H. Senn**. 2006. Probabilistic quotient normalization as robust method to account for dilution of complex biological mixtures. Application in ^{1}H NMR metabonomics. Anal Chem **78**:4281-4290.

23. **Elbein, A. D., Y. T. Pan, I. Pastuszak, and D. Carroll**. 2003. New insights on trehalose: a multifunctional molecule. Glycobiology **13**:17R-27R.

24. **Fiehn, O., J. Kopka, P. Dormann, T. Altmann, R. N. Trethewey, and L. Willmitzer**. 2000. Metabolite profiling for plant functional genomics. Nat Biotechnol **18**:1157-1161.

25. **Halsall, D. M., and D. E. Catcheside**. 1971. Structural genes for DAHP synthase isoenzymes in *Neurospora crassa*. Genetics **67**:183-188.

26. **Halsall, D. M., D. E. Catcheside, and C. H. Doy**. 1971. Some properties of the 3-deoxy-D-arabino-heptulosonate 7-phosphate synthase isoenzymes from mutant strains of *Neurospora crassa*. Biochim Biophys Acta **227**:464-472.

27. **Halsall, D. M., and C. H. Doy**. 1969. Studies concerning the biochemical genetics and physiology of activity and allosteric inhibition mutants of *Neurospora crassa* 3-deoxy-D-arabino-heptulosonate 7-phosphate synthase. Biochim Biophys Acta **185**:432-446.

28. **Hill, E. P., and A. S. Sussman**. 1964. Development of Trehalase and Invertase Activity in *Neurospora*. J Bacteriol **88**:1556-1566.

29. **Hogg, J. A., and M. Richardson**. 1968. Biosynthesis of betaine in *Neurospora crassa*. Arch. Mikrobiol. **62**:153-156.

30. **Horikoshi, K., and Y. Ikeda**. 1966. Trehalase in conidia of *Aspergillus oryzae*. J Bacteriol **91**:1883-1887.

31. **Horne, D. W., and H. P. Broquist**. 1973. Role of lysine and -N-trimethyllysine in carnitine biosynthesis. I. Studies in *Neurospora crassa*. J. Biol. Chem. **248**:2170-2175.

32. **Jewett, M. C., G. Hofmann, and J. Nielsen**. 2006. Fungal metabolite analysis in genomics and phenomics. Curr. Opin. Biotechnol. **17**:191-197.

33. **Kaiser, K. A., Barding, G.A., Larive, C.K.** 2009. Metabolic profiling of plants by ^{1}H-NMR: A comparison of metabolite extraction strategies using rosette leaves of the model plant *Arabidopsis thaliana*. Magn. Reson. Chem. **47**:S147-S156.

34. **Kaiser, K. A., Merrywell, C.E., Fang, F., and Larive, C.K.** 2008. Metabolic Profiling, p.233-267*In* I. Wawer, U. Holzgrabe, and B. Diehl (eds.), NMR spectroscopy in pharmaceutical analysis. Elsevier, Oxford, UK.

35. **Kanamori, K., T. L. Legerton, R. L. Weiss, and J. D. Roberts**. 1982. Effect of the nitrogen source on glutamine and alanine biosynthesis in *Neurospora crassa*. An in vivo ^{15}N nuclear magnetic resonance study. J. Biol. Chem. **257**:14168-14172.

36. **Kasuga, T., J. P. Townsend, C. Tian, L. B. Gilbert, G. Mannhaupt, J. W. Taylor, and N. L. Glass**. 2005. Long-oligomer microarray profiling in *Neurospora crassa* reveals the transcriptional program underlying biochemical and physiological events of conidial germination. Nucleic Acids Res **33**:6469-6485.

37. **Kays, A. M., and K. A. Borkovich**. 2004. Severe impairment of growth and differentiation in a *Neurospora crassa* mutant lacking all heterotrimeric G α proteins. Genetics **166**:1229-1240.

38. **Kays, A. M., P. S. Rowley, R. A. Baasiri, and K. A. Borkovich**. 2000. Regulation of conidiation and adenylyl cyclase levels by the Gα protein GNA-3 in *Neurospora crassa*. Mol. Cell. Biol. **20**:7693-7705.

39. **Koelle, M. R.** 2006. Heterotrimeric G protein signaling: Getting inside the cell. Cell **126**:25-27.

40. **Kuepfer, L., U. Sauer, and L. M. Blank**. 2005. Metabolic functions of duplicate genes in *Saccharomyces cerevisiae*. Genome Res. **15**:1421-1430.

41. **Lerch, K.** 1981. Metal ions in biological systems, vol. 13. Marcel Dekker Inc., New York, NY.

42.   **Li, L., and K. A. Borkovich**. 2006. GPR-4 Is a Predicted G-Protein-Coupled Receptor Required for Carbon Source-Dependent Asexual Growth and Development in *Neurospora crassa*. Eukaryot. Cell **5**:1287-1300.

43.   **Li, L., S. J. Wright, S. Krystofova, G. Park, and K. A. Borkovich**. 2007. Heterotrimeric G protein signaling in filamentous fungi. Annu. Rev. Microbiol. **61**:423-452.

44.   **Lin, C. Y., H. F. Wu, R. S. Tjeerdema, and M. R. Viant**. 2007. Evaluation of metabolite extraction strategies from tissue samples using NMR metabolomics. Metabolomics **3**:55-67.

45.   **Linden, H., P. Ballario, and G. Macino**. 1997. Blue light regulation in *Neurospora crassa*. Fungal Genet. Biol. **22**:141-150.

46.   **Lindon, J. C., E. Holmes, and J. K. Nicholson**. 2003. So what's the deal with metabonomics? Anal. Chem. **75**:384A-391A.

47.   **Lowe, R. G., J. W. Allwood, A. M. Galster, M. Urban, A. Daudi, G. Canning, J. L. Ward, M. H. Beale, and K. E. Hammond-Kosack**. 2010. A combined ^{1}H nuclear magnetic resonance and electrospray ionization-mass spectrometry analysis to understand the basal metabolism of plant-pathogenic *Fusarium* spp. Mol Plant Microbe Interact **23**:1605-1618.

48.   **Martin, F. P., M. E. Dumas, Y. Wang, C. Legido-Quigley, I. K. Yap, H. Tang, S. Zirah, G. M. Murphy, O. Cloarec, J. C. Lindon, N. Sprenger, L. B. Fay, S. Kochhar, P. van Bladeren, E. Holmes, and J. K. Nicholson**. 2007. A top-down systems biology view of microbiome-mammalian metabolic interactions in a mouse model. Mol Syst Biol **3**:112.

49.   **Marzluf, G.** 1997. Genetic regulation of nitrogen metabolism in the fungi. Microbiol. Mol. Biol. Rev. **61**:17-32.

50.   **Munkres, K. D.** 1968. Genetic and Epigenetic Forms of Malate Dehydrogenase in *Neurospora*. Ann. NY Acad. Sci. **151**:294-306.

51.   **Orbach, M. J., M. S. Sachs, and C. Yanofsky**. 1990. The *Neurospora crassa arg-2* locus. Structure and expression of the gene encoding the small subunit of arginine-specific carbamoyl phosphate synthetase. J Biol Chem **265**:10981-10987.

52.   **Pall, M. L.** 1981. Adenosine 3',5'-phosphate in fungi. Microbiol. Rev. **45**:462-480.

53.   **Pall, M. L., and C. K. Robertson**. 1988. Regulation of lactate/pyruvate ratios by cyclic AMP in *Neurospora crassa*. Biochem. Biophys. Res. Commun. **150**:365-370.

54.   **Perkins, D. D., A. Radford, and M. S. Sachs**. 2001. The *Neurospora* compendium: chromosomal loci. Academic Press, San Diego, CA.

55.   **Pillonel, C., and T. Meyer**. 1997. Effect of Phenylpyrroles on Glycerol Accumulation and Protein Kinase Activity of *Neurospora crassa*. Pestic. Sci. **49**:229-236.

56.   **Plesofsky-vig, N., D. Light, and R. Brambl**. 1983. Paedogenetic conidiation in *Neurospora crassa*. Exp. Mycol. **7**:283-286.

57.   **Plesofsky, N., and R. Brambl**. 1999. Glucose metabolism in *Neurospora* is altered by heat shock and by disruption of HSP30. Biochim. Biophys. Acta **1449**:73-82.

58.   **Radford, A.** 2004. Metabolic highways of *Neurospora crassa* revisited. Adv Genet **52**:165-207.

59.   **Ringner, M.** 2008. What is principal component analysis? Nat Biotechnol **26**:303-304.

60.   **Robertson, D. G.** 2005. Metabonomics in toxicology: a review. Toxicol Sci **85**:809-822.

61.   **Sachs, M. S., and C. Yanofsky**. 1991. Developmental expression of genes involved in conidiation and amino acid biosynthesis in *Neurospora crassa*. Dev Biol **148**:117-128.

62.   **Schmit, J. C., and S. Brody**. 1975. *Neurospora crassa* conidial germination: role of endogenous amino acid pools. J. Bacteriol. **124**:232-242.

63.   **Schmit, J. C., and S. Brody**. 1976. Biochemical genetics of *Neurospora crassa* conidial germination. Bacteriol. Rev. **40**:1-41.

64.   **Solomon, P. S., O. D. C. Waters, C. I. Jörgens, R. G. T. Lowe, J. Rechberger, R. D. Trengove, and R. P. Oliver**. 2006. Mannitol is required for asexual sporulation in the wheat pathogen *Stagonospora nodorum* (glume blotch). Biochem. J. **399**:231-239.

65.   **Solomon, P. S., O. D. C. Waters, and R. P. Oliver**. 2007. Decoding the mannitol enigma in filamentous fungi. Trends Microbiol. **15**:257-262.

66. **Springer, M. L.** 1993. Genetic control of fungal differentiation: The three sporulation pathways of *Neurospora crassa*. BioEssays **15**:365-374.

67. **Springer, M. L., and C. Yanofsky**. 1989. A morphological and genetic analysis of conidiophore development in *Neurospora crassa*. Genes Dev. **3**:559-571.

68. **That, T. C., and G. Turian**. 1978. Ultrastructural study of microcyclic macroconidiation in *Neurospora crassa*. Arch. Microbiol. **116**:279-288.

69. **Turian, G., and D. E. Bianchi**. 1972. Conidiation in *Neurospora*. Botanical Review **38**:119-154.

70. **Turner, G. E., and R. L. Weiss**. 2006. Developmental expression of two forms of arginase in *Neurospora crassa*. Biochim. Biophys. Acta **1760**:848-857.

71. **van den Berg, R. A., H. C. Hoefsloot, J. A. Westerhuis, A. K. Smilde, and M. J. van der Werf**. 2006. Centering, scaling, and transformations: improving the biological information content of metabolomics data. BMC Genomics **7**:142.

72. **Viant, M. R., E. S. Rosenblum, and R. S. Tieerdema**. 2003. NMR-based metabolomics: a powerful approach for characterizing the effects of environmental stressors on organism health. Environ Sci Technol **37**:4982-4989.

73. **Villas-Boas, S. G., J. Hojer-Pedersen, M. Akesson, J. Smedsgaard, and J. Nielsen**. 2005. Global metabolite analysis of yeast: evaluation of sample preparation methods. Yeast **22**:1155-1169.

74. **Ward, J. L., J. M. Baker, and M. H. Beale**. 2007. Recent applications of NMR spectroscopy in plant metabolomics. FEBS J **274**:1126-1131.

75. **Zhang, S., C. Zheng, I. R. Lanza, K. S. Nair, D. Raftery, and O. Vitek**. 2009. Interdependence of signal processing and analysis of urine ^{1}H NMR spectra for metabolic profiling. Anal Chem **81**:6080-6088.

Chapter 4: Utilization of yeast 2 hybrid screens to identify proteins that interact with GNA-3 and RIC8

Introduction

First introduced by Fields and Song in 1989 (12), the Yeast 2 Hybrid system has proven itself to be an effective tool for discovering protein-protein interactions. Since its inception, this system has been modified for other purposes, including the Yeast 3 Hybrid system that tests RNA-protein interactions (48), a 3-hybrid system for detecting small ligand-protein receptor interactions (30), a 1-hybrid system for assaying interaction between DNA and protein (28) and a multi-protein (tertiary) complexes assaying system (40).

The interaction at the heart of Yeast 2 Hybrid assay, signifying association between 2 proteins, is between short stretches of amino acids or interaction pockets in these proteins (59). This binding brings together the activation domain (AD) of the GAL4 transcription factor fused to one protein with the binding domain (BD) fused to the other, thus reconstituting an active Gal4p transcription factor. In the assay, this interaction leads to expression of amino acid and other reporter genes that allow survival of the yeast on media lacking certain key nutrients (e.g., histidine and adenine).

The Yeast 2 Hybrid system has been used to screen cDNA libraries obtained from mRNA of organisms of various species, including mouse T-cells (49), human ribosomes (46), and tobacco floral buds (21). Screening the cDNA library allows identification of many potential interacting proteins (27). By testing interaction with one protein (bait)

with all other proteins generated by the cDNA library, researchers gain a huge amount of information as to the potential protein-protein interaction network of their protein of interest. Such insight can lead to construction of a signal transduction cascade for a particular cellular process.

Signal transduction cascades are the main way cells receive and react to external input from the environment (1). These cascades are a relay of protein interactions that begins with an input source (usually a ligand) interacting with a receptor on the membrane, all the way to a transcription factor in the nucleus of the cell that manipulates expression of a gene(s). Model organisms can be used to understand and further research into signal transduction cascades. Model organisms must be simple to grow and manipulate, and possess robust genetics. One system ideally suited for this purpose is *Neurospora crassa*, a filamentous fungus. This eukaryotic system's cellular machinery allows study of the heterotrimeric G-protein system, a major signaling pathway in mammals and hence targets of pharmaceuticals (3, 20).

GNA-3 is one of the Gα-subunits of heterotrimeric G-proteins in *Neurospora* (23). Δ*gna-3* mutants possess many distinct phenotypes, including short aerial hyphae and hyperconidiation on solid medium, inappropriate conidiation in submerged cultures, female sterility, and reduced mass on poor carbon sources (23), indicating an effect of GNA-3 on multiple signaling pathways. In the absence of GNA-3, levels of cyclic AMP are dramatically decreased because of reduced amounts of adenylyl cyclase protein (23). The involvement of GNA-3 in numerous cellular processes implies that it has many interaction partners. However, GNA-3 interacting proteins are currently unknown.

RIC8 is a non-receptor Guanine nucleotide Exchange Factor (GEF) in many species, including *Neurospora* (53). In *Caenorhabditis elegans,* it is involved in embryogenesis (35), and in *Drosophila melanogaster,* it is required for asymmetric cell division in neural progenitors (53). In *Neurospora,* the deletion mutant has a severe growth defect, conidiates in submerged conditions, has almost no aerial hyphae, and is female sterile (57). It has been shown to interact physically with GNA-1 and GNA-3 in Yeast 2 Hybrid assays, with a stronger interaction with GNA-3 (57). However, other RIC8-interacting proteins are currently unknown.

To better understand and clarify the signal transduction cascade involving GNA-3 and RIC8, a Yeast 2 Hybrid cDNA library screening was conducted to search for interactors. The results of such screens will reveal possible protein interactors that can be subjected to future confirmation and elucidation, as well as suggest pathways modulated by GNA-3 and RIC8.

Materials and Methods

Saccharomyces cerevisiae strains AH109 and Y187 were used for the Yeast 2 Hybrid screens according to the Clontech Matchmaker system (Clontech Laboratories, Mountainview, CA). Growth conditions and culture media were according to specifications described in the Yeast Protocols Handbook (Clontech).

The *Neurospora a* cDNA library cloned into the pGAD-TRec vector as well as the GNA-3 pGBKT7-Y2H vector (Borkovich lab strain #86) were previously made (Sara Wright and HyoJeong Kim, unpublished). The RIC8 pGBKT7-Y2H vector (Borkovich

lab strain #173) was made by Sara Wright. Both of the "bait" vectors were made the same way; briefly, the exons of the gene were amplified using PCR to remove introns. *Bam*HI and *Eco*RI restriction sites were added to the 5' end of the first exon and to the 3' end of the last exon, respectively. These exon fragments were inserted using yeast recombinational cloning (Clontech manual) into pRS426. Finally, *ric8* was excised from pRS426 using *Bam*HI and *Eco*RI, and ligated into pGBKT7 vector digested with the same enzymes. Finally, yeast strain Y187 was transformed with this vector. All yeast strains were stored as glycerol stocks at -80˚C. Table 1 lists the vectors and Table 2 the strains used for this work.

In order to mate the cells containing library clones to the bait strain, 5 ml of strain Y187 containing the "bait" plasmid (GNA-3 or RIC8) was grown in SD-trp liquid medium overnight in the dark at 30˚C with shaking at 200 rpm. A 1-ml aliquot of the AH109 yeast strain containing the library was thawed in a room temperature water bath. Subsequently, it was mixed with 5ml of the Y187 strain containing the bait plasmid in a sterile 2-liter flask. To the flask, 45ml of 2x YPDA supplemented with kanamycin (50µg/ml) was added with gentle swirling. The microcentrifuge tube containing the library was rinsed with 1 ml of 2x YPDA supplemented with kanamycin (50µg/ml) twice and the contents poured into the flask. The flask was incubated at 30˚C for 24 hours at 50 rpm. After incubation, a small aliquot was withdrawn to inspect for zygotes (indicating successful mating). The contents of the flask were transferred to 2-50 ml conical tubes and centrifuged at 1000xg for 10 min. The flask was rinsed twice with 20 ml of 0.5X YPDA supplemented with 50 µg/ml of kanamycin. This was used to

resuspend the pelleted yeast cells. The mixture was centrifuged again at 1000xg for 10minutes. Finally, the pelleted yeast cells were resuspended in 10 ml of 0.5X YPDA supplemented with kanamycin (50μg/ml). This suspension was plated on SD minus leu,trp plates (150mm x 15mm) and incubated at 30˚C in the dark for 2 days.

Using a sterile toothpick, colonies that grew to at least 2mm in diameter on a Double Drop-Out (DDO) medium (SD minus leucine, tryptophan) plate were streaked onto another DDO plate and incubated at 30˚C in the dark. After 2 days of growth, single colonies were picked and streaked onto another plate in order to ensure that only one pGAD plasmid resided in the yeast cell. Finally, a single colony was picked from the DDO plate and streaked onto a Quadruple Drop-Out (QDO) plate (SD minus adenine, histidine, leucine and tryptophan). Strains that grew on this medium were considered potential interactors and carried onto the next phase.

Plasmids from individual yeast strains that encoded interactors were isolated from the yeast using the "Smash and Grab" method. This method involves growing the yeast strain in 5ml of SD liquid medium lacking the amino acid tryptophan. This ensures that any yeast strain that grew in this medium would have the plasmid expressing the gene for tryptophan synthesis (pGBKT7). After overnight growth, the culture was pelleted by centrifugation and the supernatant removed. An aliquot containing 200μl of lysis buffer (2% Triton X-100, 1% SDS, 100mM NaCl, 10mM Tris pH 8.0, 1mM EDTA), 200μl of phenol/chloroform) and 0.3g of 0.45mm glass beads were added to the microcentrifuge tube. The tube was capped and sealed with parafilm and vortexed three times for 1 minute with 1minute rests in between. The tube was centrifuged for 10 minutes, and the

supernatant removed to a fresh tube. To the supernatant, 0.3M NaOAc and 2.5 volume of

100% ethanol were added. This mixture was placed in the -20˚C freezer for 30minutes

before centrifuging again. The supernatant was discarded and the pellet was washed

using 1ml of 70% ethanol, followed by centrifugation for 5 minutes. Finally, the tubes

were air-dried on Kimwipes until they were completely dry and 50µl of elution buffer

(10mM Tris-Cl, pH 8.5) was added to each tube. The tubes were vortexed to resuspend

DNA.

The extracted yeast plasmids were electroporated into electro-competent (REF)

DH5α *E. coli* cells using the Eppendorf 2510 electroporator at 1800 volts. The plasmids

were introduced into *E. coli* because the yield of plasmid from *E. coli* is much greater

than from *Saccharomyces cerevisiae*. *E. coli* cells had to be electroporated instead of

chemically transformed because contaminants in the "Smash and Grab" preparation make

transformation of *E. coli* quite inefficient.

E. coli cultures containing plasmids were grown by inoculating 5 ml of LB liquid-

medium containing 100 µg/ml of ampicillin with a colony that was picked from the

LB+ampicillin (100 µg/ml) agar plate using a sterile toothpick. The culture was allowed

to grow overnight at 37˚C with shaking at 225 rpm in the dark. Plasmids were extracted

using the Qiagen Miniprep kit (Qiagen Sciences, Maryland, USA). Extracted plasmids

were then transformed back into yeast strain AH109 by chemical transformation, as

described previously. Then, the transformed yeast strain was crossed with a yeast Y187

strain containing the negative control plasmid (pGBKT7 without any inserted gene). The

mated strain was streaked onto DDO media (SD minus leu, trp) to ensure that both

plasmids were present in the same yeast cell. Then, a single colony was picked and streaked onto Triple Drop-Out (TDO) medium (SD minus leu, trp, ade) to determine whether the positively interacting protein is indeed self-activating. If the colony grew on the TDO medium, then it was discarded as a self-activator.

I.   GNA-3

All plasmids containing GNA-3 interactors were sequenced by the UC Riverside Core Facility. After the plasmid inserts were sequenced, the raw data was analyzed using Finch TV trace viewer (Version 1.4, Geospiza). The sequence of the insert was BLASTed against the *Neurospora crassa* database hosted by the Broad Institute (http://www.broadinstitute.org/annotation/genome/neurospora/MultiHome.html) in order to identify the gene.

II.   RIC8

In order to determine whether there were multiple occurrences of the same clone, a dot-blot strategy was employed. Here, 1 μl of each plasmid was spotted on a nitrocellulose membrane and allowed to dry. Then, the membrane was UV-cross-linked (1200×100 μJ/cm^2) and prehybridized in a hybridization bottle with hybridization solution (0.5 M Na_2HPO_4, 1 mM EDTA, 7% SDS, 1% BSA) with rotation in an oven at 65˚C for 1 hour. At the same time, 5 μl of one of the plasmids (chosen randomly) was used to make a ^{32}P-labeled probe. Briefly, the following steps were taken: first, 5 μl of the plasmid was boiled for 5 minutes to denature the DNA. Second, 10 μl of 5X labeling buffer (Promega: Madison, WI), 3 μl of dNTPs without dCTP, 5 μl of biotinylated BSA, 1.4 μl of Klenow fragment, and 5 μl of ^{32}P-labeled dCTP were added to the plasmid.

This mixture was incubated at room temperature for 1 hour. At the end of the hour, solution containing labeled plasmid was boiled for 5 minutes and then added to the hybridization bottle and incubated with constant rotation overnight. Next morning, the membrane was washed twice with Wash Buffer 1 (1 M Na_2HPO_4, 0.5 M EDTA, 5% w/v SDS, 0.5% w/v BSA) and Wash Buffer 2 (1 M Na_2HPO_4, 0.5 M EDTA, 1% w/v SDS) before exposing to an X-ray film using an intensifying screen. After the film was developed, the location of intense signal where the probe hybridized was correlated with the plasmid (fig. 1). The plasmids that hybridized were considered to be the same as the probe and marked as duplicates. This process was repeated for a total of 3 plasmids. Then, each of the plasmids that were used to make the probe as well as plasmids that did not hybridize to any of the probes were sequenced by the UC Riverside Core Facility. Ultimately, the method led to identification of all plasmids that interacted with RIC8 in the Yeast 2 Hybrid cDNA library screening, and the dot-blot reduced the amount of sequencing necessary. After the plasmids were sequenced, the raw data was analyzed using Finch TV trace viewer (Version 1.4, Geospiza). The sequence of the plasmid was BLASTed against the *Neurospora crassa* database hosted by the Broad Institute (http://www.broadinstitute.org/annotation/genome/neurospora/MultiHome.html) in order to identify the gene.

Most of the deletion mutants of the genes that interacted with RIC8 were readily available in the *Neurospora* genome project collection in the Borkovich laboratory at UC Riverside. The following phenotypic assays were conducted on deletion mutants of RIC8 interactors:

a.   Growth (apical extension rate) assay

Conidia from 7-day-old cultures of the deletion mutants (grown 2 days in 30˚C, dark

conditions and then brought out to room temperature with 12 hours of photoperiod for 5

additional days) grown in a foam-plugged, 250 ml flask filled with 50 ml of VM-agar

were collected with sterile water by agitation, filtered through sterile cheese-cloth to

remove all tissue types except conidia, and transferred to a sterile 50 ml conical tube.

The conidial suspension was centrifuged at 2500 rpm for 5 minutes to concentrate the

conidia. Then 25 ml of sterile water was added to the conical tube and centrifuged again

before pouring out the water. The concentrated conidial suspension was transferred to a

sterile microcentrifuge tube. After determining the conidial concentration using a

hemacytometer, a dilution stock of $1x10^6$ conidia/µl was made. One µl of the dilution

stock was placed in the center of a VM-agar plate (30ml/plate), incubated at 30˚C,

checked every 4 hours for growth, and the growth edge marked. Wild-type and Δ*ric8*

strains (collected and inoculated in the same manner) were also grown on a VM plate as a

reference.

b.   Female fertility assay

Synthetic Crossing Medium (SCM) plates were inoculated with the conidia of the

deletion mutants and incubated at 25˚C with constant light for 6 days. At the end of 6

days, conidia from wild-type strain of the opposite mating type was swabbed onto half of

the plate using a sterile swab, while the other half was swabbed with sterile water (as a

negative control). The plate was placed back into the incubator and grown for another 9

days. Then the plates were examined under a dissecting microscope for the presence of

perithecia or ascospores adhering to the underside of the petri-dish cover that have ejected from the ostioles.

c. Male fertility assay

A SCM plate was inoculated with the conidia of the wild-type strains (both mating types) and incubated at 25˚C with constant light for 6 days (enough duration to form protoperithecia). At the end of 6 days, conidia from the deletion mutant strains of the opposite mating type was swabbed onto half of the plate using a sterile swab, while the other half was swabbed with sterile water (as a negative control). The plate was placed back into the incubator and grown for another 9 days. Then, the plates were examined under a dissecting microscope for presence of perithecia or ascospores adhering to the underside of the petri-dish cover that have ejected from the ostioles of perithecia.

d. Aerial hyphae assay

A test tube containing 1 ml of VM liquid-medium was inoculated with conidia from the deletion mutant strains to a concentration of $1x10^6$ conidia/ml. Conidia from the wild-type strain were used as a reference. These test tubes were placed in an incubator set at 30˚C in the dark. The height of the aerial hyphae was measured after every 12 hours of growth for 2 days.

e. Submerged culture morphology assay

A 25 ml Erlenmeyer flask containing 6 ml of VM liquid medium was inoculated with $1x10^6$ conidia/ml from each deletion mutant strains. The flasks were sealed with sterile aluminum foil and incubated with shaking at 200 rpm at 30˚C, in the dark. After 16 hours of incubation, the flasks were removed and a 20 ml sample containing hyphae

pipetted out using a 200 ml pipet tip with the tip cut with a scissors. The sample was placed on a microscope slide, covered with a coverglass, and examined under an Olympus BX41 compound microscope at 40X magnification. Each strain was checked 3 times for consistency.

RESULTS

I.   GNA-3 interactors

From screening the cDNA library with GNA-3 as "bait", 42 "hits" were found. Out of these, many duplicates were identified after sequencing, resulting in 22 unique proteins that physically interacted with GNA-3 in the Y2H screening (Table 3). A total of 5 "hits" were hypothetical proteins. Below are the genes encoding the proteins that interact with GNA-3:

1. NCU00211 encodes the mitochondrial ribosomal protein subunit L31. In
    Saccharomyces cerevisiae, it was shown to have two domains, one that associates
    with the ribosome and another that had mRNA selectivity for mitochondrial *cox2*,
    cytochrome oxidase subunit II (55).

2. NCU00242 is the *v-snare* gene that encodes the Soluble NSF (N-ethylmaleimide
    Sensitive Fusion) attachment protein receptor (SNARE) proteins complex that plays a
    central role in membrane fusion and vesicle transport of eukaryotic organisms (8). In
    Magnaporthe grisea, a homolog called *MoVam7* is involved in growth, conidiation,
    appressorium formation, and pathogenicity. In the deletion mutant, either there were
    no conidia formed or only aberrant ones. Without MoVam7, vacuoles were

fragmented. In *Saccharomyces cerevisiae*, it was shown that Vam7p contains a PX domain that aids the protein for targeting to the plasma membrane (14).

3. NCU00467 encodes *csn-5*, which is a component of the Cop9 signalosome (CSN) that controls the ubiquitin-mediated protein degradation pathway in eukaryotes (54). CSN mediates the assembly and disassembly of the Cullin-RING ubiquitin ligases (CRLs) that polyubiquitinate proteins marked for degradation. It is thought that the major function of CSNs is to stabilize CRLs. In *Neurospora crassa*, this complex is formed of 7 subunits. Loss of any one of the *csn* leads to instability of CRLs. When a subunit is missing (*csn-5* included), the fungus is defective in conidiation, growth, and circadian rhythm.

4. NCU00971 encodes the ribosomal protein S12, a part of a complex that in conjunction with ribosomal RNA, make up the ribosomal subunits involved in the cellular process of translation (31). Interestingly, in *Podospora anserina*, a homolog called *as1* was responsible for premature death syndrome of the fungus by site-specific deletion of mitochondrial DNA (7).

5. NCU02357 encodes importin subunit β-3. Also known as karyopherin, these proteins contain 19-20 helical repeats named HEAT (58). They bind unique proteins or RNA and are mediated by Ran GTPase to enter the nucleus by the Nuclear Pore Complex.

6. NCU02400 encodes a metacaspase-1B. Metacaspases are found only in plants, protists, and fungi (6); they behave similarly to cascapses in that these are enzymes that degrade proteins. The homologous protein in yeast is Yca1p, which is

upregulated during heterokaryotic incompatibility (19). Also, this protein has been implicated in oxidative stress-induced cell death.

7. NCU02668

   Interestingly, this gene also is upregulated during heterokaryotic incompatibility (19). It encodes a cell-wall synthesis protein. In *Schizosaccharomyces pombe*, a homolog called *psu1* (36% identity) is essential for cell-wall synthesis (39).

8. NCU02998 encodes nicotinate-nucleotide pyrophosphorylase, also known as quinolinate phosphoribosyltransferase (decarboxylating), catalyses the conversion of nicotinate D-ribonucleotide, pyrophosphate and carbon dioxide into pyridine-2,3-dicarboxylate and 5-phospho-alpha-D-ribose 1-diphosphate. This enzyme is a type II phosphoribosyltransferase that provides the *de novo* source of nicotinate mononucleotide (NAMN) for NAD biosynthesis in both prokaryotes and eukaryotes (13).

9. NCU04388 encodes a phosphotidylglycerol/phosphatidylinositol transfer protein. Its function is to transfer phospholipids between membranes (56). It shares 53% identity with its homolog in *Aspergillus oryzae* (42). It plays a role during protein secretion via the Golgi complex and localization has been shown to be in the cytoplasm by association with Golgi-like vesicles.

10. NCU05995 encodes ubiquitin, arranged as 4 tandem repeats (50). It is a 76 amino acids long and is involved in the degradation pathway of intracellular proteins targeted for degradation. In *Saccharomyces cerevisiae*, it has been shown that GPCR

Ste2p can be ubiquitinated for endocytosis (17). Furthermore, the Gα-subunit Gpa1 was shown to be ubiquitinated in response to cell cycle change (51).

11. NCU06440 encodes the s20 proteasome component PRE6. S20 proteasome is a component of the S26 proteasome complex that degrades short-lived proteins (18). In *Saccharomyces cerevisiae*, it encodes an α-type subunit (16). It was demonstrated that s20 complex is associated with the nuclear envelope-endoplasmic reticulum network in yeast.

12. NCU06550 encodes *pdx-1* (*pyridoxine 1*), responsible for pyridoxine (vitamin B6) metabolism (2). It's homolog in yeast is called SNZ and is upregulated during growth arrest (4). *snz* appears to have a role during nutrient limitation and growth arrest: conditions leading to conidiation.

13. NCU06892 encodes 40S ribosomal protein S20. In *Neurospora crassa*, it is also known as cytoplasmic ribosomal protein-26 (crp-26) (41). In bacteria, it was shown that G-proteins influence the ribosome during times of nutrient limitation (22).

14. NCU08389 encodes the 60S ribosomal protein L20 (11).

15. NCU09816 encodes cytochrome c1, a subunit of the ubiquinol-cytochrome reductase (29). It is composed of a large hydrophilic portion that extends from the mitochondrial inner membrane into the inner membrane space, interacting with cytochrome c. There's also the hydrophobic part that anchors this protein to the bilayer.

16. NCU10058 is phosphoglycomutase 2, one of 2 phosphoglucomutase isozymes. In *Neurospora sitophila*, the 2 genes *rg-1* and *rg-2* encode phosphoglucomutase (36). In

Neurospora crassa, this gene was originally identified in a mutant called "ragged", which contained 6 times higher level of glucose-1-phosphate (the substrate for the phosphoglycomutase) than wild type (5).

17. NCU10572 is short chain oxidoreductase, also known as SCOR, are class of enzymes that catalyze transfer of electrons from the donor to the acceptor and are present in bacteria, fungi, plants, insects, and mammals (9).

II.   RIC8 Interactors

From screening the cDNA library with RIC8 as "bait", 71 "hits" were found. Out of these, many duplicates were identified by the dot-blot test, resulting in 8 unique proteins that physically interacted with RIC8 in the Y2H screening (Table 4). Below are the genes encoding the interacting proteins:

1. NCU11324 encodes an unidentified protein containing a PX domain, a phosphoinositide binding module that is involved in protein targeting to the membrane, specifically the region enriched with the phosphoinositide (47). This is a mechanism by which eukaryotic cells recruit proteins to the membranes. These domains are involved in cell signaling, vesicle trafficking, and cell polarity. In *Schizosaccharomyces pombe*, two proteins with PX domains that are involved in forespore formation, Vps5p and Vps17p, associate with the phosphoinositides in the membrane (25). The authors speculate that PX-domain proteins could be involved in vesicle trafficking between the membrane and the Golgi apparatus, moving proteins to the forespore location in order to orchestrate directional growth and development.

2. NCU03530 is called *acw-6*, Anchored Cell Wall-6. It is a member of the CFEM

superfamily. There was no homolog in the *Saccharomyces* Genome Database (SGD).

CFEM domains are cysteine-rich EGF-like domains and are prevalent in extracellular

regions of proteins imbedded in membranes (26). Proteins with this domain often have a

signal peptide or a GPI anchor that causes them to associate with membranes. According

to Maddi *et al*., this protein is found in vegetable and conidial cell walls (32).

3. NCU00636 encodes the mitochondrial protein ATP synthase D chain that is (52) is

necessary for conversion of ADP to ATP. Mass-spectrometry demonstrates that this

protein associates with the Woronin body (33), a vesicle specific to filamentous

ascomycetes that is filled with a dense protein making up the solid core, that plugs up the

septal pore in instances of cellular damage (60).

4. NCU08131 encodes α-amylase, an enzyme that hydrolyzes starch into simpler

molecules, such as glucose (43). Specifically, α-amylases act on glucose residues linked

through α-1-1, α-1-4, α-1-6, glycosidic bonds. A potential purpose for this enzyme is to

assist in fungal cell wall reorganization; a similar enzyme in *Aspergillus fumigatus* was

shown to be involved in cell wall biosynthesis (10).

5. NCU00455 encodes an adaptor protein called STE50. It is involved in the MAPK

pathway in other fungi and so was picked for study in detail. The results are described in

Chapter 5.

6. NCU01162. The homolog of this gene in *Saccharomyces cerevisiae* is called *gas5*

(45). It is a glycosylphosphatidylinositol-anchored glucan-remodeling enzyme that is

expressed in vegetative hyphae. The (1,3)-glucanase/transglycosidase activity is crucial

for the incorporation and remodeling of (1,3)-glucan into the cell wall and for creating attachment sites for the anchoring of mannoproteins and chitin (34).

7. NCU09632 is a hypothetical protein that contains a phosphodiesterase/alkaline phosphatase D precursor domain (NCBI protein BLAST).

8. NCU10207 has been removed from the 5th annotation of the *Neurospora crassa* genome database; it was miscalled as a gene. In the previous annotation, it was described as a 129 nucleotides long. However, there are no "hits" when checked in NCBI protein BLAST.

Phenotypic assay for deletion mutants of RIC8 interactors

Deletion mutants of RIC8 interactors that were readily available from the *N. crassa* Genome Project collection of Borkovich lab were assembled for the series of phenotypic assays; they were cultured on VM agar slants to assess their general growth phenotype (Figure 2).

Apical extension rates of the deletion mutants were examined on VM plates (Figure 3). Δ*NCU00636* and Δ*NCU03530* grew at a similar apical extension rate as the wild-type. Δ*NCU01162* and Δ*NCU08131* resembled Δ*ric8* in their apical growth rate. Δ*NCU00455* and Δ*NCU09632* grew slower than wild-type but faster than Δ*ric8*.

The ability of the mutants to act as males or females in sexual crosses was checked (Figure 4). The results indicate that all of the deletion mutant strains are male-fertile. Strains Δ*NCU00636* and Δ*NCU09632* were female-fertile. However, Δ*NCU00455, ΔNCU01162, ΔNCU03530, ΔNCU08131* did not produce any unfertilized female reproductive structures (protoperithecia), similar to Δ*ric8* mutants.

The abundance and height of aerial hyphae, a structure that gives rise to asexual spores (conidia) was assessed in the mutants over a 48-hour period (Figure 5). Strains Δ*NCU03530* and Δ*NCU00636* grew to similar heights as the wild type strain (these deletion mutants appeared to have slightly longer aerial hyphae but were not statistically different from that of wild type). Δ*NCU00455* was shorter than wild-type. Finally, aerial hyphae from strains Δ*NCU01162* and Δ*NCU08131* was very short, just slightly longer than Δ*ric8*.

Submerged hyphae cultures from the mutants were analyzed for phenotypes (data not shown). The mutants appeared normal and none conidiated in submerged conditions, in contrast to Δ*ric8* mutants.

DISCUSSION

I.   GNA-3

Proteins that interact with GNA-3 can be grouped into 3 categories: protein degradation, vesicle trafficking, and ribosome-associated. The proteins that are involved in the protein degradation pathway are NCU00467, NCU05995, and NCU06440. Deletion of NCU00467 leads to shorter aerial hyphae (15), a phenotype also found in Δ*gna-3*.

The category of vesicle trafficking contains proteins NCU00242, NCU02357, NCU02668, and NCU04388. A homolog of NCU00242 in *Magnaporthe orizae*, MoVam7, is required for conidiation; hence, another connection to GNA-3. Without NCU00242, conidiation is blocked. However, when *gna-3* is deleted in *Neurospora*

crassa, hyperconidiation occurs (23), suggesting that GNA-3 may act as a negative regulator of NCU00242.

The third category of proteins includes ribosomal proteins NCU00211, NCU00971, NCU06892, and NCU08389. NCU00211 is interesting in that it is associated with the mitochondrial ribosome. There is not much reported in the literature regarding G-proteins interacting with ribosomal subunits. However, an interesting finding is that RACK1, a protein with WD-domains that is a Gβ homolog (44) is associated with the ribosome (38). In *Neurospora crassa*, CPC-2 is the RACK1 homolog with approximately 70% positional identity to Gβ (37). It is possible that the presence of a β-like protein associated with the ribosome recruits GNA-3 also to the same complex, but further investigation is necessary.

Finally, there are proteins that interact with GNA-3 that do not fall into a large class. Some, such as NCU02998, NCU10058, and NCU06550, are proteins involved in synthesis of a metabolite. NCU09816 encodes a SCOR enzyme involved in oxidation/reduction reactions. NCU10572 encodes a protein involved in mitochondrial electron transport chain. The last interacting protein is NCU02400; this protein has a role in heterokaryotic incompatibility.

One caveat from these results is that Yeast2Hybrid assays have been shown to include false positives. Therefore, further experiment must be conducted to verify interaction between GNA-3 and the interactors.

II.   RIC8

The genes encoding 6 out of 8 hits that interacted with RIC8 had already been mutated by the *Neurospora* Genome project. Of the other 2 genes, NCU11324 and NCU10207, the latter was removed from gene annotation from the *Neurospora crassa* genome project in the latest version (Annotation 5). Hence, these 2 were not included in the phenotypic assays. Also, Δ*NCU00455* obtained from the Fungal Genetics Stock Center turned out to be a heterokaryon (which was confirmed by a Southern blot analysis). Therefore, a new knockout mutant strain was made and confirmed to be a homokaryon by Southern blot analysis (detailed in chapter 5).

Δ*NCU03530* resembles the wild-type strain in growth assays (apical extension and aerial hyphae) but is female-sterile; this mutant is blocked at the step of producing protoperithecia. This suggests that this anchored cell wall protein is involved in female fertility, particularly for producing protoperithecia.

NCU01162 is crucial for remodeling of the fungal cell wall; (1,3)-glucanase/transglycosidase activity necessary for cell wall remodeling and attachment of membrane protein anchoring function is crucial for cell wall integrity. Lacking this protein would lead to a severe growth defect. This is evident from the apical extension and the aerial hyphae assays, in which the Δ*NCU01162* showed the greatest defects. Its phenotypic similarity to Δ*ric8* is a good indication that the positive Y2H result is valid; RIC8 may interact with this protein to regulate growth of hyphae.

Disruption of female fertility could be due to the fact that Δ*NCU01162* is required for a great portion of cell wall generation, and that this disruption leads to failure to construct

126

cell wall. Hence, structure formation (such as protoperithecia and trichogynes) could be impaired, effectively blocking female fertility.

The significance of the interaction between RIC8 and protein product of NCU08131 is that this protein is a major player in the cell wall synthesis in filamentous fungi. Doung showed that in *Aspergillus fumigatus*, lacking the α-amylase leads to lack of α-1,3 glucans from the cell wall (10). Such a significant detriment to the cell wall explains the poor growth of this deletion mutant. Furthermore, lacking RIC8 (which interacts with NCU08131) leads to massive growth defect, leading to structures that are poorly developed.

NCU00636 is a bit unusual, in that this interaction is occurring in the mitochondrion. Also, there are no references for RIC8 localizing to the mitochondrion. Therefore, it seems unlikely that this Yeast2Hybrid result is valid. Phenotypic analysis also supports this view. Δ*NCU00636* strain behaves like wild-type strain in that it has similar apical extension rate and aerial hyphae growth rate, as well as female fertility.

A certain picture begins to take shape, based on the predicted roles of these interactors. NCU08131, NCU01162, and NCU03530 are genes that produce proteins that are, in some respect, responsible for cell-wall synthesis. It is possible that RIC8 is involved in guiding this process, especially pertaining to asymmetric growth.

One interesting possibility from the "hits" identified from the RIC8 Y2H assay is *ncu10207*. Because it is so short (only 129 bp in length), there is potential that it could be a ligand for RIC8. By comparison, two pheromones (modified polypetides) CCG-4 and MFA-1 are 900 bp and 75 bp long, respectively (24).

It is difficult to make more specific predictions regarding the interaction because of the preliminary nature of the results. Greater delving into the functions of the interacting protein as well as confirmation of the interaction (utilizing co-immunoprecipitation or other methods) must be performed.

Table 1. List of plasmids used for this work.

Borkovich lab #	name	type	marker	comment	source
86	pHK11	pGBKT7	Kan^R	*gna-3* cDNA	HyoJeong Kim
173	pSM24	pGBKT7	Kan^R	*ric8* cDNA	Sara Wright

Table 2. List of yeast strains used for this work.

Borkovich lab strain #	name	genotype	comment	source
1	AH109	*his3, trp1-901,ade2-101,leu2-3-112*		lab strain
2	Y187	*his3, trp1-901,ade2-101,leu2-3-112*		lab strain
86	HK11	Y187 + trp	*ric8* cDNA	Sara Wright
173	pSM24	pGBKT7	*ric8* cDNA	Sara Wright
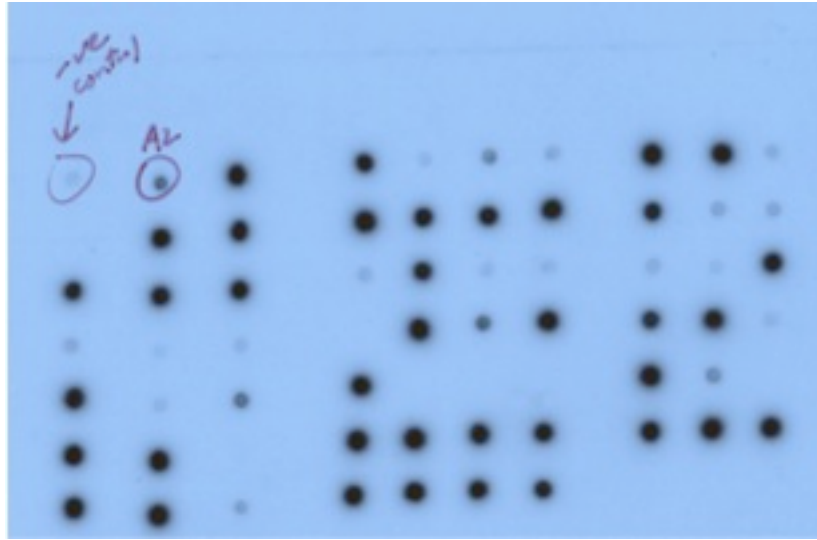
Figure 1. Dot-blot analysis of plasmids containing genes that are potential interactors with RIC8. The top left position on the membrane is spotted with the negative control (empty vector). Just to the right is spotted the positive control (1μl of purified vector that positively interacted with RIC8 in the Y2H assay (designated as "A2" in this example)). Any spot (designated with a vector that is a positive interactor of RIC8) that shows a signal as strong or stronger than the positive control is concluded to be the same gene.
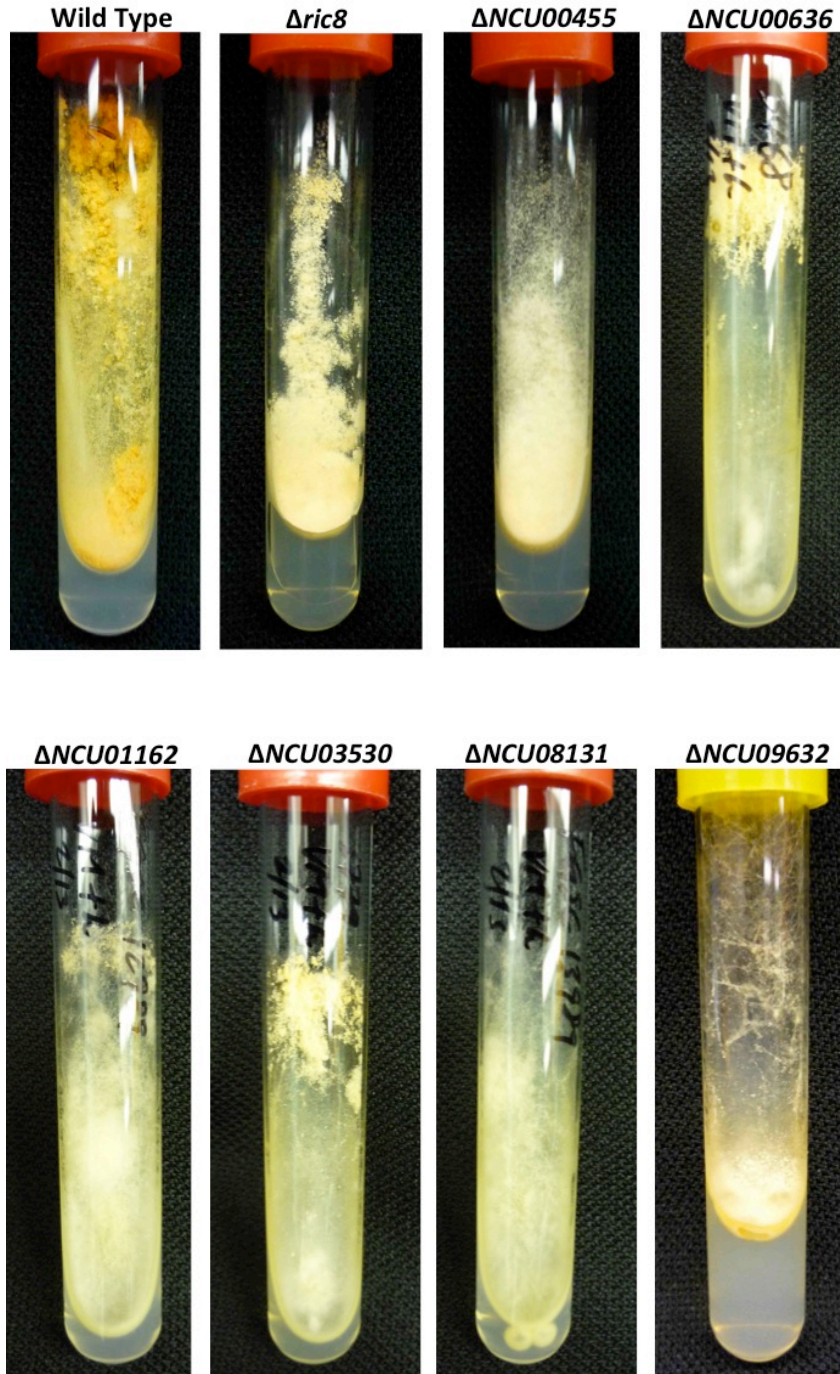
Figure 2. Slant cultures of deletion mutants in genes encoding proteins that interact with RIC8 in the Yeast 2 Hybrid assay. The deletion mutants were grown in VM-slanted agar in 13X100mm test tubes. These cultures were grown at 30°C, without light for 2 days. They were then moved to room temperature, with ~12hour photoperiod for 3 more days of incubation before being photographed.

Table 3. GNA-3 interactors identified through Yeast2Hybrid assay. There were 22 hits from screening the *N. crassa* cDNA library using GNA-3 as bait. Out of these 22, 5 were hypothetical proteins. The rest are described in detail in subsection I of the Results section. NCU# column is the gene number designated from the *Neurospora crassa* genome. "# of hits" refers to the number of clones containing the gene.

NCU #	Gene ID	# of hits
00211	*mitochondrial ribosomal protein subunit L31*	1
00242	*v-snare*	1
00467	*csn-5*	1
00971	*ribosomal protein S12*	4
02357	*importin subunit beta-3*	1
02400	*metacaspase-1B*	1
02668	*cell-wall synthesis protein*	2
02998	*nicotinate-nucleotide pryphosphrylase*	1
03365	*conserved hypothetical protein*	1
03735	*conserved hypothetical protein*	3
03857	*conserved hypothetical protein*	1
04388	*phosphotidylglycerol/phosphatidylinositol transfer protein*	1
05995	*ubiquitin*	2
06440	*proteasome component PRE6*	1
06550	*pyridoxine 1*	1
06892	*40S ribosomal protein S20*	13
08389	*60S ribosomal protein L20*	1
09174	*hypothetical protein*	1
09816	*cytochrome c1*	1
10058	*phosphoglycomutase 2*	2
10572	*short chain oxidoreductase*	1
10747	*conserved hypothetical protein*	1

Table 4. RIC8 interactors identified through Yeast2Hybrid assay. There were 8 hits from screening the *N. crassa* cDNA library screening using RIC8 as bait. These are described in detail in subsection II of the Results section. NCU# column is the gene number designated from the *Neurospora crassa* genome. "# of hits" refers to the number of clones containing the gene.

NCU #	Gene ID	# of hits
01162	Similar to 1,3-β-glucanotransferase Gel1	48
03530	protein containing CFEM domain	9
11324	protein containing PX domain	6
00636	ATP synthase D chain, mitochondrial	3
09632	phosphodiesterase/alkaline phosphatase D precursor	2
08131	Conserved hypothetical protein (alpha-amylase)	1
10207	Predicted protein (no homology in GenBank)	1
00455	MAPKKK cascade protein kinase regulator Ste50 (*Aspergillus fumigatus*)	1
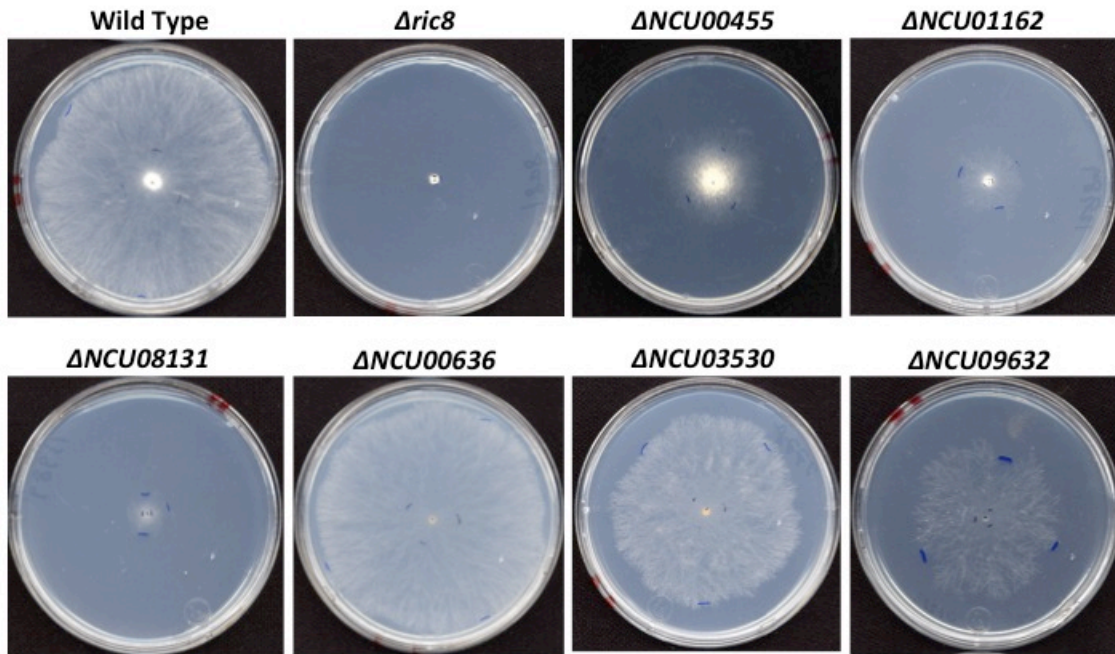
Figure 3. Colony morphology assay of deletion mutants of genes that interacts with RIC8 in Yeast2Hybrid assay. Cultures were inoculated in the center of 30 ml of VM-agar plates and incubated at 30°C, dark conditions. The pictures of each plate were taken 24 hours after inoculation.

ΔNCU01162

ΔNCU08131

ΔNCU00455

ΔNCU03530

ΔNCU09632

ΔNCU00636
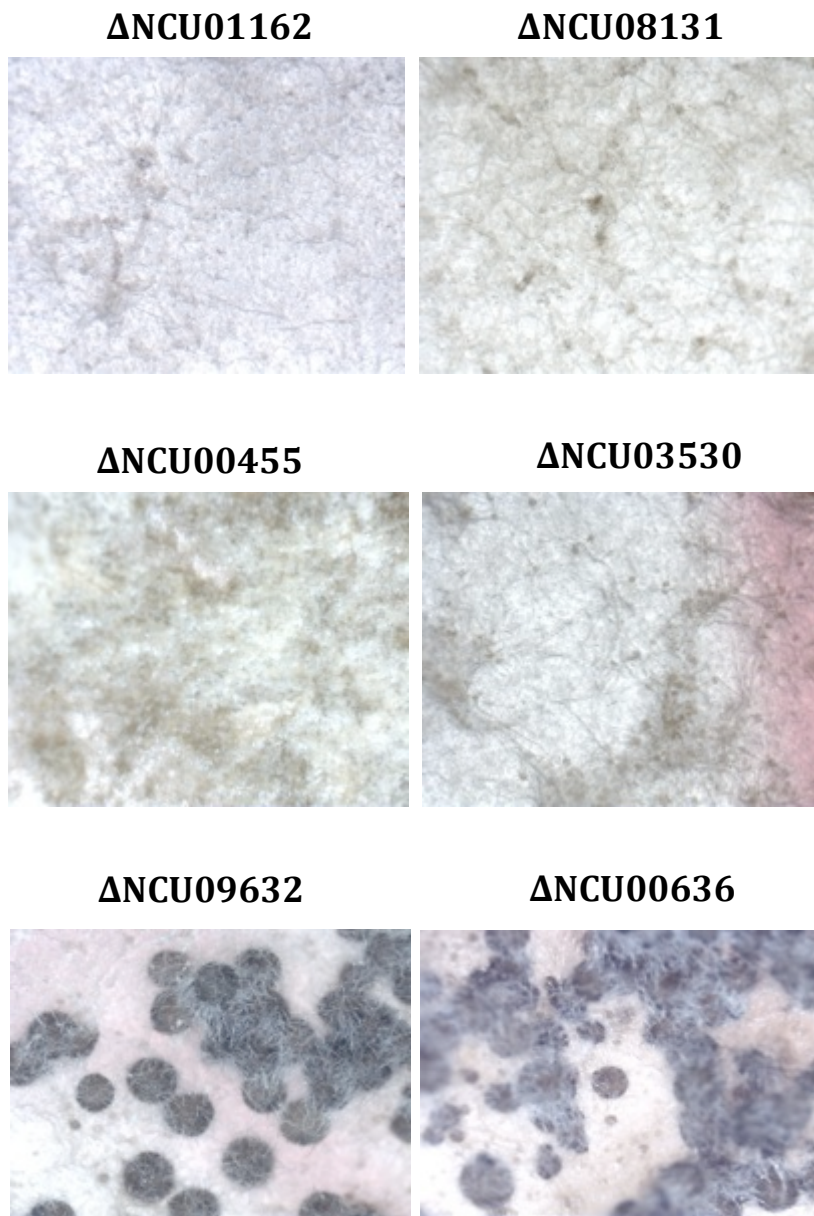
Figure 4. Female fertility assay of the deletion mutants of RIC8 interactors after they were fertilized. The cultures of the deletion mutants were inoculated onto 30ml SCM-agar plates and incubated at 25°C in constant light for 9 days. The plates were checked for development of protoperithecia under a dissection microscope. Finally, using a sterile cotton swab, wild-type conidia of the opposite mating type were rubbed onto the surface of the SCM plates to ensure good contact with the protoperithecia for a successful fertilization (this was done even to the plates of the deletion mutants that didn't show any protoperithecia).
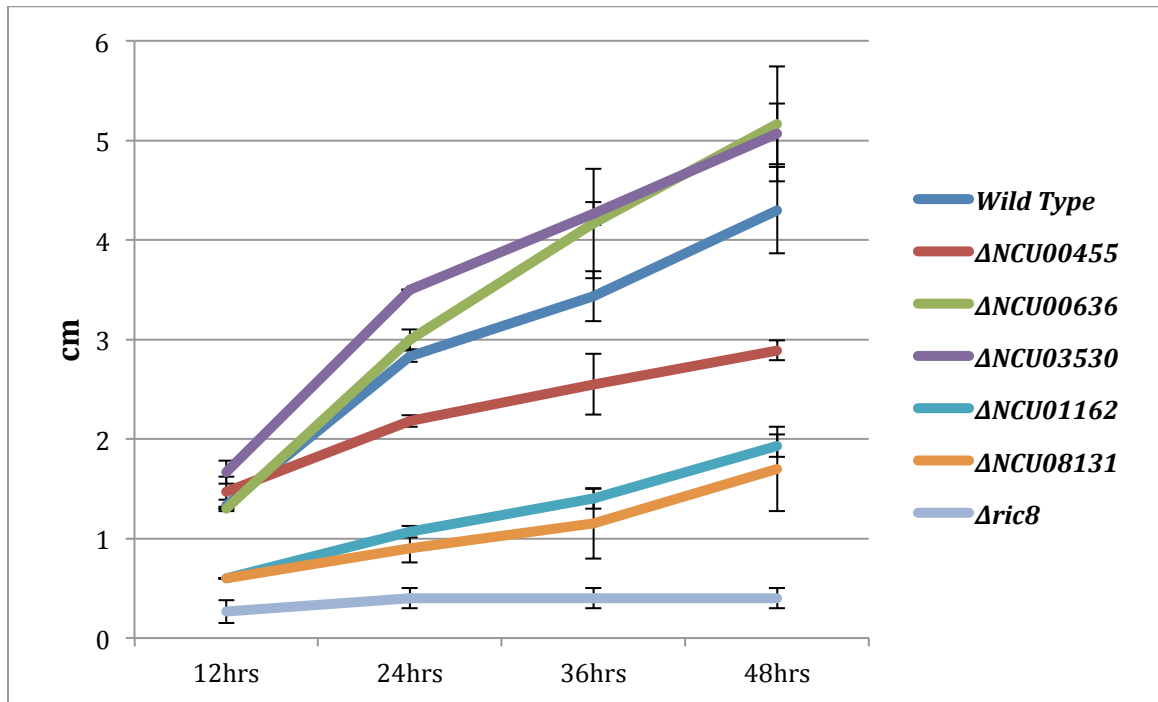
Figure 5. Aerial hyphae height assay of deletion mutants in RIC8 interactors. One ml of VM-liquid medium was dispensed into a 10x13 mm test tube and inoculated with each strain to make a concentration of $1x10^6$ conidia/ml. Each strain was tested in triplicate. The height of the aerial hyphae were marked after each 12 hour period. Error bars indicate one standard deviation.

REFERENCES

1. **Bahn Y.S., C. Xue, A. Idnurm, J. C. Rutherford, J. Heitman, and M. E. Cardenas**. 2007. Sensing the environment: lessons from fungi. Nature Reviews. Microbiology **5**:57-69.

2. **Bean L. E., W. H. Dvorachek, E. L. Braun, A. Errett, G. S. Saenz, M. D. Giles, M. Werner-washburne, M. A. Nelson, and D. O. Natvig**. 2001. Analysis of *pdx-1* (*snz-1/sno-1*) Region of the *Neurospora crassa* Genome: Correlation of Pyridoxine-Requiring Phenotypes With Mutations in Two Structural Genes. Genetics **157**:1067-1075.

3. **Borkovich K. A., L. A. Alex, O. Yarden, M. Freitag, G. E. Turner, N. D. Read, S. Seiler, D. Bell-pedersen, J. Paietta, N. Plesofsky, M. Plamann, M. Goodrich-tanrikulu, U. Schulte, G. Mannhaupt, F. E. Nargang, A. Radford, C. Selitrennikoff, J. E. Galagan, J. C. Dunlap, J. J. Loros, D. Catcheside, H. Inoue, R. Aramayo, M. Polymenis, E. U. Selker, M. S. Sachs, G. A. Marzluf, I. Paulsen, R. Davis, D. J. Ebbole, A. Zelter, E. R. Kalkman, R. O. Rourke, and F. Bowring**. 2004. Lessons from the Genome Sequence of *Neurospora crassa*: Tracing the Path from Genomic Blueprint to Multicellular Organism. Microbiology and Molecular Biology Reviews **68**:1-108.

4. **Braun E. L., E. K. Fuge, P. A. Padilla, and M. Werner-Washburne**. 1996. A stationary-phase gene in *Saccharomyces cerevisiae* is a member of a novel, highly conserved gene family. Journal of Bacteriology **178**:6865-72.

5. **Brody S., and E. L. Tatum**. 1967. Phosphoglucomutase mutants and morphological changes in *Neurospora crassa*. Proceedings of the National Academy of Sciences of the United States of America **58**:923-930.

6. **Carmona-Gutierrez D., K.U. Fröhlich, G. Kroemer, and F. Madeo**. 2010. Metacaspases are caspases. Doubt no more. Cell Death and Differentiation **17**:377-8.

7. **Dequard-Chablat M., and C. H. Sellem**. 1994. The S12 ribosomal protein of *Podospora anserina* belongs to the S19 bacterial family and controls the mitochondrial genome integrity through cytoplasmic translation. The Journal of Biological Chemistry **269**:14951-6.

8. **Dou X., Q. Wang, Z. Qi, W. Song, W. Wang, M. Guo, H. Zhang, Z. Zhang, P. Wang, and X. Zheng**. 2011. MoVam7, a Conserved SNARE Involved in Vacuole Assembly, Is Required for Growth, Endocytosis, ROS Accumulation, and Pathogenesis of *Magnaporthe oryzae*. PloS One **6**:e16439.

9. **Duax W. L., V. Pletnev, A. Addlagatta, J. Bruenn, and C. M. Weeks**. 2003. Rational proteomics I. Fingerprint identification and cofactor specificity in the short-chain oxidoreductase (SCOR) enzyme family. Proteins **53**:931-43.

10. **Duong K. L.** 2010. Master's Thesis. Amylases and *Aspergillus fumigatus* cell wall synthesis : new roles for classical enzymes. University of Iowa. Iowa.

11. **Fatica A., and D. Tollervey**. 2002. Making ribosomes. Current Opinion in Cell Biology **14**:313-8.

12. **Fields S., and O.-K. Song**. 1989. A novel genetic system to detect protein-protein interactions. Nature **340**:245-246.

13. **Foster J. W., and A. G. Moat**. 1980. Nicotinamide adenine dinucleotide biosynthesis and pyridine nucleotide cycle metabolism in microbial systems. Microbiological Reviews **44**:83-105.

14. **Fratti R. A., and W. Wickner**. 2007. Distinct targeting and fusion functions of the PX and SNARE domains of yeast vacuolar Vam7p. The Journal of Biological Chemistry **282**:13133-8.

15. **He Q., P. Cheng, Q. He, and Y. Liu**. 2005. The COP9 signalosome regulates the *Neurospora* circadian clock by controlling the stability of the SCFFWD-1 complex. Genes & Development **19**:1518-31.

16. **Heinemeyer W., N. Troendle, G. Albrecht, and D. H. Wolf**. 1994. PRE5 and PRE6, the Last Missing Genes Encoding 20S Proteasome Subunits from Yeast? Indication for a Set of 14 Different Subunits in the Eukaryotic Proteasome Core. Biochemistry **33**:12229-12237.

17. **Hicke L., and H. Riezman**. 1996. Ubiquitination of a yeast plasma membrane receptor signals its ligand-stimulated endocytosis. Cell **84**:277-87.

18. **Hilt W., and D. H. Wolf**. 1996. Proteasomes: destruction as a programme. Trends in Biochemical Sciences **21**:96-102.

19. **Hutchison E., S. Brown, C. Tian, and N. L. Glass**. 2009. Transcriptional profiling and functional analysis of heterokaryon incompatibility in *Neurospora crassa* reveals that reactive oxygen species, but not metacaspases, are associated with programmed cell death. Microbiology **155**:3957-70.

20. **Jacoby E., R. Bouhelal, M. Gerspacher, and K. Seuwen**. 2006. The 7 TM G-protein-coupled receptor target family. ChemMedChem **1**:761-82.

21. **Jang S., K. An, S. Lee, and G. An**. 2002. Characterization of tobacco MADS-box genes involved in floral initiation. Plant & Cell Physiology **43**:230-8.

22. **Jiang M., S. M. Sullivan, P. K. Wout, and J. R. Maddock**. 2007. G-protein control of the ribosome-associated stress response protein SpoT. Journal of Bacteriology **189**:6140-7.

23. **Kays A. M., P. S. Rowley, R. A. Baasiri, and K. A. Borkovich**. 2000. Regulation of conidiation and adenylyl cyclase levels by the Gα protein GNA-3 in *Neurospora crassa*. Molecular and Cellular Biology **20**:7693-705.

24. **Kim H. J., and K. A. Borkovich**. 2006. Pheromones are essential for male fertility and sufficient to direct chemotropic polarized growth of trichogynes during mating in *Neurospora crassa*. Eukaryotic Cell. Am Soc Microbiol **5**:544-554.

25. **Koga T., M. Onishi, Y. Nakamura, A. Hirata, T. Nakamura, C. Shimoda, T. Iwaki, K. Takegawa, and Y. Fukui**. 2004. Sorting nexin homologues are targets of phosphatidylinositol 3-phosphate in sporulation of *Schizosaccharomyces pombe*. Genes to Cells **9**:561–574.

26. **Kulkarni R. D., M. R. Thon, H. Pan, and R. A. Dean**. 2005. Novel G-protein-coupled receptor-like proteins in the plant pathogenic fungus *Magnaporthe grisea*. Genome Biology **6**:R24.

27. **Legrain P., and L. Selig**. 2000. Genome-wide protein interaction maps using two-hybrid systems. FEBS Letters **480**:32-6.

28. **Li J., and I. Herskowitz**. 1993. Isolation of ORC6, a component of the yeast origin recognition complex by a one-hybrid system. Science **262**:1870-1874.

29. **Li Y., K. Leonard, and H. Weiss**. 1981. Membrane-Bound and Water-Soluble Cytochrome c1 From *Neurospora* Mitochondria. European Journal of Biochemistry **116**:199-205.

30. **Licitra E. J., and J. O. Liu**. 1996. A three-hybrid system for detecting small ligand-protein receptor interactions. Proceedings of the National Academy of Sciences of the United States of America **93**:12817-21.

31. **Liebman S. W., Y. O. Chernoff, and R. Liu**. 1995. The accuracy center of a eukaryotic ribosome. Biochem. Cell Biol. **73**:1141-1149.

32. **Maddi A., S. M. Bowman, and S. J. Free**. 2009. Trifluoromethanesulfonic acid-based proteomic analysis of cell wall and secreted proteins of the ascomycetous fungi Neurospora crassa and Candida albicans. Fungal Genetics and Biology **46**:768-81.

33. **Managadze D.** 2007. Ph.D. Thesis. Biogenesis of Microbodies in the Filamentous Fungus *Neurospora crassa*. October. Ruhr University of Bochum. Bochum, Germany.

34. **Medina-Redondo M. de, Y. Arnáiz-Pita, C. Clavaud, T. Fontaine, F. del Rey, J. P. Latgé, and C. R. Vázquez de Aldana**. 2010. β(1,3)-glucanosyl-transferase activity is essential for cell wall integrity and viability of *Schizosaccharomyces pombe*. PloS One **5**:e14046.

35. **Miller K. G., and J. B. Rand**. 2000. A Role for RIC-8 (Synembryn) and GOA-1 (GoA) in Regulating a Subset of Centrosome Movements During Early Embryogenesis in *Caenorhabditis elegans*. Genetics **156**: 1649-1660.

36. **Mishra N. C., and E. L. Tatum**. 1970. Phosphoglucomutase mutants of *Neurospora sitophila* and their relation to morphology. Proceedings of the National Academy of Sciences of the United States of America **66**:638-45.

37. **Müller F., D. Krüger, E. Sattlegger, B. Hoffmann, P. Ballario, M. Kanaan, and I. B. Barthelmess**. 1995. The *cpc-2* gene of *Neurospora crassa* encodes a protein entirely composed of WD-repeat segments that is involved in general amino acid control and female fertility. Molecular & General Genetics **248**:162-73.

38. **Nilsson J., J. Sengupta, J. Frank, and P. Nissen**. 2004. Regulation of eukaryotic translation by the RACK1 protein: a platform for signalling molecules on the ribosome. EMBO Reports **5**:1137-41.

39. **Omi K., H. Sonoda, K. Nagata, and K. Sugita**. 1999. Cloning and characterization of psu1(+), a new essential fission yeast gene involved in cell wall synthesis. Biochemical and Biophysical Research Communications **262**:368-74.

40. **Ozenberger B. A., and K. H. Young**. 1995. Functional interaction of ligands and receptors of the hematopoietic superfamily in yeast. Molecular Endocrinology **9**:1321-1329.

41. **Radford A., T. Beck, J. Davies, and N. Navarro-Coy**. 2000. The *Neurospora crassa* e-Compendium.

42. **Record E., S. Moukha, and M. Asther**. 2001. Cloning and expression in phospholipid containing cultures of the gene encoding the specific phosphatidylglycerol/phosphatidylinositol transfer protein from *Aspergillus oryzae*: evidence that the pg/pi-tp is tandemly arranged with the putative 3-ket. Gene **262**:61-72.

43. **Reddy N. S., A. Nimmagadda, K. R. S. S. Rao, C. Biotechnology, and N. Nagar**. 2003. An overview of the microbial α-amylase family. African Journal of Biotechnology **2**:645-648.

44. **Rodriguez M. M., D. Ron, K. Touhara, C.-H. Chen, and D. Mochly-Rosen**. 1999. RACK1, a Protein Kinase C Anchoring Protein, Coordinates the Binding of Activated Protein Kinase C and Select Pleckstrin Homology Domains in Vitro. Biochemistry **38**:13787-13794.

45. **Rolli E., E. Ragni, M. de Medina-Redondo, J. Arroyo, C. R. V. de Aldana, and L. Popolo**. 2011. Expression, stability and replacement of glucan remodelling enzymes during developmental transitions in *Saccharomyces cerevisiae*. Molecular Biology of the Cell **22**:1585-1598.

46. **Sato M., Y. Saeki, K. Tanaka, and Y. Kaneda**. 1999. Ribosome-associated protein LBP/p40 binds to S21 protein of 40S ribosome: analysis using a yeast two-hybrid system. Biochemical and Biophysical Research Communications **256**:385-90.

47. **Seet L.-F., and W. Hong**. 2006. The Phox (PX) domain proteins and membrane traffic. Biochimica et Biophysica Acta **1761**:878-96.

48. **SenGupta D. J., B. Zhang, B. Kraemer, P. Pochart, S. Fields, and M. Wickens**. 1996. A three-hybrid system to detect RNA-protein interactions in vivo. Proceedings of the National Academy of Sciences of the United States of America **93**:8496-501.

49. **Staudinger J., M. Perry, S. J. Elledge, and E. N. Olson**. 1993. Interactions among vertebrate helix-loop-helix proteins in yeast using the two-hybrid system. The Journal of Biological Chemistry **268**:4608-11.

50. **Taccioli G. E., E. Grotewold, G. O. Aisemberg, N. D. Judewicz, V. D. Obligado, and B. Aires**. 1989. Ubiquitin expression in *Neurospora crassa*: cloning and sequencing of a polyubiquitin gene. Nucleic Acids Research **17**:6153-6165.

51. **Torres M. P., S. T. Clement, S. D. Cappell, and H. G. Dohlman**. 2011. Cell cycle-dependent phosphorylation and ubiquitination of a G protein α subunit. The Journal of Biological Chemistry **286**:20208-16.

52. **Viebrock A., A. Perz, and W. Sebald**. 1982. The imported preprotein of the proteolipid subunit of the mitochondrial ATP synthase from *Neurospora crassa*. Molecular cloning and sequencing of the mRNA. The EMBO Journal **1**:565-71.

53. **Wang H., K. H. Ng, H. Qian, D. P. Siderovski, W. Chia, and F. Yu**. 2005. Ric-8 controls *Drosophila* neural progenitor asymmetric division by regulating heterotrimeric G proteins. Nature Cell Biology **7**:1091-8.

54. **Wang J., Q. Hu, H. Chen, Z. Zhou, W. Li, Y. Wang, S. Li, and Q. He**. 2010. Role of Individual Subunits of the *Neurospora crassa* CSN Complex in Regulation of Deneddylation and Stability of Cullin Proteins. PLoS Genetics **6**:e1001232.

55. **Williams E. H., X. Perez-Martinez, and T. D. Fox**. 2004. MrpL36p, a highly diverged L31 ribosomal protein homolog with additional functional domains in *Saccharomyces cerevisiae* mitochondria. Genetics **167**:65-75.

56. **Wirtz K. W.** 1991. Phospholipid transfer proteins. Annual Review of Biochemistry **60**:73-99.

57. **Wright S. J., R. Inchausti, C. J. Eaton, S. Krystofova, and K. A. Borkovich**. 2011. RIC8 is a Guanine-nucleotide Exchange Factor for Gα Subunits that Regulates Growth and Development in *Neurospora crassa*. Genetics **189**:1-45.

58. **Xu D., A. Farmer, and Y. M. Chook**. 2010. Recognition of nuclear targeting signals by Karyopherin-β proteins. Current Opinion in Structural Biology **20**:782-90.

59. **Young K. H.** 1998. Yeast two-hybrid: so many interactions, (in) so little time... Biology of Reproduction **58**:302-11.

60. **Yuan P., G. Jedd, D. Kumaran, S. Swaminathan, H. Shio, D. Hewitt, N.-H. Chua, and K. Swaminathan**. 2003. A HEX-1 crystal lattice required for Woronin body function in *Neurospora crassa*. Nature Structural Biology **10**:264-70.

Chapter 5: Characterization of STE50, a MAPK adaptor protein that interacts with a novel GEF, RIC8, in *Neurospora crassa*

INTRODUCTION

Originally identified in *Saccharomyces cerevisiae*, STE50 is an adaptor protein (20) integral to Mitogen Activated Protein Kinase (MAPK) signaling that is involved in the pheromone sensing pathway, pseudohyphal growth/invasive, filamentous growth pathway, and the osmosensing pathway (9, 20). *ste50* is composed of a Ras-like (RA) domain located on the N-terminus (30) and a Sterile-Alpha Motif (SAM) domain that is located on the C-terminus (33). The SAM domain is conserved and often involved in protein-protein interactions and signal transduction, mediating homo- and heterodimerization. In fact, more than 300 proteins that possess this motif are involved in signal transduction and transcriptional activation/repression. NMR structural analysis has shown that the SAM domain of Ste50p shares the same folding structure as that of Ste11p (33). Using NMR, the authors were able to deduce that monomeric Ste50p is able to bind dimeric Ste11p, ultimately forming a heterotrimeric complex. They also postulated that the SAM-SAM interaction between Ste50p and Ste11p could be activating Ste11p by keeping it in a conformation that perpetuates the MAPK signal. There are homologs of STE50 in both Ascomycete and Basidiomycete fungi. In the latter, STE50 also possesses a SH3 domain, which is crucial for infection in some fungal pathogens, such as *Ustilago maydis* (14).

Cdc42p is a Rho-type small G-protein that is anchored to the membrane by prenylation (11) in *S. cerevisiae*. Cdc42p binds to Ste50p using the RA domain, causing the Ste50p-Ste11p complex to translocate to the plasma membrane; interestingly, this contact can occur whether Cdc42 is GDP or GTP-bound. This membrane tethering of the Ste50p-Ste11p complex due to interaction with Cdc42p is crucial for signaling in the filamentous growth and HOG signaling pathways (30); without Ste50p, filamentous growth of *S. cerevisiae* is halted (30). Cdc42p also binds to Ste20p, a PAK (p21-activated protein kinase)-like kinase, and activates it (29). Hence, the role of Cdc42p is to bring the Ste50p-Ste11p complex to the PAK-like kinase at the membrane, acting as a bridge between the two components. Activated Sho1p (a membrane protein that functions as an osmosensor and is required for the HOG pathway) will bind to the Ste50p-Ste11p complex and also to the MAPKK Pbs2p, allowing Ste11p to phosphorylate Pbs2p (29). This leads to a signal transduction cascade, whereby transcription factors activate transcription of genes responsible for production of glycerol, offsetting the harmful effects of solutes in the environment that are responsible for osmotic stress (26). Thus, the major role of Ste50p is to bind Ste11p (MAPKKK) using the SAM-SAM interaction and bring it to the plasma membrane for interaction with Cdc42p by its RA-domain.

Non-MAPK components have also been implicated in protein-protein interactions with STE50p. In *S. cerevisiae*, an integral membrane protein called Opy2p physically interacts with Ste50p in Yeast2Hybrid and co-immunoprecipitation assays (33). GFP-tagged Opy2p is localized to the cell periphery, indicating that Opy2p is a membrane

protein. This association is important for the HOG pathway, because it provides a way

for Ste50p to be recruited to the plasma membrane to carry out its function. The C-

terminal RA-like domain of Ste50p physically and constitutively interacts with the C-

terminal region of Opy2p, termed as SID (Ste50-Interacting Domain). A more detailed

description of Opy2p divided the protein into 4 regions: short conserved regions A, B, C,

D that can interact with Ste50p (35); depending on which SID region is bound by Ste50p,

Opy2p can have a positive or a negative influence on the function of Ste50p. Since

Opy2p has a single transmembrane domain, interaction with it will bring Ste50 to the

plasma membrane (6). When Ste50p (associated with Ste11p (MAPKKK)) is present at

the membrane, it can then interact with Sho1p, to transduce signals that lead to activation

of the HOG pathway in *S. cerevisiae*. However, when Ste50p is bound to Conserved

Region-B of Opy2p, it does not interact with the Ste7p (MAPKK), disrupting the HOG

pathway. Hence, Opy2p has a significant effect on activation of Ste50p in yeast.

Recently, it has been shown that Ste50p can be phosphorylated and that this leads

to its activation in yeast (9). Initially, it was reported that this phosphorylation was due to

the Hog1p MAPK, and that this phosphorylation event limits the duration of pathway

activation; acting as a negative feedback loop that makes sure that MAPK pathway is

tightly controlled. However, new report indicates that Ste50p can be phosphorylated by

other MAPKs, such as Fus1p or Kss1p (35). Furthermore, phosphorylation of Ste50p

prevents it from binding to three sites on Opy2p that act as a positive regulator (35). This

could have a negative effect on the osmosensing pathway. For the Hog1p MAPK

pathway, phosphorylation of Ste50p leads to shortening the duration of Hog1p activation

after osmotic stress. As for the pheromone sensing MAPK pathway, phosphorylation of Ste50p leads to a reduced state of activation without external stimulus.

MST50, a Ste50 homolog in the rice blast fungus *Magnaporthe grisea,* has also been characterized (36). It was shown by Yeast2Hybrid assay that MST50 interacts strongly with the MAPKK MST7 (a Ste7 homolog) and weakly with the MAPKKK MST11 (similar to Ste11p in *S. cerevisiae* and NRC-1 in *N. crassa*) (36). The authors postulate that MST50 could be facilitating the formation of a complex that brings MST11 (MAPKKK) and MST7 (MAPKK) together for interaction. Without MST50, the fungus is not able to infect rice leaves (19) because it is not able to form an appressorium, a specialized cell-type that is able to adhere to surface of the rice plant leaf and penetrate the cell to initiate the infection process.

In *Cryptococcus neoformans*, an opportunistic, yeast-like fungal pathogen that preys on immunocompromised animal hosts, STE50 interacts with both STE11 (MAPKKK) and STE20, an upstream PAK kinase in the pheromone response pathway (8). This was shown using a Yeast2Hybrid assay, where only the region of STE20 that includes the CRIB and PH domains was used in order to prevent a conformation that would block interaction (8). In addition to the SAM and RA-like domains, *C. neoformans* STE50 also has two SRC Homology 3 (SH3) domains, commonly found in basidiomycete STE50 proteins (8). It was shown that STE50 is required for cell fusion, sexual filamentation, sexual reproduction, and response to pheromone in *C. neoformans*.

Recent findings in the yeast *Kluyveromyces lactis* showed that STE50 interacts with the Gα subunit of a heterotrimeric G-protein (28). Sanchez-Paredes *et al.* (2011)

demonstrated that STE50 interacts with both forms of the Gα subunit, inactive (GTP-bound) and the active (GDP-bound); however, STE50 interacts more strongly with the GTP-bound form of Gα. This capability of STE50 to recognize the active vs. inactive form of Gα makes it a sensitive modulator of the mating response in *K. lactis*. Interestingly, the authors also showed that Gα binds to both the RA domain and the SAM domain of Ste50p. In *K. lactis*, the mating pathway is stimulated partly by interaction of the Gα subunit and Ste50p. Deletion of *ste50* leads to a 50% reduction in mating (28). This is because the Gα subunit brings Ste50p to the membrane where it can interact with the components of the MAPK pathway, increasing the intensity of the signal.

In mammalian cells, a protein called OSM (Osmosensing Scaffold for MEKK3) operates similarly to STE50 in the osmosensing pathway (31). It physically interacts with MEKK3 (STE11 homolog) and MKK3 (STE20 homolog) to regulate signal transduction during hyperosmotic shock by activating p38 MAPK, the mammalian homolog of Hog1, as demonstrated by Bimolecular Fluorescence Complementation (BiFC) and co-immunoprecipitation (31). Also, its localization pattern is very much like that of *Saccharomyces cerevisiae* Ste50p; when tagged with GFP, the protein is diffusely localized throughout the cell. However, with hyperosmotic shock, the GFP signal localizes to the plasma membrane, specifically to ruffle-like structures. Finally, OSM was shown to interact with both GDP and GTPγS-loaded small GTPase Rac1 (31); this is quite similar to the way Ste50p of *Saccharomyces cerevisiae* interacts with Cdc42. Hence, the role of OSM is similar to its fungal counterparts in that it is necessary for osmoregulation by MEKK3-mediated activation of p38, the Hog1 homolog in yeast. The

148

model for the signal transduction cascade activated by osmotic stress in mammalian cells flows from RAC (GTPase) that regulates the OSM/MEKK3 complex to activate MKK3, which in turn activates p38, leading to transcription of genes necessary for osmoregulation.

One phenotype associated with the MAPKs in filamentous fungi is cell-cell fusion (24). *N. crassa* forms specialized cells called Conidial Anastomosis Tubes (CATs) during conidial germination (25). CATs of adjacent germlings home towards one another, facilitating cell fusion. These CATs are distinct from germ tubes which are thicker, display indeterminant growth, and branch. CATs, on the other hand, are thinner and shorter (>15μm), display determinant growth, and do not branch. Furthermore, mutants known to be defective in hyphal fusion are also defective in CAT fusion, in that they are not able to detect the chemical signal from other CATs and so do not fuse. These mutants include Δ*mak-2* (MAPK) and Δ*nrc-1* (MAPKKK).

In this chapter, I present analysis of the STE50 protein from *N. crassa*. From a Yeast-two-hybrid (Y2H) screen of a cDNA library made from *Neurospora crassa*, using a novel guanine nucleotide exchange factor RIC8 as "bait", several interacting proteins were identified, one of which was STE50. I characterized a Δ*ste50* knockout mutant and demonstrated several phenotypes in common with Δ*ric8*. Furthermore, coimmunoprecipitation experiments supported a physical interaction between RIC8 and STE50. Finally, a MAPK assay was done to explore the effect of STE50 on MAK-1 and MAK-2 MAPK pathways.

MATERIALS AND METHODS

Strains and Culture conditions

N. crassa strains used in this study are listed in Table 1. Vegetative hyphae were grown on Vogel's Minimal medium, and sexual crosses were made on SCM medium. Hygromycin B (Calbiochem.) was added at a concentration of 200 μg/ml.

To collect conidia for inoculation, 250 ml flasks containing approximately 50ml of VM agar were inoculated with conidia from the desired strain. After 5 days of growth (2 days at 30°C without light and 3 days at room temperature with 12 hours of light/dark alternating photoperiod), the conidia in the flasks were collected by adding sterile water to the flasks, agitating the flasks with a vortexer, and collecting the conidia by straining the liquid through a sterile layer of shop towel (Chix Masslinn; Benson, NC) over a sterile flask. The liquid containing conidia was transferred to a 50 ml conical tube and centrifuged at 2500 rpm for 5 minutes. Then, the supernatant was poured off, leaving only the conidial pellet. A volume of 1 ml of water was added to the pellet, which was then transferred to a sterile microcentrifuge tube and placed on ice. The conidial suspension was vortexed before removing 10 μl to prepare a 1:100 diluted sample. 10 μl of the dilution was used to estimate the conidia concentration in the stock by placing onto a hemacytometer and counting under a compound microscope at 40X magnification. After calculating the conidial concentration in the stock, a diluted working concentration of 1×10^6 conidia/ml was prepared.

When mating two strains of *N. crassa*, Synthetic Crossing Medium (SCM; recipe for 1 L: 1 g KNO_3, 0.7 g K_2HPO_4, 0.5 g KH_2PO_4, 0.5 g $MgSO_4.7H_2O$, 0.1 g NaCl, 0.1 g

CaCl$_2$.2H$_2$0, 50 µl biotin stock soln, 100 µl trace element stock soln) slant tubes were used. The SCM tubes were inoculated with the strain that would serve as the female and kept at 25°C with constant light for 9 days (or until abundant protoperithecia were visible). Then, a sterile, wet cotton-swab was used to rub clean inside glass area where ascospores would eventually shoot. Afterwards, another sterile, cotton swab was used to rub the conidia from a male strain of opposite mating type onto the agar surface where the protoperithecia protrude. The fertilized SCM crossing tubes were then kept at room temperature with an approximately 12 hours of photoperiod, with the surface of the agar facing the light source (because ascospores are shot towards the light orientation). After approximately two weeks (when ascospores can be seen deposited on the glass surface with the naked eye), a sterile, cotton swab was used to rub a small area of the inside glass and plunged several times into 500 µl of sterile water in a 1.5 ml microcentrifuge tube to dislodge all ascospores. The ascospores were pelleted in the microcentrifuge tube by centrifugation at 500xg for 5 min. The supernatant was pipeted off and more sterile water added to the tubes. The tubes were placed in waterbath set at 60°C for 30 min. Afterwards, the microcentrifuge tubes were allowed to cool to room temperature before centrifugation. The water was pipette off and 500 µl of 0.1% agar solution added (to prevent ascospores from settling). A volume containing 50 µl of this ascospore suspension was pipetted onto the surface of FGS plates, spread and the plate incubated at 30°C in the dark for approximately 24 hours. Then, with the aid of a dissecting microscope and a sterile needle, germinated ascospores were picked and gently placed into a VM-agar slant with the appropriate components.

After transformation of *N. crassa* strain, the microconidiation procedure was

sometimes used to obtain homokaryons. The transformant was inoculated onto a

microconidiation medium (0.1X SCM, 5% sucrose, 2% agar, 1 mM sodium iodoacetate)

and incubated at 25˚C with constant light for 7 days. Then, 1 ml of sterile water was

pipetted into the test tube and the tube vortexed in order to dislodge the microconidia

from the hyphae. Using a sterile, disposable pipet, the liquid was collected and filtered

through a 5 micron syringe-filter. The filtered liquid containing the microconidia was

collected in a sterile microcentrifuge tube, washed by centrifugation and pelleting, and

plated on FGS medium.

Plasmid Construction/procedure

Plasmids were propagated in *E. coli*, DH5α strain. For plasmid extraction, the *E.

coli* strain containing the vector was streaked onto a LB plate containing 100 µg/ml of

ampicillin (or kanamycin, depending on the selectable marker) and incubated overnight at

37˚C. The following day, a sterile toothpick was used to pick a single colony grown on

the LB plate and placed into 5 ml of LB liquid-medium containing 100 µg/ml of

ampicillin and incubated with shaking at 200 rpm for approximately 16 hours at 37˚C.

Plasmids were extracted and purified using Qiagen Miniprep kit (Qiagen Sciences,

Maryland, USA).

Western blotting

Protein samples run on 10% SDS-PAGE gels were electroblotted onto a

nitrocellulose membrane (GE Nitrobind 0.45 micron #EP4HY00010) for 3 hours at 200

mV. After the transfer, the membrane was washed twice in 30 ml TBS for 5 minutes at

room temperature with gentle shaking using an orbital shaker. The membrane was then

blocked in 5% nonfat dry milk dissolved in TBS (20 ml) for 30 minutes at room

temperature with gentle shaking using an orbital shaker. The membrane was incubated

with primary and secondary antibodies and washed, as described in sections, below.

In order to visualize the results of the Western, 1 ml each of the 2 solutions in the

Thermo Scientific Super Signal West Pico Chemiluminescent Substrate kit (Pierce,

Rockford, IL) in a conical tube was mixed. The washed membrane was placed in a clean

plastic box that was large enough to hold the membrane and substrate solution poured

over the blot with a gentle rocking back-and-forth motion. Finally, the substrate solution

was poured off, the membrane lifted using tweezers and the corner of the membrane

blotted on a paper towel. The membrane was sandwiched between two pieces of

transparency film and exposed using a Chemiluminescent Detection System (UVP

Biochemi System).

Generation of Δ*ste50* mutants

Using the gene-replacement approach, *ste50* in *N. crassa* was knocked out using a

hygromycin B phosphotransferase (*hph*) cassette as a replacement at the native locus

according to protocol found in Colot *et al*. (4). Briefly, a knock-out (KO) cassette that

was already designed by the *N. crassa* Genome Project containing approximately one

kilobase upstream and one kilobase downstream of the *ste50* Open Reading Frame (ORF)

was fused to the 5' and 3' ends of the *hph* cassette using yeast recombinational cloning

(23). This method allows for fusion of long DNA fragments into a single fragment by

recombining ends of the fragments where overlap of at least 20 bp exists. When the

DNA fragments are transformed into yeast strain FY384 (along with linearized yeast shuttle-vector pRS426), the yeast cellular machinery is able to recombine the fragments into a circle, which can be extracted from yeast. The recombined insert fragment can then be excised out with an appropriate restriction enzyme or using PCR (Table 2 is a list of all yeast strains used for constructing plasmids and strains). Following this method to produce the knock-out cassette, the digested products were electrophoresed on a 1% agarose gel in TAE buffer. Judging how long to run the gel according to the position of the loading dye, it was stained with ethidium bromide (EtBr) and visualized in a UVP transilluminator (UVP, Upland, CA). The 4473 nucleotide (nt) sized-band representing the *ste50* KO cassette was excised with a razor blade and placed into a microcentrifuge tube. Using Qiagen QIAEX II Gel-Extraction kit (Qiagen, USA), the *ste50* KO cassette was extracted from the agarose block and 1 µl of eluted DNA visualized on an EtBr-stained agarose gel. A volume containing 10 µl of *Hin*dIII-digested λ gDNA was loaded into a lane of the same gel so that the amount of cassette present in 1 µl could be compared with digested bands of the λ genomic DNA and the quantity of DNA estimated.

Once the KO cassette has been made, purified, and quantity estimated, it was electroporated into 7 day-old conidia of the Δ*mus-51* strain FGSC #9718 (16) (*N. crassa* strain defective in non-homologous end-joining repair of double-stranded DNA breaks due to replacement of *mus-51* gene with the *bar* cassette); this mutant (homolog of the human KU70 gene) facilitates homologous recombination to near 100% success, compared to ~30% in wild type strain. Briefly, conidia from a 7 day-old culture of Δ*mus-*

154

51 grown in a foam-plugged, 250 ml flask filled with 50 ml of VM-agar were collected

with sterile water by agitation and filtered through sterile layer of shop towel to remove

all tissue types except conidia, which flow through. The conidial solution was

centrifuged at 2500 rpm for 5 min. The supernatant was poured out, and the conidial

pellet resuspended in 25 ml of sterile, cold sorbitol (1 M), and concentrated by

centrifugation at 2500 rpm for 5 min, with the supernatant poured off again. A volume of

1 ml, cold 1 M sorbitol was added, and the conidial concentration was determined with a

haemacytometer and adjusted to 2.5 x 10^9 conidia/ml using sorbitol. A volume

containing 40 μl of conidial solution was pipetted into an electroporation cuvette along

with 25 ng of the KO cassette and electroporated immediately in Eppendorf

electroporator (model #2510). Immediately, 1 ml of cold sorbitol (1 M) was added to the

electroporated conidial suspension. The suspension was pipette into a 15 ml conical tube,

to which 4 ml of VM liquid medium was added. The tube was placed in a shaker at 50

rpm for 2 hours at 30°C (recovery step). After the incubation, 5 ml of warm (60°C)

regeneration agar (for 100 ml of media: 2 ml of 50x Vogel's, 18.2 g of sorbitol, 2 g of

yeast extract, 1 g of agar, 84 ml of H_2O) was added into the conical tube. Then the

contents were well-mixed and gently poured on top of petri plates containing 20 ml of

FGS + hygromycin (200 μg/ml) medium (for 100 ml of media: 2 ml of 50x Vogel's, 1 g

of agar, 88 ml of H2O, and 10 ml of 10x FGS). The plates were incubated at 30˚C in the

dark. After approximately 48 hours, single colonies could be visualized; these were

picked off the plate with a sterile Pasteur pipet and into a test tube containing 2 ml of

VM-agar supplemented with 200 μg/ml of hygromycin. The test tubes were incubated at

30˚C without light and checked daily for signs of growth. After 2 days of growth in the 30˚C, dark incubator, the cultures were moved out to room temperature with ambient lighting conditions and allowed to grow for 3 more days before being placed in the refrigerator (to suppress growth). Strains that grew on VM + hygromycin agar were carried onto the next phase of verification.

To confirm that the DNA integrated at the native locus and not ectopically, genomic DNA from each of the strains was extracted and subjected to Southern analysis. Briefly, a sterile wooden stick was used to transfer a small amount of conidia from each of the transformed strains into 5 ml of VM liquid-medium. The inoculated cultures were incubated at 30˚C, 200 rpm, and dark conditions for approximately 16 hours. Afterwards, the hyphal mass from the inoculated cultures was vacuum-filtered to remove media, rinsed with DI water, placed in microcentrifuge tubes, and stored on ice for genomic DNA extraction. The fungal tissue was flash frozen with liquid nitrogen and pulverized with a plastic rod until the consistency of the tissue turned into a fine powder. Then, QIAGEN Fungal Tissue DNA Extraction kit (Qiagen, USA) was used to extract genomic DNA from the fungal tissue.

For Southern analysis, 8ul of genomic DNA was digested with the restriction enzyme *Hind*III overnight and then electrophoresed on a 1% agarose gel. After staining with ethidium bromide, a gel image was taken with a ruler (to gauge location of the ladder relative to size of the gel). The gel was then shaken in denaturation solution (for 1 L: 20 g of NaOH, 58.4 g of NaCl) for 45 minutes, transferred to neutralization solution (for 1 L: 78.8 g tris base, 87.6 g of NaCl, pH 7.4) and shaken for another 45 minutes.

156

The gel was soaked in 2x SSC solution (for 1 L: 17.53 g of NaCl, 8.82 g of trisodium citrate) for 10 minutes. The gel was finally placed under a 0.45 micron nylon transfer membrane (GE Water & Process Technologies, N00HY00010) within a container of 2x SSC solution to transfer DNA onto the membrane by upward capillary action with the aid of a filter paper and paper towels serving as a wick. After approximately 16 hours, the nitrocellulose membrane was peeled off of the gel and both sides of the membrane UV-crosslinked at 1200×100 $\mu J/cm^2$.

To make the probe for Southern analysis, the following steps were performed: first, 200 ng of purified *ste50* KO cassette was boiled for 5 minutes to denature the DNA. Second, 10 μl of 5X labeling buffer (Promega: Madison, WI), 3 μl of dNTPs without dCTP, 5 μl of biotinylated BSA, 1.4 μl of Klenow fragment, and 5 μl of ^{32}P-labeled dCTP were added to the single-stranded *ste50* KO cassette. This mixture was incubated at room temperature for 1 hour. At the same time, the nitrocellulose membrane was placed into a hybridization bottle along with 30 ml of hybridization solution and incubated at 65˚C with rotation for 1 hour. At the end of the hour, the solution containing labeled *ste50* KO cassette was boiled for 5 minutes and then added to the hybridization bottle and incubated with constant rotation overnight. The next morning, the radioactive fluid in the hybridization bottle was poured off into the radioactive waste container, and 15 ml of wash buffer I (40 mM Na_2HPO_4, 1 mM EDTA, 5% SDS, 0.5% BSA) added, with rotation for 15 minutes at 65˚C. This step was repeated once. Wash buffer II (40 mM Na_2HPO_4, 1 mM EDTA, 1% SDS) was then used to wash the membrane 2 times, using the procedure described for Wash buffer I. The membrane was then removed from

the hybridization bottle, wrapped with plastic wrap, and exposed to X-ray film (Denville Scientific: Metuchen, NJ) within a film cassette using an intensifying screen. The film was developed after ~6 hours of exposure, and the banding examined for the predicted pattern for Δ*ste50*.

Since *N. crassa* cells have more than one nucleus (and rarely do all nuclei within a cell transform), the Δ*ste50* transformant (a heterokaryon) was used as a male to cross with a wild-type strain (used as a female) as described above in order to obtain a homokaryon. Initially, ascospore plated from this cross failed to germinate on sorbose plates. However, the the progeny were plated on VM + hygromycin (200 μg/ml) plates with success.

After obtaining many strains that grew on VM + hygromycin slants, 36 were subjected to Southern analysis to identify homokaryons without ectopic integration of the *ste50* KO cassette, as described above. After preliminary screening of phenotypes, representative Δ*ste50* strain #2333 was selected for further study. Table 1 lists all strains used for this study.

Phenotypic assays of Δ*ste50* mutants

1. <u>Growth (apical extension rate) assay.</u> Conidia from a 7-day old culture of Δ*ste50* were collected as described above. After counting the conidial concentration using a hemacytometer, a dilution stock of 1×10^6 conidia/μl was made. One μl of the dilution stock was placed in the center of a VM-agar plate (30 ml/plate), incubated at 30˚C, checked every 4 hours for growth, and the growth edge marked. Wild-type strain

FGSC#4200 (collected and inoculated in the same manner) was grown on a VM plate as a reference.

2. Female fertility assay. To test whether STE50 is required for *N. crassa* to make protoperithecia (female sexual structures) and to be successfully fertilized, a SCM plate was inoculated with Δ*ste50* and incubated at 25˚C with constant light for 6 days. At the end of 6 days, conidia from a wild-type strain of opposite mating type were swabbed onto half of the plate using a sterile swab, while the other half was swabbed with sterile water (as a negative control). The plate was then incubated for another 9 days. The plates were examined under a stereomicroscope for the presence of perithecia or ascospores that had ejected from the ostioles of perithecia. Wild-type FGSC#4200, Δ*mak-1* (strain #1601), Δ*mak-2* 1046A (strain #1608), and Δ*ric8* 1a (strain #1811) strains were also tested in this manner.

3. Aerial hyphae assay. To test if STE50 is necessary for production of normal aerial hyphae, 1 ml of VM liquid-medium in a test tube was inoculated with conidia from the Δ*ste50* strain for final concentration of 1×10^6 conidia/ml. Conidia from a wild-type strain were used as a reference. These test tubes were placed in an incubator set at 30˚C without light. The height of the aerial hyphae was measured after 24 hours of growth. The same strains tested for female fertility were also tested in this manner.

4. Conidia germination assay. Conidia from Δ*ste50* mutants were collected as described above and 8×10^6 conidia were spread on a VM-agar plate. Conidia from a wild-type strain were used as a reference. These plates were placed in an incubator set at 30˚C without light. After every 2 hours of incubation, thin sections of agar containing

germinated conidia were sliced out using a razor blade, placed on a microscope slide, and checked under an inverted microscope at 60X magnification (Olympus IX71, Japan)(Camera QIClick, QIMAGING). Then, 100 conidia per strain were checked to determine the ratio of germinated versus ungerminated conidia. This was done at 2 hour intervals until the 10th hour. The same strains tested for female fertility were also tested in this manner.

5. CAT fusion assay. Approximately 8×10^6 conidia of wild-type FGSC #4200 (strain #1749), Δ*mak-2* 1046A (strain #1608), Δ*ric8* 1a (strain #1811), and Δ*ste50* (strain #2333) were plated (with a sterile, bent glass-rod) were planted on 100x15 mm plates containing 30 ml of VM-agar. The plates were placed into an incubator set at 30˚C, without lights. After 4, 6, and 8 hours, plates were taken out of the incubator and thin sections of agar containing germinated conidia were sliced out using a razor blade, placed on a microscope slide, and checked under an inverted microscope. CATs were viewed under Differential Interference Contrast (DIC), at 60X magnification.

Yeast Two Hybrid Assay

A possible interaction between STE50 and the Gα-subunits of *N. crassa* was explored using a Yeast2Hybrid assay. A Ste50-pGADT7 vector (pGAD-ste50) was transformed into *S. cerevisiae* strain AH109 (Mating type a) by lithium acetate-mediated chemical transformation as described (Yeast Protocols Handbook; Clontech) with modifications. A single colony was picked off from the plate using a sterile toothpick and placed into a test-tube containing 5 ml of YPDA liquid medium. This culture was incubated with shaking at 200 rpm at 30˚C overnight. The next morning, 1 ml of the

culture was pipetted into a sterile, baffled flask containing 50 ml of YPDA liquid-medium and incubated at the same condition. After 4 hours, the OD of the culture was checked in a spectrophotometer at 600 nm. If the OD had not reached a value of 1.0, then the flask was returned to the shaker for more incubation. Once an OD of 1.0 was reached, the culture was collected into a 50 ml conical tube and centrifuged at 2500 rpm for 5 minutes to pellet the yeast cells. The supernatant was poured off and 25 ml of sterile water was added to the tube in order to resuspend the yeast cells and wash away residual YPDA. The conical tube was centrifuged at 2500 rpm for 5 minutes to pellet the yeast cells. Subsequently, 1 ml of 100 mM lithium chloride (LiCl) was used to suspend the yeast pellet before pipetting into a sterile microcentrifuge tube. The tube was kept at room temperature until transformation. Carrier DNA (salmon sperm) was boiled for 5 minutes for denaturation and then kept on ice to prevent reannealing of the DNA strands. Finally, plasmid and transformation mix (240 µl 50% PEG 3350(w/v), 29 µl water, 50 µl salmon sperm DNA) were added to the yeast cells. The contents of the microcentrifuge tube were mixed, the solution incubated at 30˚C for 30 minutes and then at 42˚C (water bath) for 30 minutes. After incubation, 1 ml of sterile water was added to the transformation tubes, the solution mixed and the tube centrifuged briefly to pellet the yeast cells. After removal of most of the supernatant, the transformed yeast cells were plated onto Synthetic Dextrose (SD) medium lacking a particular amino acid that would be supplied by the gene on the transformed vector.

Yeast Mating: Y187 yeast cells (mating type α) transformed with GNA-1, GNA-2, and GNA-3 in pGBKT7 vectors (by HyoJeong Kim) were streaked onto SD-leucine

plates and incubated in the dark at 30˚C for 48 hours. Colonies (~2mm colony diameter) were picked using a sterile toothpick and inoculated onto the surface of a YPDA plate. This mating plate (STE50 x Gα) was incubated at 30˚C for 12 hours and checked for successful fertilization; a sterile toothpick was used to scrape a small portion of the plate where the streaks from the 2 different strains crossed and placed on a glass slide for examination under the compound microscope. At 40X magnification, the cultures were checked for zygotes (which are larger than a haploid yeast cell) or tetrads. In order to isolate diploids containing both pGAD*ste50* and pGBKT7 containing a Gα-subunit, the area where the 2 different strains were cross-streaked was scraped with a sterile toothpick and streaked onto a SD-leu, trp plate and incubated for 48 hours in the dark at 30˚C. A single colony was picked from each plate and streaked onto both SD-ade, leu, trp plate (TDO) and a SD-ade, his, leu, trp plate (QDO); these plates were incubated at 30˚C for 48 hours in the dark and then examined for growth of colonies.

Finally, to gauge the interaction between STE50 and components of the various MAPK pathways, Yeast2Hybrid vectors containing components of the MAPK pathways were obtained from Dr. Stephan Seiler (Table 3 lists all strains used for the interaction study), transformed into appropriate yeast strains, and mated to opposite mating type yeast containing *ste50* Yeast2Hybrid vector as described above. Ste50 Yeast2Hybrid vector obtained from the interactor discovered during the cDNA library screening with RIC8 as "bait". Hence, it was truncated and did not have the RA-domain. However, the SAM-domain was still present. Table 3 shows all of the yeast strains made or obtained for this purpose.

Construction of a *ste50*-GFP complementation strain

In order to be certain that the phenotypes caused by deletion of *ste50* were indeed due to the absence of the gene, a complementation study was conducted in which a wild-type copy of the *ste50* gene was transformed into the Δ*ste50::hph*$^+$ mutant. This was accomplished by taking advantage of the *his-3* targeting vector, pMF272 (7). This vector, reported in Freitag *et al.* (2004), takes advantage of the relatively high rate of recombination at the *his-3* locus. A construct containing the wild-type *his-3* gene inserted next to another fragment of DNA can be efficiently targeted by recombination to the *his-3* locus of a *his-3* mutant, thus rescuing the requirement for histidine supplementation. Using pMF272, I generated a construct (pJK-ste50-gfp) in which a translational fusion of *ste50* and *GFP* is under the control of the *ccg-1* (Clock-Controlled Gene, essentially a constitutive promoter) promoter. This vector can be used for both complementation and localization studies of *ste50*.

The 1570 bp fragment containing the *ste50* ORF with a glycine linker was inserted upstream of the *gfp* gene in pMF272, generating pJK-ste50-gfp. The recipient for transformation was a Δ*ste50, his-3* A (strain #2474). Strain A was constructed by crossing Δ*ste50* (strain #2333, mating type A) to a *his-3* strain 77a (strain #1208, mating type a). pJK-ste50-gfp was transformed using electroporation, as described above. The transformants were plated on FGS agar-medium containing 200 µg/ml of hygromycin, but lacking histidine. Therefore, only transformants that have successfully recombined the pJK-ste50-gfp construct at the *his-3* locus would be able to grow.

To verify that the transformants carried a functional copy of *gfp*, conidia from each transformant were placed on a glass slide with 15 µl of VM liquid-medium, covered with a cover glass, and examined using an inverted microscope at 60X (Olympus, IX71, Japan) magnification. Wild-type conidia were used as a negative control: a baseline setting was needed to establish cutoff for fluorescence to distinguish strains that fluoresced from those that did not. Using Metamorph software to control imaging, 100% gfp signal, 100ms exposure, gamma setting of 1, and gain of 0.7 was found to unambiguously distinguish conidia that fluoresced. Only strains that exhibited fluorescence were carried to the next phase of the confirmation.

Southern analysis was used to determine whether the strains contained the ste50-gfp construct integrated at the *his-3* locus. The 9.4 kb *Hin*dIII fragment of *his-3* from pMF272 was isolated from an agarose gel, labeled with ^{32}P-dCTP and used as the probe. Southern analysis was conducted as described above. The wild-type strain has a 9.6 kb band, while the *ste50-gfp, his+* strain possesses 6.7 kb and 2.7 kb bands. Two strains exhibiting the correct Southern band pattern, resistance to hygromycin, and GFP-fluorescence were chosen for purification to homokaryons using microconidiation. A total of 32 strains were obtained after the microconidiation purification. From these, Southern analysis was repeated as above, and two homokaryons (9(F1) and 10(F2)) and with resistance to hygromycin, GFP-fluorescence, and correct Southern banding pattern were chosen for long-term storage. Strain 9(F1) (#2537) was used for localization and phenotypic analysis.

Localization studies of STE50-GFP

VM-agarose plates were inoculated with conidia from the strain 9(F1) and

incubated in the dark at 30˚C for 4, 6, and 8 hours. At these times, a slice of VM-agarose

(avoids background due to agar autofluorescence) was excised from the plate using a

razor blade and then placed on top of 15 µl of VM liquid medium that had previously

been pipetted onto a microscope slide. A cover-glass was placed on top of the agarose

slice and a drop of immersion oil placed on top of the cover glass. The assembly was

inverted and examined using the Olympus inverted microscope at 60X magnification. To

view GFP, Metamorph Image Analysis software (Version 7.0.0, Sunnyvale, CA) was

used to control the inverted microscope. The settings for viewing localization of STE50-

GFP were GFP fluorescence of 100%, 100ms exposure, gamma setting of 1, and gain of

0.7.

Since STE50 homologs regulate the mating MAPK pathway in yeasts, I also

wished to determine whether STE50-GFP is localized in protoperithecia. Synthetic

Crossing Medium (SCM) plates were made, substituting agarose for agar. The plates

were inoculated with the *ste50-gfp* strain 9(F1) and incubated at 25˚C with constant light

for optimal protoperithecial formation. After 7 days, the plates were removed, thin slices

of agarose excised, conidia rinsed from the strip using a water bottle, and fluorescence

checked under the inverted microscope.

Mislocalization studies

To investigate whether the loss of RIC8 leads to mislocalization of STE50 (and

vice versa), *ste50-gfp, Δric8* and *ric8-gfp, Δste50* strains were constructed. *ste50-gfp*

strain 9(F1) was crossed to Δ*ric8* strain 1-5a (strain #1811) and *ric8-gfp* strain *ric8-gfp*

(strain #1820, mat A) was crossed to Δ*ste50* strain B (strain #2475, mat a). Mating was performed on SCM cross tubes and ascospores collected 2 weeks after fertilization, as described above. Ascospore progeny were plated on hygromycin-containing VM or FGS plates and picked onto VM+hygromycin (200 μg/ml) slants. Conidia from the slants were checked for green fluorescence. Only the strains that fluoresced were carried into the next phase, in which genomic DNA was isolated and the genotype of the strain confirmed by PCR. Since deletion of both *ste50* and *ric8* was carried out by replacement of the ORF with the *hph* cassette, PCR with a forward primer corresponding to a sequence approximately 1 kb upstream of the start codon of the gene and a reverse primer corresponding to a sequence within the *hph* cassette was used to detect the knockout mutants (Δ*ric8* diagnostic-PCR conditions: 95°C for 1 min, (repeated 30 cycles: 95°C for 30 sec, 47°C for 1 min, 68°C for 2 min), 68°C for 5 min) (Δ*ste50* diagnostic-PCR conditions: 95°C for 1 min, (repeated 30 cycles: 95°C for 30 sec, 52°C for 30 sec, 68°C for 1 min), 68°C for 5 min). Once the strains were verified (by diagnostic PCR and GFP-fluorescence), they were used for localization studies with the inverted microscope.

MAPK phosphorylation assays

Since STE50 homologs in other fungi regulate MAPK pathways, I conducted MAP kinase phosphorylation assays. In these assays, the phosphorylation status of MAP kinases is detected using Western analysis with antibodies specific for the phosphorylated MAPK protein. In our laboratory, we have developed assays for all 3 MAP kinases in *N. crassa*, MAK-1, MAK-2 and OS-2 (12, 18) .

Strains were grown in 50ml of VM agar medium inside a sterile 250 ml flask

enclosed with a foam stopper: For these studies, conidia (isolated as described above)

from wild-type (FGSC#4200, strain #1749), Δ*ste50* (strain #2333)*, Δric8* 1a (strain

#1811)*, Δos-2* (FGSC#2239, strain #1957)*, Δmak-1* (strain #1601)*, Δmak-2* 1046A (strain

#1608) were used to inoculate 100ml of VM liquid medium at a concentration of $1x10^6$

conidia/ml. After 16 hours, tissue from each strain was collected using vacuum filtration

with a filter funnel holding a Whatman #3 filter.

Collected tissue was flash-frozen with liquid nitrogen to prevent protein degradation.

Protein extraction was according to the protocol described in Aldabbous *et al.* (1).

Briefly, the harvested mycelium was ground into a fine powder with a mortar and pestle

in liquid nitrogen, transferred to a microcentrifuge tube using a spatula, and extraction

buffer [50 mM HEPES pH7.5, 2 mM EGTA, 2 mM EDTA, 1% Triton X-100, 10%

glycerol, 100 mM NaCl, 1 mM phenylmethylsulfonyl fluoride, 50 µl Fungal Protease

Inhibitor Cocktail (Promega)] and phosphatase inhibitors (1 mM sodium orthovanadate

and 1 mM sodium fluoride) added to the frozen ground fungal mycelium. After thawing

the frozen fungal tissue mixture on ice, it was centrifuged at 4000xg for 30 minutes at

4°C and the supernatant transferred to a new tube. The concentration of protein in the

extracts was determined using the BCA Protein Assay (Pierce Chemical, Rockford, IL).

To carry out the immunoblot analysis, 25 µg of total protein (per sample) was separated

on a 10% SDS-polyacrylamide gel by electrophoresis. Protein was transferred onto a

nitrocellulose membrane by wet electroblotting (Bio-Rad Transblot Cell), and a duplicate

gel stained with Coomassie Brilliant Blue to verify that the lanes contained equal

amounts of protein. Membranes were rinsed several times with double-distilled water

and then blocked for 3 hours by shaking in Tris-buffered saline (50 mM Tris pH7.5, 150

mM NaCl) also containing 0.1% Tween20 and 5% nonfat dried milk (Stater's Brothers

brand) at room temperature.

To detect and distinguish the phosphorylated forms of the two *N. crassa* MAP

kinases MAK-1 (51,580 Da) and MAK-2 (41,080 Da), membranes were incubated with

anti-phospho p44/42 MAP kinase antibody (1:1000 dilution) (Cell Signaling Technology)

in Tris-buffered saline (50 mM Tris pH7.5, 150 mM NaCl), 0.1% Tween20 and 1%

nonfat dried milk with gentle shaking overnight on an orbital shaker at 4˚C.

Phosphorylated versions of MAK-1 and MAK-2 are both recognized by this antibody

(17). After labeling with primary antibody, the blots were washed 3 times for 5minutes

each in the wash buffer (Tris-buffered saline and 0.1% Tween 20). Membranes were

then incubated with horseradish-peroxidase conjugated secondary antibody (1:2000

dilution; Sigma, #A0545) for 1 hour at room temperature with gentle shaking. Finally,

chemiluminescence detection was accomplished according to manufacturer's protocol

(Pierce SuperSignal West Pico kit (product #34079), Rockford, IL) and reactive bands

visualized using a Biochemie Chemilluminescence Detection system (UVP, Upland,

CA).

For the OS-2MAP kinase assay, the protocol previously described in Jones *et al.*

(13) was used. Briefly, cultures were grown, tissue collected, and ground as described

above. Then, 1 ml of cold 3 mM phenylmethylsulfonylfluoride (PMSF) in 95% ethanol

was added, along with 0.2 g of 0.5 mm glass beads in a 2 ml screw-cap microcentrifuge

tube. The tubes were vortexed for 1 min and chilled for another minute on ice (this was

repeated 3 times). Afterwards, these tubes were kept at -20°C for at least 16 hours.

Then, they were centrifuged at 14000 rpm for 15 minutes, supernatant removed, and

tubes vacuum concentrated for 30 minutes. A volume containing 250 μl of 1%SDS was

added to the tubes to reconstitute the proteins. The tube was heated at 85°C for 5 minutes

before centrifuging at 14000 rpm for 5 minutes. The supernatant was removed and saved

in a different microcentrifuge tube. The BCA assay (Pierce Chemical, Rockford, Il.) was

performed to determine the amount of protein in each sample. Finally, western analysis

was conducted as described above.

For the OS-2 MAPK assay, anti-Hog1p antibody (cat #SC-9079, Santa Cruz

Technologies, Santa Cruz, CA) was used at a concentration of 1:600 to detect OS-2. For

detection of phospho-OS-2, anti-phospho p38 antibody (cat #9211, Cell Signaling

Technology, Beverly, MA) was used at a concentration of 1:1000.

Co-immunoprecipitation studies

In order to confirm that STE50 interacts with RIC8, co-immunoprecipitation (Co-

IP) studies were performed. To carry out this experiment, a "knock-in" approach was

taken, wherein a copy of the wild-type gene with an epitope tag was placed at the native

locus via homologous recombination. Figure 1 illustrates the strategy used to make this

strain. In this case, a cassette (pJK-ste50-FLAG) containing the *ste50* ORF with a *flag*

epitope-tag sequence plus a *nourseothricin* resistance gene (as a selectable marker) was

"knocked-in" to the native locus of *ste50* (Figure 2). The same procedure was previously

performed to create a *ric8* "knock-in", but with a V5 epitope-tag; this strain was made by

Patrick Schacht in our laboratory. The "knock-in" cassette was assembled by yeast recombinational cloning as previously described. After electroporation of the cassette into *N. crassa* conidia of Δ*mus-51* strain 51-18-1 (strain #2776, *mat a*), transformants were selected on VM agar-plates supplemented with 100 µg/ml of nourseothricin. Transformants were picked onto VM + nourseothricin slants. Then, their genomic DNA was extracted and tested by PCR. Briefly, two PCRs were conducted to verify correct DNA sequence of the inserts in these transformants: 'S50 diag FW' and 'FLAG RV' to amplify the 2319 bp fragment encompassing the *ste50* open reading frame plus FLAG sequence, and 'FLAG FW' and 'STE50 RV' to amplify the 1995 bp fragment encompassing the FLAG sequence plus nourseothricin marker and 3'UTR portion of *ste50*. Strains exhibiting the expected amplified fragments were used for next step.

In order to obtain a homokaryon, the nourseothricin-resistant transformants were purified by microconidiation. I could not cross to wild type and pick ascospores on to nourseothricin medium, as ascospores rarely germinate on medium containing this antibiotic. When small colonies could be observed under the dissecting microscope (10X), a sterile needle was used to pick up individual colonies and placed into test tubes containing 2 ml of VM agar-medium. These tubes were incubated at 30˚C without light for 2 days before moving them into room temperature with ~12 hours of light/dark cycling conditions. After 5 days of growth, each individual strain was spot-tested on VM + nourseothricin (100 µg/ml) agar slants and VM + Ignite (200 µg/ml) slants (only susceptible strains were kept because this meant that *mus* mutation (*mus* gene was replaced with bar cassette that gives resistance to Ignite) was removed). Genomic DNA

was extracted only from the strains that grew on VM + nourseothricin. Diagnostic PCR was used to determine that the strains were indeed correct as described above.

ste50-FLAG strain 9(F1) (female) was crossed to ric8-V5 (male) using the protocol described above. Germinated ascospores from this cross (initially picked onto VM-agar slants) were transferred to VM + nourseothricin (100 μg/ml) slanted-agar test-tubes and incubated at 30°C and dark condition for 2 days before moving them to room temperature with a 12-hour photoperiod. Conidia from the slants were transferred to VM-agar flasks (as described above) and grown for 5 days (2 days in 30°C, dark and 3 days at room temperature with ~12 hour photoperiod). Conidia from each strain were collected as described above, and used to inoculate 50 ml of VM liquid medium in a 250 ml flask to a concentration of $1x10^6$ conidia/ml. Flasks were incubated for 16 hours at 30°C at 200 rpm in the dark. Tissue was collected by vacuum filtration as described above. Finally, total cell extract (containing cytosolic protein) was extracted from the tissue by method described below: the collected tissue was ground in liquid nitrogen with the aid of mortar and pestle. Then, the fine powder was spooned into Oakridge centrifuge tubes kept on ice with the addition of 4 ml of Co-IP extraction buffer (cold). These tubes were centrifuged at 46000 x g, 4°C for 1 hr. Supernatant was transferred to a 15ml conical tube and protein concentration measured using the Bradford assay.

Extracted protein from each of the progeny from the cross between ste50-FLAG and ric8-V5 were tested for expression of the tagged proteins using Western analysis as described above, with the exception that anti-FLAG primary antibody (1:700 dilution, Cell Signaling #2368) and anti-V5 primary antibody (Bethyl, cat#A190-120A) were

used. The RIC8-V5 fusion protein produces a band of 54 kDa, while the STE50-FLAG fusion protein is 53.1 kDa. One strain tested positive for expression of both RIC8-V5 and STE50-FLAG proteins and was designated as R8-V5, S50-F 1 (strain #2532).

To conduct the co-immunoprecipitation experiment, a whole-cell extract from the RIC8-V5, STE50-FLAG strain (strain #2532) was isolated and protein level quantified using the method described above. Subsequently, anti-FLAG agarose beads were prepared; 80 µl of a bead suspension [Sigma Anti-FLAG M2 agarose from Mouse (cat #A2220)] was transferred to an Eppendorf tube and centrifuged for 1 minute at 100 x g at 4˚C. The supernatant was discarded and 1 ml of (cold) Co-IP buffer (10 mM Tris-Cl at pH 7.5, 250 mM NaCl) was added to gently resuspend the pellet. Subsequently, 1 ml of the protein extract (10 mg of protein) was added to the agarose bead pellet, followed by gentle mixing using a nutator at 4˚C overnight. After incubation, the supernatant was removed from the beads by centrifugation (4˚C, 10 sec, 100 x g) and the beads washed 3 times with ice-cold Co-IP buffer. The contents of the Eppendorf tube were transferred to a fresh tube before elution to remove any particulates that might be adhering to the tube surface. The agarose bead pellet was resuspended in 30 µl of cold Co-IP buffer, after which 10 µl of 4x Laemmli Sample Buffer (13 ml of buffer B (30.2 g of tris base, 2 g of SDS, reconstitute to 500 ml with water, pH to 6.8), 10 ml of glycerol, 2 g of SDS, 5 ml of beta-mercaptoethanol and a few crystals of bromophenol blue) was added. The mixture was heated at 95˚C for 3 minutes, centrifuged at 15,000 rpm for 1 minute in a microcentrifuge at room temperature and the supernatant containing immunoprecipitated proteins transferred to a new Eppendorf tube.

Western analysis using FLAG or V5 antibodies was conducted as described above. The blot was incubated in a 1:700 dilution of FLAG antibody (Cell Signaling #2368) in TBST (0.1% Tween) (20 ml solution) overnight at 4˚C with rotation using a Nutator. The membrane was washed three times in 30 ml TBS for 5 minutes at room temperature with gentle shaking using an orbital shaker. The membrane was incubated with the secondary antibody (Sigma goat anti-rabbit peroxidase conjugate #A0545) diluted 1:2000 in 5% milk dissolved in TBS (20 μl antibody in 40 ml solution) for 1 hour at room temperature with gentle shaking on an orbital shaker. The membrane was washed three times in 30 ml TBS for 5 minutes at room temperature with gentle shaking using an orbital shaker. The co-immunoprecipitation results were visualized with chemilluminescence as described above.

RESULTS

Phenotypes of the Δ*ste50* mutant

Loss of STE50 caused *N. crassa* to grow in a manner similar to Δ*ric8* and the Δ*mak-2* mutant (Figure 2). All three deletion mutants exhibited a "flat" phenotype on the agar surface, with little aerial hyphae, in contrast to the wild-type strain. Δ*ste50* and Δ*mak-2* mutants grew at a considerably slower rate than that of wild-type on a VM-agar plate after 24 hours of growth (Figure 3). However, Δ*ric8* grew significantly slower than the other two mutant strains (Figure 3).

Even before Δ*ste50* was crossed with the opposite mating type, it was noticed that there were no signs of protoperithecia (Figure 4). After 14 days of growth on the SCM

plate, there was still no signs of protoperithecia on the Δ*ste50* mutant; on the other hand, the wild-type strain showed ample protoperithecia after 7 days of growth (data not shown). Similarly, both Δ*mak-1* and Δ*mak-2* mutants also failed to form protoperithecia on SCM plates (data not shown).

After 48 hours of growth, the aerial hyphae assay showed that Δ*ste50* developed significantly shorter aerial hyphae compared to wild-type (Figure 5). However, aerial hyphae development in Δ*ste50* was still significantly greater than that of the Δ*ric8* strain. Aerial hyphae development was comparable in Δ*ste50* and Δ*mak-2* strains (Figure 5).

STE50 is required for formation of CATs in *Neurospora crassa*.

Since mutants deficient in many components of MAPK pathways exhibit defects in CAT formation, the Δ*ste50* strain was also tested in the CAT assay. After 4 hours, Wild-type conidia were checked; they had germinated and formed CATs (Figure 6). However, no CATs were present in the Δ*ste50* sample. After 8 hours incubation on a VM-agar plate, the conidia of Δ*ste50* were checked under the inverted microscope, but only germination tubes were detected under inspection; there was no CAT formation (Figure 6). Hence, without STE50, *N. crassa* does not form CATs.

Wild-type conidia begin to germinate after 4 hours (data not shown; see below). However, germination of Δ*ste50* and Δ*ric8* conidia is much slower (data not shown; see below).

The Δ*mak-2* mutant also did not produce CATs, even after 8 hours of incubation (Figure 6). Δ*ric8*, however, eventually did form CATs after 8 hours; the reason for this delay is that its germination was very slow.

STE50 does not interact with GNA-1, GNA-2, GNA-3, or GNB-1 in *Neurospora crassa*.

It was reported that in yeast *K. lactis*, Ste50p interacts with the Gα subunit, KlGα (28). Also, in *S. cerevisiae*, Ste50p interacts with all components of the heterotrimeric G-protein: Gα, Gβ, Gγ (34). However, after mating yeast strains containing Y2H vectors expressing 3 Gα-subunits (GNA-1, GNA-2, and GNA-3) or Gβ with Y2H vector expressing *ste50* in the opposite mating type strain, no interaction could be detected between them. Therefore, using the Yeast2Hybrid assay, it was concluded that in *N. crassa*, STE50 does not associate with the heterotrimeric G-proteins GNA-1, GNA-2, GNA-3, or GNB-1.

STE50 interacts with a component of the MAPK pathway in *Neurospora crassa*.

From the interaction study between STE50 and the MAPK pathway components, only MEK-2 (MAPKK of cell-fusion MAPK pathway) interacted with STE50. Also, this was a weak interaction since the growth only appeared on TDO medium (SD$_{-leu,-trp,-ade}$).

Complementation of STE50 leads to a wild-type phenotype.

The complemented strain of Δ*ste50* resembled wild-type in all of the phenotypes exhibited (Figure 7, data not shown). First, the complemented strain formed aerial hyphae that was of same height as the wild type (Figure 7). Second, after 7 days, normally formed protoperithecia could be seen under the dissecting microscope in a complemented *ste50* strain. Also, the complemented strain was female-fertile when crossed to the wild-type strain of the opposite mating type. Fourth, the germination rate

of the complemented strain was similar to wild type and not to that of the Δ*ste50*.

Finally, the complemented strain was able to form Conidial Anastamosis Tubes (CATs).

STE50 localizes to the septa and to the endoplasmic reticulum or tubular vacuoles.

A *ste50*-complemented strain (containing a *ste50-gfp* fusion) was inspected for

GFP fluorescence. STE50-GFP localized to septa in hyphal cultures and was also visible

in the cytoplasm (Figure 8). Also, it localized to either the endoplasmic reticulum or

tubular vacuoles. Finally, STE50-GFP could not be detected in protoperithecia (data not

shown).

Mislocalization studies

Loss of *ste50* had did not effect localization of RIC8 in *N. crassa*; RIC8-GFP was

still visible in the cytoplasm. Likewise, loss of *ric8* had no effect on the localization of

STE50; it was still generally visible in the cytoplasm of *N. crassa* as well as distinctly in

hyphal septa (data not shown).

Loss of STE50 leads to a decreased phosphorylation for MAK-1 and MAK-2, but

not OS-2.

MAK-1, MAK-2, and OS-2 are the three MAPKs in *N. crassa*. Therefore,

comparing phosphorylation states of these 3 MAPKs in Δ*ste50* to that of the wild-type

strain should give an indication regarding MAPK pathways regulated by STE50 in *N.*

crassa.

Phosphorylation of OS-2 was not affected by deletion of STE50 or RIC8 (Figure

9). However, Δ*ste50* had almost no phosphorylated MAK-2 and the MAK-1

phosphorylation level was less than half compared to wild-type (Figure 8) (measured by

ImageJ; data not shown). In contrast, Δ*ric8* mutants exhibited elevated MAK-1-phosphate amounts (measured with ImageJ; data not shown) relative to wild type. These results are consistent with STE50 as a positive regulator of the MAK-1 and MAK-2 Erk MAPK pathways. As for RIC8, it is a negative regulator of MAK-1 phosphorylation.

Coimmunoprecipitation experiments confirm a physical association between STE50 and RIC8

Since Yeast 2 Hybrid assays have been previously shown to yield false positive results (3), Co-IP confirmation has become an industry standard for verification of protein-protein interactions (2). The FLAG epitope-tag (5) has been used successfully in *Neurospora crassa* and demonstrated to be an useful tool in isolation of protein complexes (10) (Figure 11). Using a strain expressing FLAG-tagged STE50 and V5-tagged RIC8, immunoprecipitation of both proteins was demonstrated using anti-V5 conjugated beads. A wild-type strain lacking both constructs was used as a negative control and did not exhibit any specific immunoprecipitating proteins (Figure 11).

DISCUSSION

CAT fusion is disturbed in *N. crassa* mutants, such as Δ*nrc-1* and Δ*mak-2*, lacking MAPK pathway components that control hyphal fusion and female fertility pathway (15). Also, it has been shown that Δ*ste50* also is defective in CAT formation. This lends support to a mechanism in which STE50 is functioning in the hyphal fusion and female fertility MAPK pathways.

From the Y2H assay, it was interesting to find that STE50 interacts with MEK-1. In *Magnaporthe grisea*, STE50 homolog was shown to interact with STE7 (36). This could be that a full-length STE50 might interact with other components of the MAPK pathway.

Even though STE50 homologs were shown to interact with Gα and other subunits of heterotrimeric G-proteins in other fungi, this was not the case in *N. crassa*. One possible reason for this is that in *N. crassa*, RIC8 has been shown to interact with GNA-1 and GNA-3, both Gα-subunits. And since STE50 has been shown to physically interact with RIC8, it may not need to interact with Gα subunits. And since *K. lactis* and *S. cerevisiae* are both yeasts and do not have a homolog of *ric8* in their genome, it could be that these yeast organisms must have Ste50p interact with the Gα because they do not have a RIC8 homolog to act as a bridge between the two components. However, *N. crassa* bypasses this interaction by associating STE50 with RIC8 instead.

Δ*ric8* has very poor growth rate compared to wild type. However, Δ*ste50* does not grow poorly but is on par with the wild-type growth rate. Even though RIC8 and STE50 physically interact, the signal transduction pathway governing growth rate must function independently of STE50. That is, RIC8 must interact with another protein that does not require STE50 to function as an adapter.

Δ*ste50* is not only female infertile, but does not form protoperithecia, similar to Δ*mak-1* and Δ*mak-2* mutants. This shared trait suggests that STE50 functions in the sexual fertility MAPK pathway. Interestingly, Δ*ric8* is also female-sterile, without any protoperithecia.

Conidia of the wild-type strain germinate after about 4 hours. However, Δste50 is much slower than that, at about 8 hours post-plating. Δric8 also germinates very slowly (first sign of germination after 8 hours). Since both genes are necessary for timely germination of conidia, it seems likely that they are somehow involved in the germination process of the conidia in *N. crassa*.

STE50 (this thesis) and RIC8 (32) are both present in the cytoplasm, indicating the possibility of association between the two proteins. However, STE50-GFP and RIC8 do not colocalize in other cellular compartments. RIC8 does not localize to the septum, in contrast to STE50, suggesting that STE50 is functioning in a RIC8-independent role. Interestingly, another protein that is localized to septa is RHO-4, a small GTPase (21). Without RHO-4, hyphae are aseptate and show alterations in hyphal morphology in *N. crassa*. Also, Δrho-4 grows at much slower rate than the wild-type strain. Finally, similar to STE50, RHO-4 localizes to the hyphal septa, but not to the conidial septa (22). This correlation of localization between STE50 and RHO-4 suggests a possible interaction between the two proteins. Such a scenario would be similar to the situation in *S. cerevisiae*, where Ste50p interacts with Cdc42p (a small GTPase). It could be that this interaction in *Neurospora crassa* is substituted with RHO-4 as the interaction partner. Although *N. crassa* does have a homolog of Cdc42, its phenotype does not correlate with that of Δste50; it has a directional growth defect and grows in a zigzag manner (27).

Previous work has shown that RIC8 is a GEF that facilitates exchange of GDP for GTP on Gα subunits (32) (Figure 12). Also, RIC8 is involved in female structure (protoperithecium) formation as well as aerial hyphae development. Without RIC8, *N.*

crassa has a defective phenotype regarding these two morphologies. Loss of STE50 also leads to similar phenotypes. This study has shown that RIC8 has a negative influence on phosphorylation of MAK-1, where as STE50 has a positive influence on phosphorylation of both MAK-1 and MAK-2.

STE50 has RIC8-independent roles that involves MAK-2 MAPK pathway. This is illustrated by the fact that Δ*ste50* cannot form CATs while Δ*ric8* can. In conjunction with the evidence of decreased phosphorylation of MAK-2 in Δ*ste50* and defective CAT formation, STE50 must be an integral component of the MAK-2 MAPK pathway (Figure 13).

Table 1. These are strains used for this study.

Borkovich lab strain #	Strain	Relevant genotype	Comments	Source/ reference
1601	Δ*mak-1*	Δ*mak-1::hph*$^+$ mat a	Δ*mak-1 homokaryon*	
1608	Δ*mak-2*	Δ*mak-2::hph*$^+$ mat A	*1046A*	Dan Ebbole
1749	wild type	wild type mat a	74A-ORS-SL6a, FGSC #4200	FGSC
1811	Δ*ric8 1a*	Δ*ric8::hph*$^+$ mat a	Δ*ric8* homokaryon	Sara Wright
1957	Δ*os-2*	Δ*os-2::hph*$^+$ mat a	*FGSC #2239*	Carol Jones
2333	Δ*ste50*	Δ*ste50::hph*$^+$ mat A	Δ*ste50* homokaryon	this study
2776	Δ*mus-51*	Δ*mus-51::bar*$^+$	resistant to Ignite	
2537	*ste50*-GFP 9(F1)	Δ*ste50::hph*$^+$ *ste50-GFP::his-3*$^+$	*ste50* complemented	this study
2538	*ste50*-GFP 10(F2)	Δ*ste50::hph*$^+$ *ste50-GFP::his-3*$^+$	*ste50* complemented	this study
2476	Δ*mus-51 51-18-1*	Δ*mus-51::nat*$^+$ mat a	*mus-51* replaced with neorseothricin marker	James Kim

Table 2. Yeast strains used for construction of plasmids and strains for this study.

Borkovich lab strain #	name	genotype	comment	source
1	AH109	*his3, trp1-901,ade2-101,leu2-3-112*		lab strain
2	Y187	*his3, trp1-901,ade2-101,leu2-3-112*		lab strain
86	HK11	Y187 + trp	*ric8* cDNA	Sara Wright
78	FY834			
173	pSM24	pGBKT7	*ric8* cDNA	Sara Wright

Table 3. yeast strains made for the Yeast2Hybrid interaction study with STE50.

| Borkovich lab strain #	Gene	NCU #	vector	MAPK pathway	Provider
213	*nrc-1*	6182	pGAD	MAPKKK of hyphal fusion and female fertility	Stephen Seiler
214	*nrc-1*	6182	pGBK	"	Stephen Seiler
215	*ste-7*	4612	pGAD	MAPKK of hyphal fusion and female fertility	Stephen Seiler
216	*ste-7*	4612	pGBK	"	Stephen Seiler
217	*mak-2*	2393	pGAD	MAPK of hyphal fusion and female fertility	Stephen Seiler
218	*mak-2*	2393	pGBK	"	Stephen Seiler
219	*mek-1*	6419	pGAD	MAPKK of cell wall integrity	Stephen Seiler
220	*mek-1*	6419	pGBK	MAPKK of cell wall integrity	Stephen Seiler
221	*mek-1 $_{aa1-216}$*	6419	pGAD	MAPKK of cell wall integrity	Stephen Seiler
222	*mek-1$_{aa216-518}$*	6419	pGAD	MAPKK of cell wall integrity	Stephen Seiler
223	*mik-1$_{aa1-1007}$*	2234	pGAD	MAPKKK of cell wall integrity	Stephen Seiler
224	*mik-1$_{aa1008-1778}$*	2234	pGAD	MAPKKK of cell wall integrity	Stephen Seiler
225	*ste20*	3894	pGAD	PAK-kinase	Stephen Seiler
226	*cla-4*	406	pGAD	PAK-kinase	Stephen Seiler
227	*cla-4*	406	pGBK	PAK-kinase	Stephen Seiler
228	*hym-1*	3576	pGBK	Adapter	Stephen Seiler
113	*os-4*	3071	pGBK	MAPKKK of osmosensing	Carol Jones
84	*gna-1*	6493	pGBK	Heterotrimeric G-protein	Sara Wright
85	*gna-2*	6729	pGBK	Heterotrimeric G-protein	Sara Wright
86	*gna-3*	5206	pGBK	Heterotrimeric G-protein	Sara Wright
87	*gnb-1*	440	pGBK	Heterotrimeric G-protein	Sara Wright
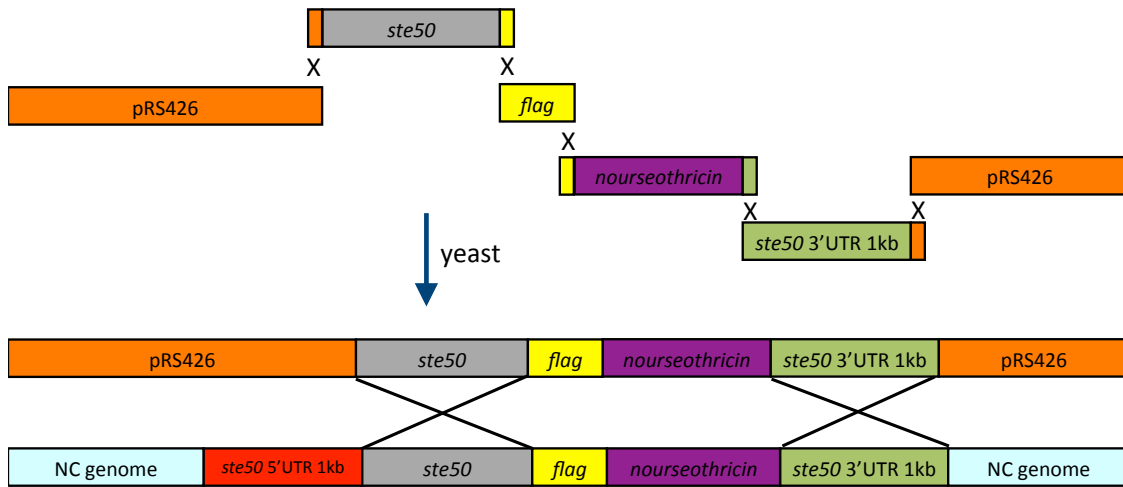
Figure 1. Schematic diagram of how STE50-FLAG strain was made. Individual DNA fragments were amplified using PCR and fused together using yeast recombinational cloning.

Wild-type   Δ*ric8*   Δ*mak-2*   Δ*ste50*
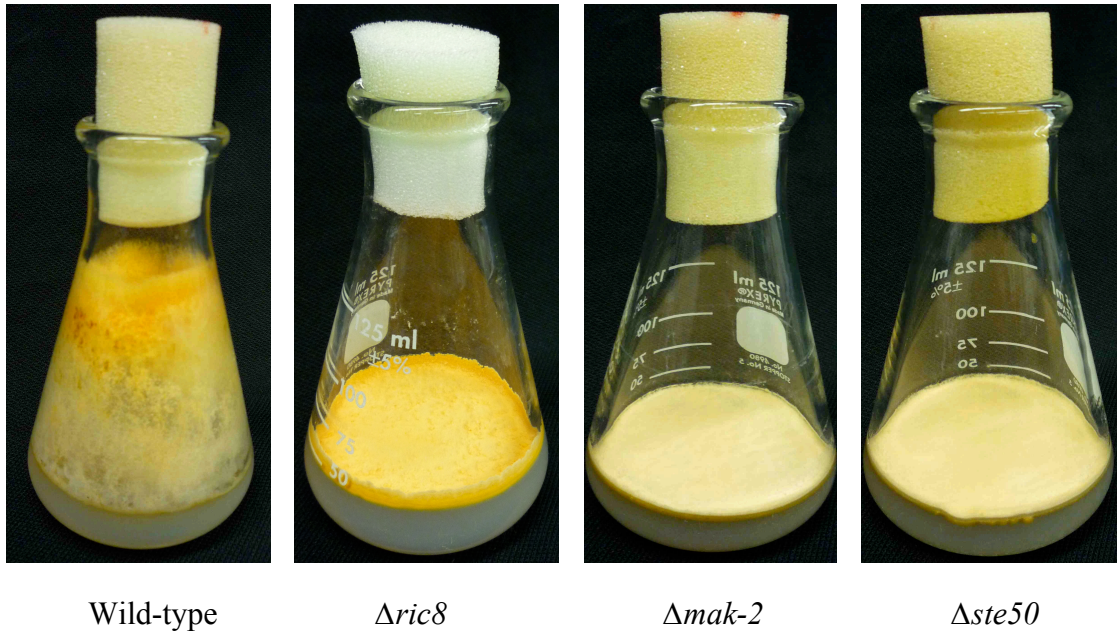
Figure 2. Comparison of Δ*ste50* with wild-type, Δ*ric8*, and Δ*mak-2* strains. All three deletion mutants share a similar phenotype, with very flat hyphal growth that hugs the surface of the agar.

Wild Type　　　　**Δste50**　　　　**Δmak-2**　　　　**Δric8**
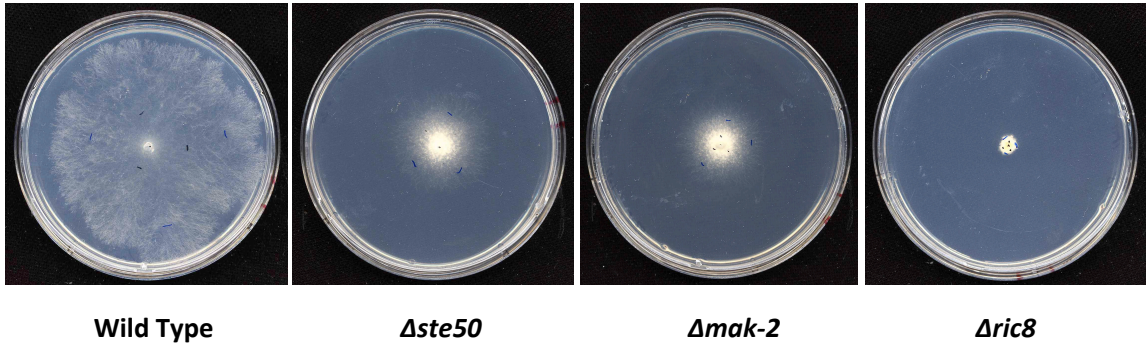
Figure 3. Colony morphology assay. Wild type grows at a much faster rate than all three deletion mutants. However, Δ*ste50* and Δ*mak-2* grow better than *Δric8*.

| | | |
| Wild-type | Δ*ric8* | Δ*ste50* |
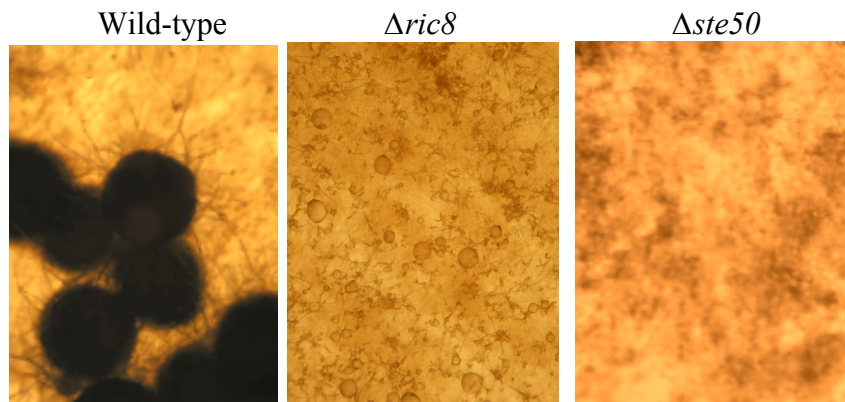
Figure 4. Female fertility phenotype of Δ*ste50*. Without STE50, *Neurospora crassa* cannot go through a regular female fertilization cycle. Furthermore, it even does not produce any protoperithecia. Δ*ric8* shares the same phenotype.
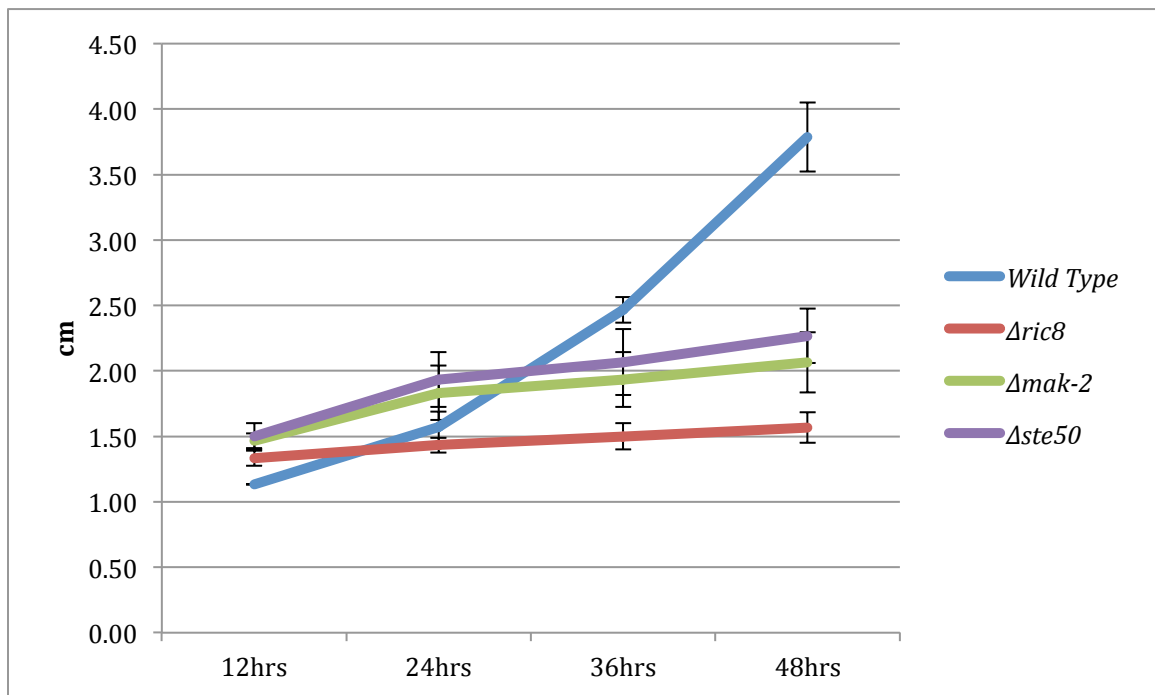
Figure 5. Aerial hyphae assay. Δ*ste50* was compared to wild type, Δ*ric8*, and Δ*mak-2*. All three deletion mutants display a similar phenotype, much shorter aerial hyphae than wild type.

Wild-type   Δ*ric8*
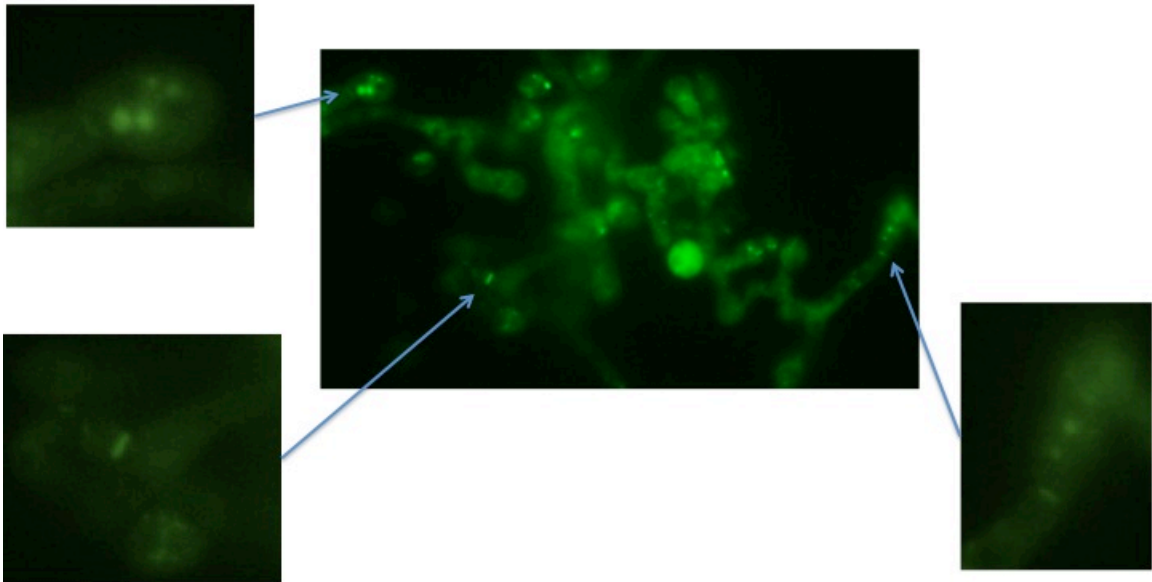
Δ*mak-2*   Δ*ste50*
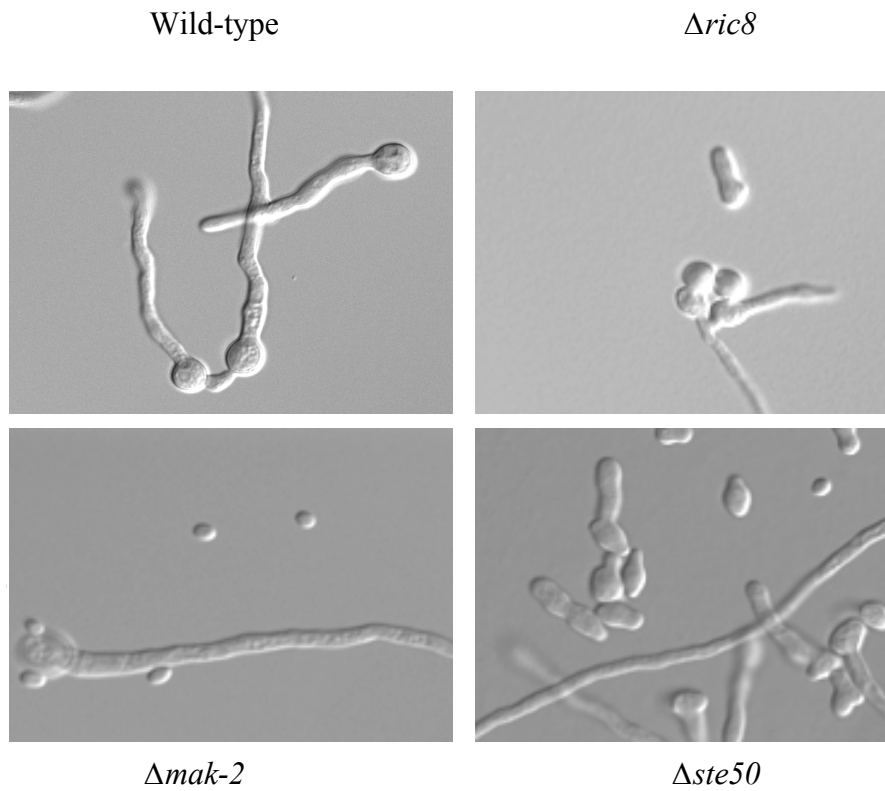
Figure 6. CAT-fusion assay. Unlike wild-type and Δ*ric8*, Δ*ste50* does not form CATs. This phenotype resembles that of Δ*mak-2*.
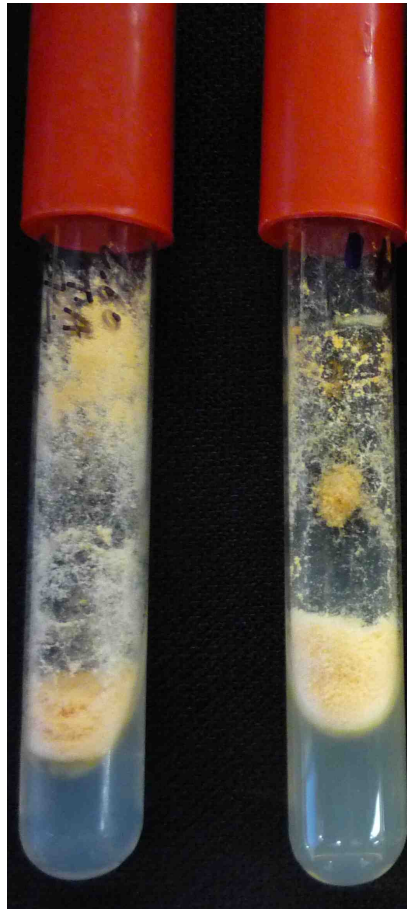
Wild-type   *ste50*-complemented

Figure 7. Complementation of *ste50*. The *ste50*-complemented strain resembles wild-type in the aerial hyphae height assay.

Figure 8. localization of STE50-GFP. Ste50-GFP strain was used to determine localization of this protein. GFP-fluorescence shows that STE50 localizes to the hyphal septa. Arrows indicate STE50 localized to the hyphal septa.
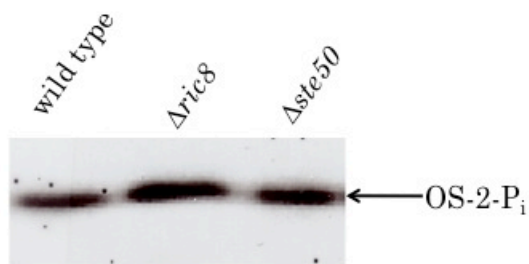
Figure 9. MAPK-phosphorylation assay reveals that STE50 does not influence phosphorylation of OS-2. Western analysis was performed using antibodies that detect phosphorylated p38 MAPK OS-2; OS-2-P$_i$ (p38 MAPK) levels are normal in Δ*ste50* and Δ*ric8* mutants.
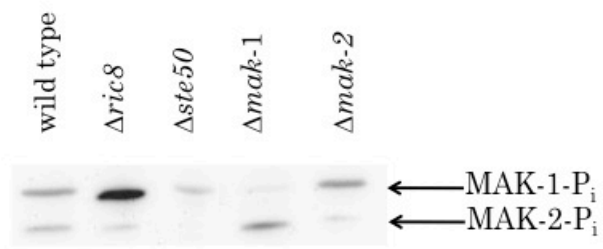
Figure 10. MAPK-phosphorylation assay reveals that STE50 influences phosphorylation of MAK-1 and MAK-2. Western analysis was done using antibodies that detect phosphorylated ERK MAPKs.
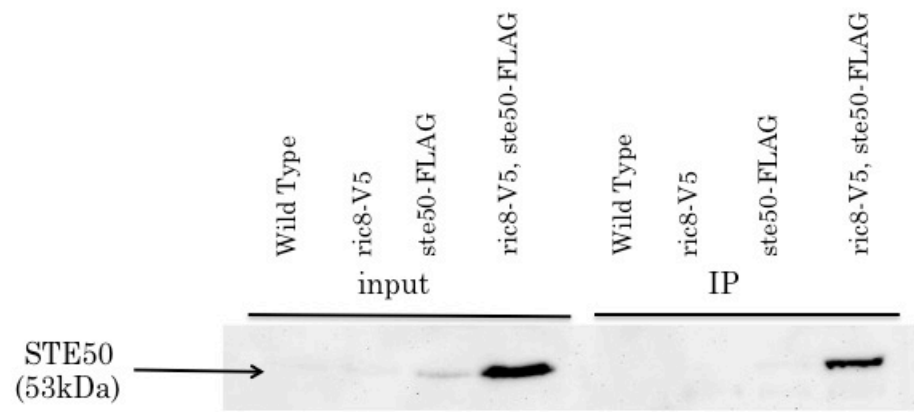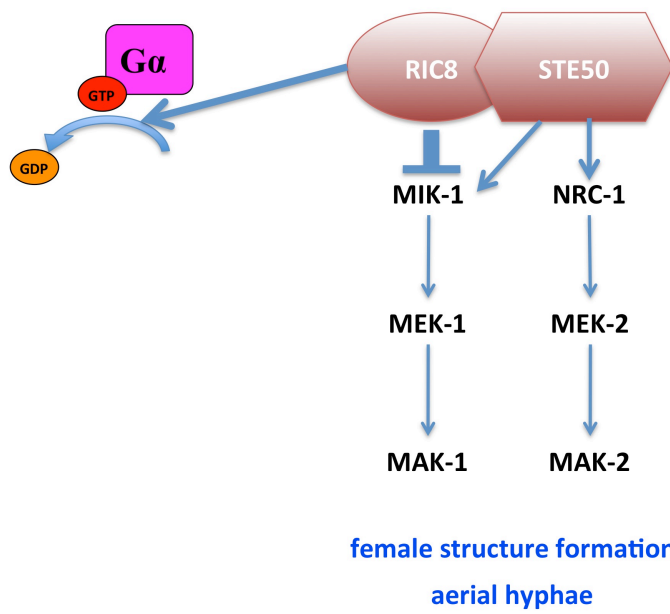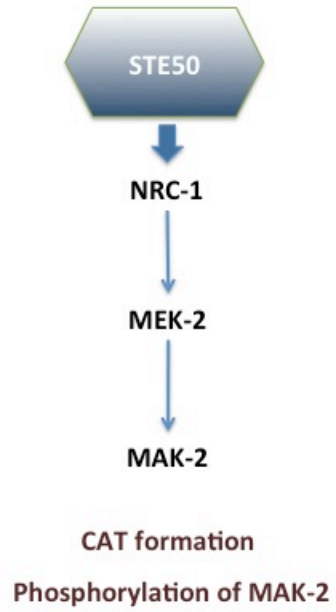
Figure 11. **Co-immunoprecipitation of RIC8-V5 and STE50-FLAG**.
Immunoprecipitation with V5-conjugated beads, Western probed with anti-FLAG 1˚
antibody.

Figure 12. RIC8 and STE50 influence the MAPK pathways (MAK-1 and MAK-2) for female structure development and aerial hyphae formation.

Figure 13. STE50 influences the MAK-2 MAPK pathway for CAT formation and phosphorylation of MAK-2.

REFERENCES

1. **Aldabbous M. S., M. G. Roca, A. Stout, I. C. Huang, N. D. Read, and S. J. Free**. 2010. The *ham-5, rcm-1 and rco-1* genes regulate hyphal fusion in *Neurospora crassa*. Microbiology **156**:2621-9.

2. **Berggård T., S. Linse, and P. James**. 2007. Methods for the detection and analysis of protein-protein interactions. Proteomics **7**:2833-42.

3. **Brückner A., C. Polge, N. Lentze, D. Auerbach, and U. Schlattner**. 2009. Yeast two-hybrid, a powerful tool for systems biology. International Journal of Molecular Sciences **10**:2763-88.

4. **Colot H. V., G. Park, G. E. Turner, C. Ringelberg, C. M. Crew, L. Litvinkova, R. L. Weiss, K. A. Borkovich, and J. C. Dunlap**. 2006. A high-throughput gene knockout procedure for *Neurospora* reveals functions for multiple transcription factors. Proceedings of the National Academy of Sciences of the United States of America **103**:10352-7.

5. **Einhauer A., and A. Jungbauer**. 2001. The FLAG peptide, a versatile fusion tag for the purification of recombinant proteins. Journal of Biochemical and Biophysical Methods **49**:455-65.

6. **Ekiel I., T. Sulea, G. Jansen, M. Kowalik, O. Minailiuc, J. Cheng, D. Harcus, M. Cygler, M. Whiteway, and C. Wu**. 2009. Binding the Atypical RA Domain of Ste50p to the Unfolded Opy2p Cytoplasmic Tail Is Essential for the High-Osmolarity Glycerol Pathway. Molecular Biology of the Cell **20**:5117-5126.

7. **Freitag M., P. C. Hickey, N. B. Raju, E. U. Selker, and N. D. Read**. 2004. GFP as a tool to analyze the organization, dynamics and function of nuclei and microtubules in *Neurospora crassa*. Fungal Genetics and Biology **41**:897-910.

8. **Fu J., C. Mares, A. Lizcano, Y. Liu, and B. L. Wickes**. 2011. Insertional mutagenesis combined with an inducible filamentation phenotype reveals a conserved STE50 homologue in *Cryptococcus neoformans* that is required for monokaryotic fruiting and sexual reproduction. Molecular Microbiology **79**:990-1007.

9. **Hao N., Y. Zeng, T. C. Elston, and H. G. Dohlman**. 2008. Control of MAPK specificity by feedback phosphorylation of shared adaptor protein Ste50. The Journal of Biological Chemistry **283**:33798-802.

10. **Honda S., and E. U. Selker**. 2009. Tools for fungal proteomics: multifunctional *Neurospora* vectors for gene replacement, protein expression and protein purification. Genetics **182**:11-23.

11. **Johnson D. I.** 1999. Cdc42: An essential Rho-type GTPase controlling eukaryotic cell polarity. Microbiology and Molecular Biology Reviews **63**:54-105.

12. **Jones C. A., and K. A. Borkovich**. 2010. Analysis of Mitogen-Activated Protein Kinase Phosphorylation in Response to Stimulation of Histidine Kinase Signaling Pathways in *Neurospora*. Methods Enzymol. **471**:319-334.

13. **Jones C. A., S. E. Greer-phillips, and K. A. Borkovich**. 2007. The Response Regulator RRG-1 Functions Upstream of a Mitogen-activated Protein Kinase Pathway Impacting Asexual Development, Female Fertility, Osmotic Stress, and Fungicide Resistance in *Neurospora crassa*. Molecular Biology of the Cell **18**:2123-2136.

14. **Klosterman S. J., A. D. Martinez-Espinoza, D. L. Andrews, J. R. Seay, and S. E. Gold**. 2008. Ubc2, an ortholog of the yeast Ste50p adaptor, possesses a basidiomycete-specific carboxy terminal extension essential for pathogenicity independent of pheromone response. Molecular Plant-Microbe Interactions **21**:110-21.

15. **Maerz S., C. Ziv, N. Vogt, K. Helmstaedt, N. Cohen, R. Gorovits, O. Yarden, and S. Seiler**. 2008. The nuclear Dbf2-related kinase COT1 and the mitogen-activated protein kinases MAK1 and MAK2 genetically interact to regulate filamentous growth, hyphal fusion and sexual development in *Neurospora crassa*. Genetics **179**:1313-25.

16. **Ninomiya Y., K. Suzuki, C. Ishii, and H. Inoue**. 2004. Highly efficient gene replacements in *Neurospora* strains deficient for nonhomologous end-joining. Proceedings of the National Academy of Sciences of the United States of America **101**:12248-53.

17. **Pandey A., M. G. Roca, N. D. Read, and N. L. Glass**. 2004. Role of a Mitogen-Activated Protein Kinase Pathway during Conidial Germination and Hyphal Fusion in *Neurospora crassa*. Eukaryotic Cell **3**:348-358.

18. **Park G., S. Pan, and K. A. Borkovich**. 2008. Mitogen-activated protein kinase cascade required for regulation of development and secondary metabolism in *Neurospora crassa*. Eukaryotic Cell **7**:2113-22.

19. **Park G., C. Xue, X. Zhao, Y. Kim, M. Orbach, and J.-R. Xu**. 2006. Multiple upstream signals converge on the adaptor protein Mst50 in *Magnaporthe grisea*. The Plant Cell **18**:2822-35.

20. **Ramezani Rad M., G. Xu, and C. P. Hollenberg**. 1992. STE50, a novel gene required for activation of conjugation at an early step in mating in *Saccharomyces cerevisiae*. Molecular and General Genetics. Springer **236**:145–154.

21. **Rasmussen C. G., and N. L. Glass**. 2005. A Rho-Type GTPase , *rho-4*, Is Required for Septation in *Neurospora crassa*. Eukaryotic Cell **4**:1913-1925.

22. **Rasmussen C. G., and N. L. Glass**. 2007. Localization of RHO-4 indicates differential regulation of conidial versus vegetative septation in the filamentous fungus *Neurospora crassa*. Eukaryotic Cell **6**:1097-107.

23. **Raymond C. K., E. H. Sims, and M. V. Olson**. 2002. Linker-mediated recombinational subcloning of large DNA fragments using yeast. Genome Research **12**:190-7.

24. **Read N. D., A. Lichius, J.-Y. Shoji, and A. B. Goryachev**. 2009. Self-signalling and self-fusion in filamentous fungi. Current Opinion in Microbiology **12**:608-15.

25. **Roca M. G., J. Arlt, C. E. Jeffree, and N. D. Read**. 2005. Cell Biology of Conidial Anastomosis Tubes in *Neurospora crassa*. Eukaryotic Cell **4**:911-919.

26. **Saito H., and K. Tatebayashi**. 2004. Regulation of the osmoregulatory HOG MAPK cascade in yeast. Journal of Biochemistry **136**:267-72.

27. **Seiler S., and M. Plamann**. 2003. The Genetic Basis of Cellular Morphogenesis in the Filamentous Fungus *Neurospora crassa*. Molecular Biology of the Cell **14**:4352-4364.

28. **Sánchez-Paredes E., L. Kawasaki, L. Ongay-Larios, and R. Coria**. 2011. The Gα Subunit Signals through the Ste50 Protein during the Mating Pheromone Response in the Yeast *Kluyveromyces lactis*. Eukaryotic Cell **10**:540-6.

29. **Tatebayashi K., K. Tanaka, T. Tomida, T. Maruoka, E. Kasukawa, and H. Saito**. 2006. Adaptor functions of Cdc42, Ste50, and Sho1 in the yeast osmoregulatory HOG MAPK pathway. EMBO Journal **25**:3033-3044.

30. **Truckses D. M., J. E. Bloomekatz, and J. Thorner**. 2006. The RA Domain of Ste50 Adaptor Protein Is Required for Delivery of Ste11 to the Plasma Membrane in the Filamentous Growth Signaling Pathway of the Yeast *Saccharomyces cerevisiae*. Molecular and Cellular Biology **26**:912-928.

31. **Uhlik M. T., A. N. Abell, N. L. Johnson, W. Sun, B. D. Cuevas, K. E. Lobel-Rice, E. A. Horne, M. L. Dell'Acqua, and G. L. Johnson**. 2003. Rac-MEKK3-MKK3

scaffolding for p38 MAPK activation during hyperosmotic shock. Nature Cell Biology **5**:1104-10.

32. **Wright S. J., R. Inchausti, C. J. Eaton, S. Krystofova, and K. A. Borkovich**. 2011. RIC8 is a Guanine-nucleotide Exchange Factor for Gα Subunits that Regulates Growth and Development in *Neurospora crassa*. Genetics **189**:1-45.

33. **Wu C., G. Jansen, J. Zhang, D. Y. Thomas, and M. Whiteway**. 2006. Adaptor protein Ste50p links the Ste11p MEKK to the HOG pathway through plasma membrane association. Genes & Development **20**:734-46.

34. **Xu G., G. Jansen, D. Y. Thomas, C. P. Hollenberg, and M. Ramezani Rad**. 1996. Ste50p sustains mating pheromone-induced signal transduction in the yeast *Saccharomyces cerevisiae*. Molecular Microbiology **20**:773-83.

35. **Yamamoto K., K. Tatebayashi, K. Tanaka, and H. Saito**. 2010. Dynamic control of yeast MAP kinase network by induced association and dissociation between the Ste50 scaffold and the Opy2 membrane anchor. Molecular Cell **40**:87-98.

36. **Zhao X. H., Y. S. Kim, G. S. Park, and J. R. Xu**. 2005. A Mitogen-Activated Protein Kinase Cascade Regulating Infection-Related Morphogenesis in *Magnaporthe grisea*. The Plant Cell **17**:1317-1329.

Chapter 6. Conclusions and Future Directions

In an effort to dissect the signal transduction cascade in *Neurospora crassa*, a chemical genomics approach was first attempted. After an arduous screening process, a small molecule that has a distinct effect on *N. crassa* was found. This molecule causes strange blebbing on the surface of the conidia as well as the hyphae of the filamentous fungus. I checked to see whether the blebbing caused by the chemical was actually related to conidial anastomosis tubes (CATs). However, testing the chemical on mutants that were defective in forming CATs confirmed that these strange protrusions were not CATs.

A possible next step for the chemical genomics project could be a RNAseq experiment. By comparing wild-type strains with negative control versus treatment with compound #5979758, expression of various genes can be measured using RNAseq and then validated with RT-PCR. This could lead to valuable information regarding genes that are affected by the chemical. Deletion mutants in highly regulated genes could be tested for sensitivity to the chemical.

An experiment that developed from the original chemical genomics project was to perform metabonomics analysis on wild type and the Δ*gna-3* mutant in the presence and absence of the conidiation inhibitor. Experiments testing the effect of low carbon on the metabonome (and effect of added peptone) were included, as low carbon induces condiation in wild type, while peptone corrects the inappropriate conidiation in Δ*gna-3* mutants. However, the results using the inhibitor were not decipherable because no clear

cut trends could be deduced from the metabolic profiles, except that the compound #6238725 affected metabolic pathways of wild type and $\Delta gna-3$ mutants of *N. crassa*. The compound #6238725 prevented conidiation in $\Delta gna-3$, but it also reduced mass (which was probably the result of the perturbation in the metabolism). However, the rest of the experiments yielded valuable results: comparison of the metabolomes of wild type vs. $\Delta gna-3$, high sucrose vs. low sucrose, conidia vs. hyphae, +/- peptone. One of the main conclusions was that the loss of GNA-3 did not significantly influence the global metabolome, although levels of specific metabolites did vary (5). Also, loss of GNA-3 led to a defect in detection of carbon source by the fungus. This is a further indication that this Gα is involved in carbon nutrient sensing by *N. crassa* (4). Furthermore, since this is the first publication of utilizing this technology for the purpose of studying the *N. crassa*'s metabolome using ^{1}H NMR, this experiment and results can serve as a blueprint for future studies of metabolites in other filamentous species.

For future studies, a possible direction is to perform metabonomics experiments on other deletion mutants. The advantage of this plan is that this approach could group mutants into collections that have similar metabolic profiles, suggesting that these mutants share a similar perturbation in a metabolic pathway. It provides a powerful support to the genomics approach by showing how a loss of a gene could lead to an unforeseen phenotype, revealing a new role for the gene. Moreover, combining the metabonomics approach with a molecular biology methodology to determine gene expression (such as microarray or RNA-seq) (1) would prove doubly worthwhile; by

202

correlating gene expression data with the metabolite levels (comparison between wild type and a deletion mutant) would possibly uncover new pathways for the gene.

A valuable finding from the Yeast2Hybrid screening of RIC8 was discovery of STE50 as an interactor. This protein was shown to physically interact with RIC8 also by co-immunoprecipitation, indicating that this interaction is not a false-positive. During this process, a STE50-FLAG strain was made. As a possible future project, conducting a Mass Spectrometry study of STE50-FLAG could lead to much information regarding interactors of this protein. Since STE50 has an adaptor protein function, identification of its associated proteins will likely reveal components in diverse pathways. For example, can a complex be obtained where RIC8 and Gαs are also present? It has already been shown that RIC8 interacts with GNA-1 in both Yeast2Hybrid (8) and mass spectrometry experiments (Michkov, Servin and Borkovich, unpublished), and weakly with GNA-3 in a Yeast2Hybrid assay (8), and this thesis research has shown that RIC8 physically interacts with STE50. The discovery that RIC8, STE50 and one or more Gα proteins are present in a complex would be most valuable because it would provide additional evidence that RIC8 plays key role in bridging two crucial signal transduction pathways of the filamentous fungi, heterotrimeric G proteins and MAPK cascades.

Another interesting interaction avenue of research is to investigate a possible interaction between STE50 and RHO-4. Since both proteins have been shown to localize to the hyphal septum, but not to the conidial septum (6, 7), it begs the question: do they physically interact? One way that this interaction can be tested is by checking for the presence of RHO-4 in the complex associated with STE50-FLAG epitope-tagged protein.

Another way would be to determine their interaction using the Yeast2Hybrid assay. Since the STE50 Yeast2Hybrid vector is already made, only the RHO4 Yeast2Hybrid vector would need to be constructed. In order to determine a possible dependence between the two proteins for localization to the hyphal septum, a mislocalization study can be conducted whereby *ste50-gfp* strain can be crossed with Δ*rho-4*. Inversely, the *rho4-gfp* mutant can be crossed to Δ*ste50*. Mislocalization of the GFP would indicate that the missing protein is responsible for proper localization of the other protein.

In *Saccharomyces cerevisiae*, it was shown that phosphorylation of STE50 leads to limiting duration of pathway activation (3). Since this thesis research showed that STE50 affects phosphorylation of both MAK-1 and MAK-2 MAPK pathways, this is a possible way of determining if there is "crosstalk" between MAPK pathways in *N. crassa*. Taking advantage of the STE50-FLAG strain and crossing it to the various MAPK deletion mutants, a strain can be engineered to be defective in only one of the three MAPK pathways. Then a MAPK assay (checking for the phosphorylation state of the MAPK proteins) can be conducted. Hao *et al*. (2008) showed that in *S. cerevisiae*, FLAG epitope-tagged Ste50p migrates at a slower rate than untagged Ste50p during electrophoresis and can be verified by Western analysis (3). Since phosphorylated STE50 migrates at a slower rate than the non-phosphorylated STE50, the effect of missing MAPK can also be checked. In *S. cerevisiae*, there are 7 serine or threonine residues within a MAPK consensus sequences (Ser or Thr followed by Pro), 5 of them are phosphorylated. In *N. crassa*, there exist 11 serine or threonine residues that are within a MAPK consensus sequence (Ser-26, Ser-36, Thr-48, Ser-222, Thr-252, Ser-257,

204

Thr-293, Ser-301, Ser-306, Thr-308, and Thr-366). It stands to reason that STE50 also becomes phosphorylated in order to limit the duration of activated MAPK signaling state. Does STE50-FLAG get less phosphorylated when a MAPK is deleted? By determining the effect of one MAPK on the remaining two (OS-2 on MAK-1/MAK-2, for example) paired with the level of phosphorylation of STE50, it can lead to evidence of crosstalk between the separate MAPK pathways in *N. crassa*.

Another interesting interaction with STE50 to explore is whether it interacts with PAKs such as the homologs of Ste20 and Cla4 from *S. cerevisiae* (2). Is STE50 only an adaptor protein for the MAPKs or does it also interact with other kinases? This information could lead to a connection between the MAPK pathway and other cellular components of *N. crassa*.

Importantly, characterization of GNA-3 Y2H interactors should be performed. Finding deletion mutants in interactors that have a phenotype similar to Δ*gna-3* would be a clue that the interactor participates in a pathway with the Gα.

Finally, the gene product of NCU10207 should be tested as a possible ligand for RIC8. There are no reports of a ligand binding to RIC8 in the literature. Still, it seems odd that there is no connection, especially since it physically interacts with RIC8 in Y2H assay. It would be interesting to see what effect a deletion of NCU10207 has on *N. crassa*. Will it explain one of many phenotypes that a Δ*ric8* mutant exhibits? Afterwards, an *in vitro* assay with purified RIC8 and synthesized polypeptide (derived from sequence of NCU10207) could show that there is an interaction between the two.

Such findings could lead to new discovery regarding this novel GEF in *Neurospora crassa* and possibly other organisms.

REFERENCES

1. **Atanasova L., and I. S. Druzhinina**. 2010. Review: Global nutrient profiling by Phenotype MicroArrays: a tool complementing genomic and proteomic studies in conidial fungi. Journal of Zhejiang University-Science B **11**:151-68.

2. **Borkovich K. A., L. A. Alex, O. Yarden, M. Freitag, G. E. Turner, N. D. Read, S. Seiler, D. Bell-pedersen, J. Paietta, N. Plesofsky, M. Plamann, M. Goodrich-tanrikulu, U. Schulte, G. Mannhaupt, F. E. Nargang, A. Radford, C. Selitrennikoff, J. E. Galagan, J. C. Dunlap, J. J. Loros, D. Catcheside, H. Inoue, R. Aramayo, M. Polymenis, E. U. Selker, M. S. Sachs, G. A. Marzluf, I. Paulsen, R. Davis, D. J. Ebbole, A. Zelter, E. R. Kalkman, R. O. Rourke, and F. Bowring**. 2004. Lessons from the Genome Sequence of *Neurospora crassa*: Tracing the Path from Genomic Blueprint to Multicellular Organism. Microbiology and Molecular Biology Reviews **68**:1-108.

3. **Hao N., Y. Zeng, T. C. Elston, and H. G. Dohlman**. 2008. Control of MAPK specificity by feedback phosphorylation of shared adaptor protein Ste50. The Journal of Biological Chemistry **283**:33798-802.

4. **Kays A. M., P. S. Rowley, R. A. Baasiri, and K. A. Borkovich**. 2000. Regulation of conidiation and adenylyl cyclase levels by the Gα protein GNA-3 in *Neurospora crassa*. Molecular and Cellular Biology **20**:7693-705.

5. **Kim J. D., K. Kaiser, C. K. Larive, and K. A. Borkovich**. 2011. Use of ^{1}H nuclear magnetic resonance to measure intracellular metabolite levels during growth and asexual sporulation in *Neurospora crassa*. Eukaryotic Cell **10**:820-31.

6. **Rasmussen C. G., and N. L. Glass**. 2005. A Rho-Type GTPase , *rho-4*, Is Required for Septation in *Neurospora crassa*. Eukaryotic Cell **4**:1913-1925.

7. **Rasmussen C. G., and N. L. Glass**. 2007. Localization of RHO-4 indicates differential regulation of conidial versus vegetative septation in the filamentous fungus *Neurospora crassa*. Eukaryotic Cell **6**:1097-107.

8. **Wright S. J., R. Inchausti, C. J. Eaton, S. Krystofova, and K. A. Borkovich**. 2011. RIC8 is a Guanine-nucleotide Exchange Factor for Gα Subunits that Regulates Growth and Development in *Neurospora crassa*. Genetics **189**:1-45.

Appendix 1: Effect of MPEB on the metabolome of *Neurospora crassa*.

Conidiation inhibitor #6238725 (MPEB) identified from the chemical screening of the Chembridge ExpressPick library (detailed in Chapter 2 of this thesis) was used to suppress conidiation in wild-type and Δ*gna-3* strains for the metabonomics study. Since the Δ*gna-3* strain inappropriately conidiates in high sucrose condition, and MPEB represses this phenotype, it was of interest to determine the influence that this chemical has on the metabolism of *Neurospora crassa*. The goal was to determine the metabolite profiles of both strains with the application of the compound and then see how the profile of Δ*gna-3* strain changes due to exposure to MPED (compared to the metabolome of conidiating Δ*gna-3* in high sucrose condition). Also, the effect of MPEB on wild type was analyzed (MPEB does not affect any phenotype related to conidiation) because it could serve as a baseline for comparison to the metabolome of Δ*gna-3*.

For this metabonomics experiment, VM + 1.5% sucrose medium was supplemented with MPEB to a final concentration of 10 μM. Previous experiments have shown that this concentration was sufficient in preventing conidiation of Δ*gna-3* in submerged condition. After treatment with MPEB and incubation, both tissues of wild-type and Δ*gna-3* strains were collected and metabolites extracted, ^{1}H NMR experiments conducted, and statistical analysis done exactly as described in Chapter 3.

Statistical analysis was conducted on individual metabolites that were identified (and quantifiable). Table 1 shows the relative levels of detectable/quantifiable metabolites. Figures 1-3 show the relative metabolite levels of amino acid, sugars, and

miscellaneous metabolites in graph form with error bars, respectively. Interestingly, levels of the amino acids arginine, ornithine, lysine, and glutamine did not resemble the metabolome of non-conidiating tissue but rather that of conidiating tissue. Also, the amino acids glycine and leucine did not follow the trends of either conidiating or non-conidiating tissue. As for the sugar metabolites, trehalose, glucose, and mannitol all resemble the metabolite levels in conidia. Intriguingly, even though the concentration of these sugars in MPEB-treated tissue resembles that of conidia, they do not conidiate.

Data was collected and principal components analysis conducted to fathom the effect of MPEB on the metabolome of *N. crassa*. Figure 4 is the PCA scores plot from the experiment, including data from treatments of both wild type and Δ*gna-3* with MPEB. The most striking impression from the scores plot is that symbols representing the MBEP-treated metabolomes of both wild type and Δ*gna-3* group are completely removed from the metabolomes of both strains in both high and low sucrose conditions (with the exception of one Δ*gna-3* outlier); this indicates that the *N. crassa* metabolome is severely affected by MPEB. Even though wild type and Δ*gna-3* strains treated with MPEB did not conidiate, the metabolic profile does not resemble that of non-conidiating tissue.

The conclusion that can be drawn is that the small molecule MPEB has a profound effect on the metabolome of *N. crassa*. However, levels of some of the quantifiable metabolites seem to indicate that the metabolic profiles of wild type and Δ*gna-3* strains treated with MPEB resemble that of conidiating tissue. The global metabolome (indicated by the PCA scores plot) shows that the metabolic profiles of tissues treated with MPEB do not group with either the non-conidiating or conidiating tissue.

After the initial discovery of MPEB from the library screening, 1 mg of this compound was ordered from Chembridge Corporation (San Diego, CA). This aliquot was still effective as a conidiation inhibitor of Δ*gna-3* strain (similar to the chemical from the stock library). However, the second aliquot of MPEB purchased did not prevent conidiation and hence led to cessation of this project.

Table 1. Relative metabolite levels for both wild type and Δ*gna-3* strains treated with conidiation inhibitor MPEB. Metabolites that were present but were not quantifiable are leveled as "NQ".

Metabolites	Integral ave.	wild type	Δ*gna-3*
histidine	7.8725	NQ	NQ
tyrosine	6.903	NQ	NQ
fumarate	6.5195	NQ	NQ
adenosine	6.082	NQ	NQ
allantoin	5.3965	NQ	NQ
glucose	5.2345	0.00053	0.00063
trehalose	5.1875	0.00969	0.00852
carnitine	4.569	0.00124	0.00075
serine	3.969	0.00868	0.00562
mannitol	3.6975	0.02731	0.02629
glycine	3.5575	0.00870	0.00461
betaine	3.2775	0.00138	0.00236
choline	3.205	0.00127	0.00358
ornithine	3.0715	0.00091	0.00054
lysine	3.0145	0.00038	0.00042
asparagine	2.878	NQ	NQ
aspartate	2.8025	0.00128	NQ
glutamine	2.4575	0.00918	0.00971
glutamate	2.3415	0.02548	0.01935
arginine	1.662	0.00243	0.00366
alanine	1.475	0.06516	0.09131
threonine	1.333	0.00398	0.00782
valine	1.0435	0.00221	0.00270
leucine	0.9645	0.00047	0.00080
isoleucine	0.9365	0.00099	0.00185
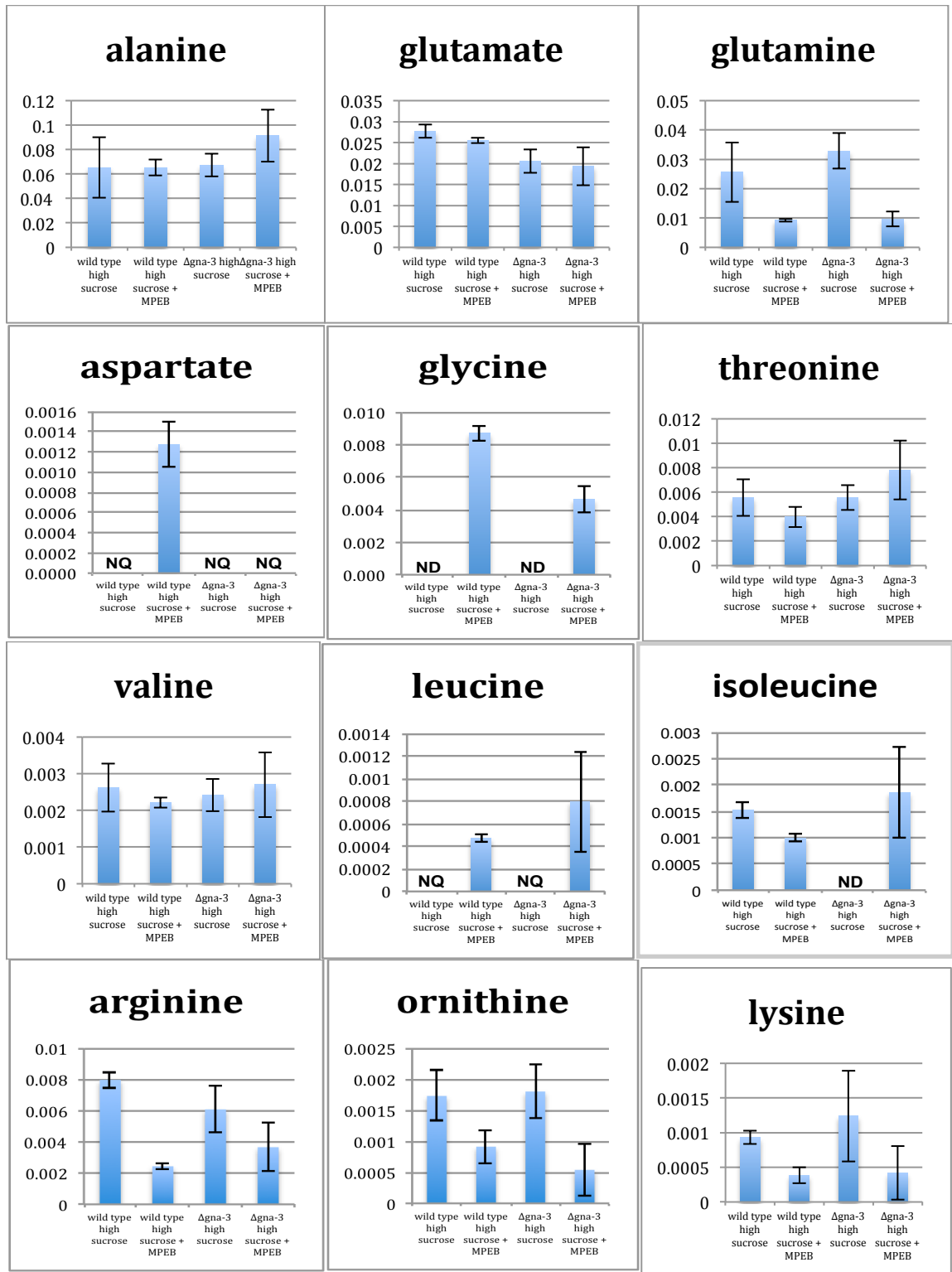
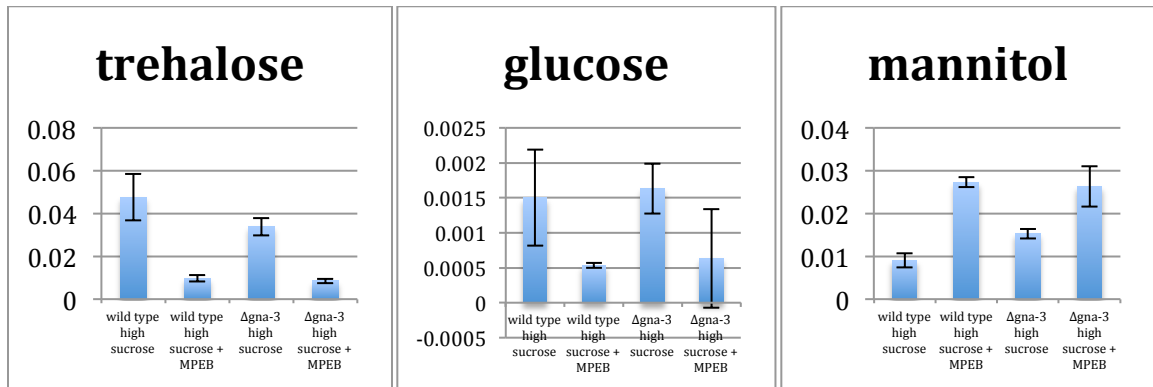**Figure 1.** Relative levels of amino acids.
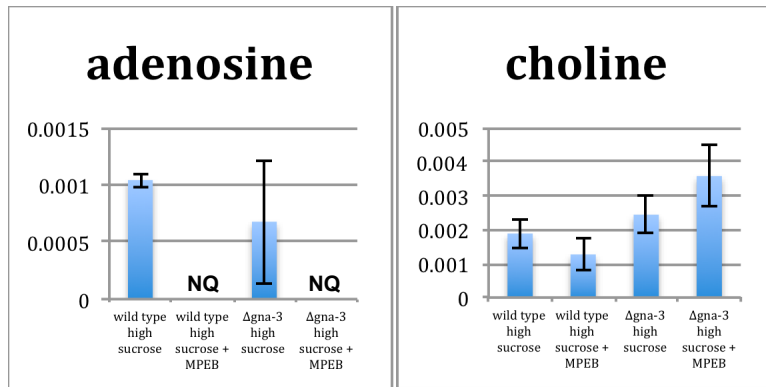
Figure 2. Relative levels of sugar metabolites.

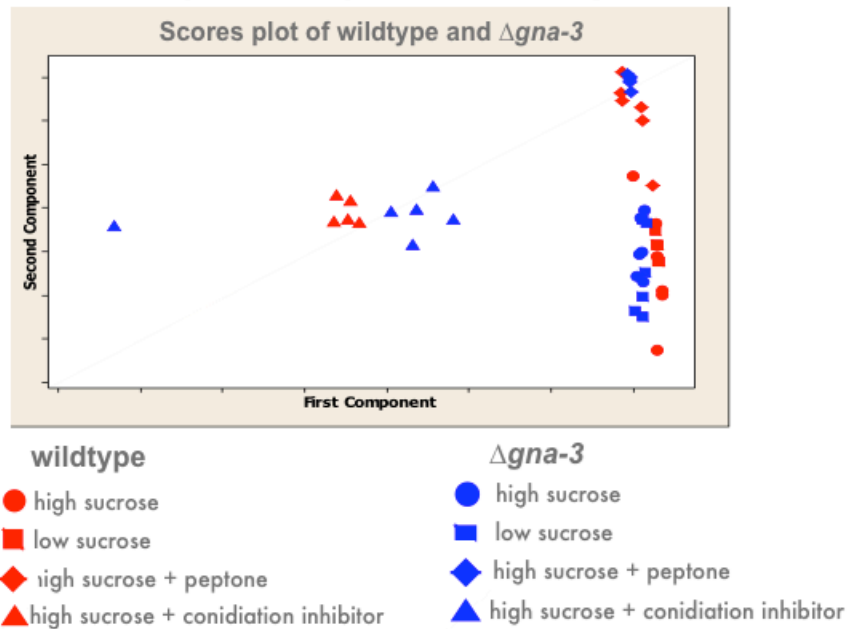Figure 3. Relative levels of miscellaneous metabolites.

Figure 4. PCA scores plot of the metabonomics project including metabolome of wild type and Δ*gna-3* treated with MPEB.